Diss. ETH No. 22686

Development of a Purification Protocol for CRF Receptor Isomers and a Structural Investigations of a Potential Interaction Between Nogo-A-△20 and S1PR2-Fragments

A dissertation submitted to
ETH ZURICH

for the degree of
Doctor of Sciences at ETH Zurich
(Dr. sc. ETH Zurich)

presented by

VIVIANE ZELENAY

Master of Science in Chemistry, ETH Zurich
born June 16, 1987
citizen of Dietlikon, Switzerland

accepted on the recommendation of
Prof. Dr. Roland Riek, examiner
Prof. Dr. Gebhard Schertler, co-examiner

2015

Contents

Abstract

G protein-coupled receptors (GPCRs) are an important class of membrane proteins. GPCRs are involved in important physiological processes such as homeostasis, inflammatory responses and cancer, therefore, they increasingly gained interests from drug companies. GPCRs are composed of seven transmembrane helices, with the N-terminus on the extracellular and the C-terminus on the intracellular side. A conformational change is induced upon ligand binding resulting in signal transduction across cell membranes.

So far, little is known about GPCRs and their ligand interaction due to the challenges in producing functional receptors and their further stabilisations. Even though it is agreed that dynamics play an important role for the GPCRs and their interactions and activations upon ligand binding, most of the solved structure are from crystallisation. However, this technique just shows static conformations. In contrast, Nuclear magnetic resonance (NMR) spectroscopy could give complementary insights to crystallography data such as ligand-receptor interactions and its influence on the dynamics of GPCRs. However, for NMR spectroscopy, high amounts of functionally active receptors are needed, which have to be grown in an expression system suitable to introduce NMR-active isotopes applicable for multi-dimensional NMR spectroscopy measurements.

Here, the corticotropin-releasing factor 2β ($CRF_{2\beta}R$), a member of the *secretin* family of the GPCR, has been chosen as a model system for NMR spectroscopy measurements due to its role in the stress induced endocrine-responses in the human

body. However, as discussed above, a prerequisite for NMR spectroscopy is a purification protocol that yields a functional receptor in the mg range. Here, a purification protocol has been established for the $CRF_{2\beta}R$ expressed in *E.coli*. The receptor has been solubilised from *E.coli* membranes in a whole cell extraction, either with the detergents n-dodecyl β-D-maltopyranoside (DDM)/n-tetradecylphosphocholine (FC14) or DDM alone. The receptor has been purified further using immobilised metal ion affinity chromatography (IMAC) in the presence of the detergent DDM.

To separate folded receptor from its unfolded form, a ligand-affinity chromatography has been developed. The antagonist of $CRF_{2\beta}R$, astressin, which binds to the N-terminus of the CRF receptors, has been used as the ligand for the affinity chromatography. It has been bound to a resin via a biotin-streptavidin interaction. A protocol for the astressin-affinity chromatography has been established using the extracellular domain (ECD) of the $CRF_{2\beta}R$, since its purification protocol is known and its NMR-derived structure has been published in 2004. The fold of the eluted ECD has been verified with a [^{15}N, ^{1}H]-HSQC, which is a NMR-based fingerprint of the structure. Additionally, the ability of the eluted ECD to bind its antagonist astressin has been confirmed via NMR spectroscopy.

The final purification protocol for the $CRF_{2\beta}R$ yields about $0.5\,\mathrm{mg}$ active receptor per litre of bacteria culture. The activity of the $CRF_{2\beta}R$ has been verified with a radioactive ligand binding assay achieving a binding activity of $11\,\mathrm{nM}$.

For NMR spectroscopy measurements, an expression protocol has been established to express the receptor ^{15}N-labelled in minimal media. A NMR spectrum has been recorded in the detergent FC14.

A purification protocol for a soluble isomer of the CRF_2R family ($sCRF_{2\alpha}R$) has also been developed. The sample has been purified using IMAC and astressin-affinity chromatography. However, folded and unfolded soluble receptor eluted simultaneously from the astressin-affinity column.

A ligand for GPCRs can also be another membrane protein. This is the case for the GPCR sphingosine-1-phosphate receptor 2 (S1PR2). Its binding partner is the mem-

brane protein Nogo-A. Nogo-A is found in the myelin sheaths of axons and is responsible for the inhibition of axons regrowth. The specific segment important for binding to S1PR2 has been elucidated via biochemical methods. This segment has been termed Nogo-A-Δ20. Nogo-A-Δ20 is an intrinsically disordered part (IDP) of the Nogo-A. To investigate the interaction between Nogo-A-Δ20 and the extracellular loops (ECL) of the S1PR2, first, 3D NMR spectroscopy measurements were performed on the protein for sequential assignment. $75\,\%$ of the amino acid residues were achieved to be assigned. Secondary structure analysis was performed on the assigned Nogo-A-Δ20 confirming its intrinsically disordered structure, which is independent on pH or temperature. The hypothesis that the extracellular loops of the S1PR2 bind to the Nogo-A-Δ20 segment could not be confirmed using NMR spectroscopy measurements.

Zusammenfassung

G-Protein-gekoppelte Rezeptoren (englisch: G protein-coupled receptors, GPCRs) bilden eine der wichtigsten und mit über 1000 Rezeptoren eine der grössten Proteinsuperfamilie. GPCRs beeinflussen wichtige physiologische Prozesse, wie zum Beispiel die Homeostasis, endokrinische Reaktionen induziert durch Entzündingen oder Krebs. Aus diesem Grund erhalten GPCRs eine hohe Aufmerksamkeit in Arztneimittelforschungen. GPCRs besitzen sieben Transmembranhelices, wobei der N-Terminus im extracellulären und der C-Terminus im intracellulären Bereich einer Zelle liegt. Sobald ein Ligand an ein GPCR bindet, induziert dieser eine strukturelle Veränderung im GPCR, welche schlussendlich eine Signalübertragung durch die Membrane auslöst.
Es ist immer noch sehr wenig über GPCRs bekannt und ihre Interaktionen mit Liganden. Dies liegt hauptsächlich an der Schwierigkeit, funktionelle Rezeptoren herzustellen und sie zu stabilisieren. Die meisten Strukturen wurden aus Kristallen, die in inaktiver Konformation kristallisiert wurden, ermittelt. Doch zeigen diese nur eine Momentaufnahme von den vielen strukturellen Konformationen eines GPCRs, in einer zudem noch sehr unnatürlichen Umgebung. Man ist sich jedoch einig, dass die Dynamik der GPCRs für deren Aktivierung durch Liganden eine wichtige Rolle spielt. Kernspinresonanz (englisch nuclear magnetic resonance, NMR) könnte hier wichtige Informationen bezüglich der Liganden-Rezeptoren Wechselwirkungen und deren Auswirkung auf die Dynamik der GPCRs liefern. Für diese Methode wird allerdings eine grosse Menge an funktionellen Rezeptor benötigt. Zusätzlich muss der Rezeptor in einem Expressionssystem produziert werden, in welchem der Rezeptor mit NMR ak-

tiven Isotopen expremiert werden kann.
Corticotropin Releasing Faktor 2β Rezeptor ($CRF_{2\beta}R$), welches ein Mitglied der *Secretin* Familie der GPCRs ist, wurde wegen seiner Bedeutung in der durch Stress induzierten endokrinischen Reaktionen für diese Arbeit gewählt. Wie jedoch erwähnt wurde, ist die Etablierung eines Protokolls für die Herstellung eines funktionellen Rezeptors in mg-Bereich Vorraussetzung für NMR-basierte strukturelle Studien. Ein solches Protokoll wurde für die Proteinaufreinigung von $CRF_{2\beta}R$ in dieser Arbeit etabliert. Der Rezeptor wurde dazu mit einer 'whole cell extraction' aus *E.coli*-Membranen solubilisiert. Für die Extraktion wurde entweder eine Mischung aus n-Dodecyl-β-D-maltopyranosid (DDM)/Tetradecylphosphocholin (FC14) Detergenzien oder DDM alleine verwendet. Anschliessend wurde der Rezeptor in DDM mit einer immobilisierten-Metallionen-Affinitätschromatographie (IMAC) aufgereinigt. Funktioneller Rezeptor wurde vom Nicht-Funktionellen mit einer Ligandenaffinitätschromatographie getrennt. Für die Ligandenaffinitätssäule wurde der Antagonist Astressin verwendet. Dieser bindet zum N-Terminus des CRF Rezeptors. Astressin wurde mit einer Biotin-Streptavidin Interaktion ans Resin gebunden.
Das Protokoll für die Astressinaffinitätschromatographie wurde mit der ersten extrazellulären Domäne (ECD) des $CRF_{2\beta}R$ etabliert. Deren Aufreinigungsprotokoll und Struktur wurde im Jahr 2004 publiziert. Die richtige Faltung der eluierten ECD wurde mittels [^{15}N, ^{1}H]-HSQC NMR Spektroskopiemessung verifiziert, welches ein NMR-basierter Fingerabdruck von der Struktur darstellt. Zusätzlich wurde auch mittels NMR Spektroskopie validiert, ob die eluierte ECD ihren Antagonisten Astressin binden konnte.
Die Ausbeute der Aufreinigung von $CRF_{2\beta}R$ beträgt ungefähr $0.5\,\mathrm{mg}$ pro Liter Bakterienkultur. Die Aktivität des Rezeptors wurde mit einem radioaktiven Ligandenbindungstest bestätigt. Die Bindungsaffinität betrug $11\,\mathrm{nM}$.
Isotopenmarkierter Rezeptor wurde mit einem neu etablierten Expressionsprotokoll in Minimalmedium hergestellt. Ein NMR-Spektrum wurde im Detergenz FC14 aufgenommen.

Ebenfalls wurde ein Protokoll für die Aufreinigung eines löslichen CRF_2R Isoforms ($sCRF_{2\alpha}R$) etabliert. Dieses Protein wurde gleichfalls mittels einer IMAC und Astressinaffinitätschromatographie aufgereinigt. Jedoch konnte hier der gefaltete nicht vom entfalteten Rezeptor getrennt werden, da beide gleichzeitig eluiert wurden.
Die Liganden für GPCRs können sehr verschiedenartig sein, wie zum Beispiel Photonen, kleine Moleküle, Hormone oder Lipide. Auch ein Membranprotein kann als Bindungspartner fungieren, wie es für den Sphingosine-1-Phosphat-Rezeptor 2 (S1PR2) der Fall ist. Der Ligand ist das Protein Nogo-A, welches in den lipidreichen Myelinmembran eines Axons zu finden ist. Nogo-A ist dafür verantwortlich, dass Nervenzellen nicht mehr zusammenwachsen, wenn sie einmal separiert wurden. Das Segment, welches spezifisch an S1PR2 bindet, wurde mit biochemischen Methoden erfasst. Dieses Segment wird Nogo-A-Δ20 genannt und ist ein intrinsisch ungeordneter Teil (IDP) des Nogo-As. In dieser Arbeit wurde isotopenmarkiertes Nogo-A-Δ20 produziert. Mit diesem wurden mehrere 3D NMR Spektren aufgenommen, um eine Aminosäurenzuordnung durchzuführen. $75\,\%$ der Aminosäuren konnten zugeordnet werden. Damit konnte mit der sekundären Proteinstrukturvorhersage das Nogo-A-Δ20 als IDP bestätigt werden, auch bei verschiedenen pHs oder Temperaturen. Es wurde vermutet, dass die extrazelluläre Domänen (englisch extracellular loops, ECL) vom S1PR2 sich bei der Interaktion mit dem Nogo-A-Δ20 beteiligen. Daher titrierte man die ECLs zum markierten Nogo-A-Δ20 dazu. Die Hypothese, dass die ECLs des S1PR2 für die Bindung an Nogo-A-Δ20 zuständig sind, konnte mittels NMR Spektroskopie nicht bestätigt werden.

Chapter 1

Introduction

This chapter starts with a general overview on G protein-coupled receptor (GPCR) membrane proteins and their importance for research in medicinal chemistry, following a discussion of the different structural features of the GPCR family and its classifications. The next chapter emphasis especially on the corticotropin releasing factor receptor (CRF R) belonging to the GPCR *secretin* family, and its ligands, the so far solved structures and its importance in medicinal chemistry.
In addition, the membrane protein Nogo-A is discussed. Its disordered extracellular segment Nogo-A-Δ20 binds the GPCR sphingosine 1-phosphate receptor 2 (S1PR2).
The introduction finishes with an overview about membrane proteins in nuclear magnetic resonance (NMR) spectroscopy, the importance of detergents and isotope labelling and the GPCR studied by NMR spectroscopy so far.

1.1 G Protein-Coupled Receptors

1.1.1 In Medicinal Chemistrty

The G protein-coupled receptors (GPCRs) are an important class of integral membrane proteins, which has about 800 encoded genes in the human genome [1]. They

control diverse biological functions in mammals such as neural, cardiovascular, immune, and endocrine processes and are thought to be responsible for many pathological diseases including physical and mental disorders such as cancer or depression [2–5]. Therefore, a lot of effort is put into elucidating the biological and structural functions of GPCR and to understand how they transduce outer signals across membranes into cells. The investigation of the interactions between GPCRs and ligands might shed light into their mechanism and how and why dynamics are critical to the functioning of GPCRs.

However, GPCRs are not only interesting from a structural point of view, but also for pharmaceutical companies. Depending on the studies, about $25\,\%$ to $30\,\%$ of the clinically approved drugs on the market target one or several GPCRs [6, 7]. In the studies only drugs were included, whose molecular target is known in the human body. The drugs targeting GPCRs can be very diverse and are used to treat *e.g.* hypertension (angiotensin receptor 1), pain and alcoholism and abuse of opioids (opioid receptors), HIV (chemokine (C-C motif) receptor 5) or osteoporosis (parathyroid receptor) [8].

1.1.2 Sturctural Overview

Despite the importance of GPCRs, very little is known about their structures and their structure-activity relationship. Only since 2000, crystal structures have been published with that of rhodopsin being the first [9]. Since then, structures of 28 different GPCRs have been published [1], most of them being molecularly engineered to be in an inactive state.

A GPCR is composed of seven α-helical transmembranes (TM) helices linked by intracellular (IC) and extracellular (EC) loops, having the N-terminus on the EC and the C-terminus on the IC side. The extracellular part of a GPCR modulates the access of its ligand to the binding site by creating either a rather closed or open structure for the ligand to penetrate. The transmembrane region is the structural core of a GPCR

[1] http://blanco.biomol.uci.edu/mpstruc/

to where the ligand binds. The ligand transduces the information to the intracellular part through via conformational changes in the TM region [10].

Figure 1.1: Snake plot of the sequence of bovine rhodopsin highlighting the seven transmembrane helices. It shows the disulphide bridge between ECL2 and TM3 (magenta filled boxes), which is conserved throughout the GPCR family. The blue circle indicate the position of helix 8 in the rhodopsin sequence. Two cysteines at the C-terminus are attached to the membrane via palmitoylation [10].

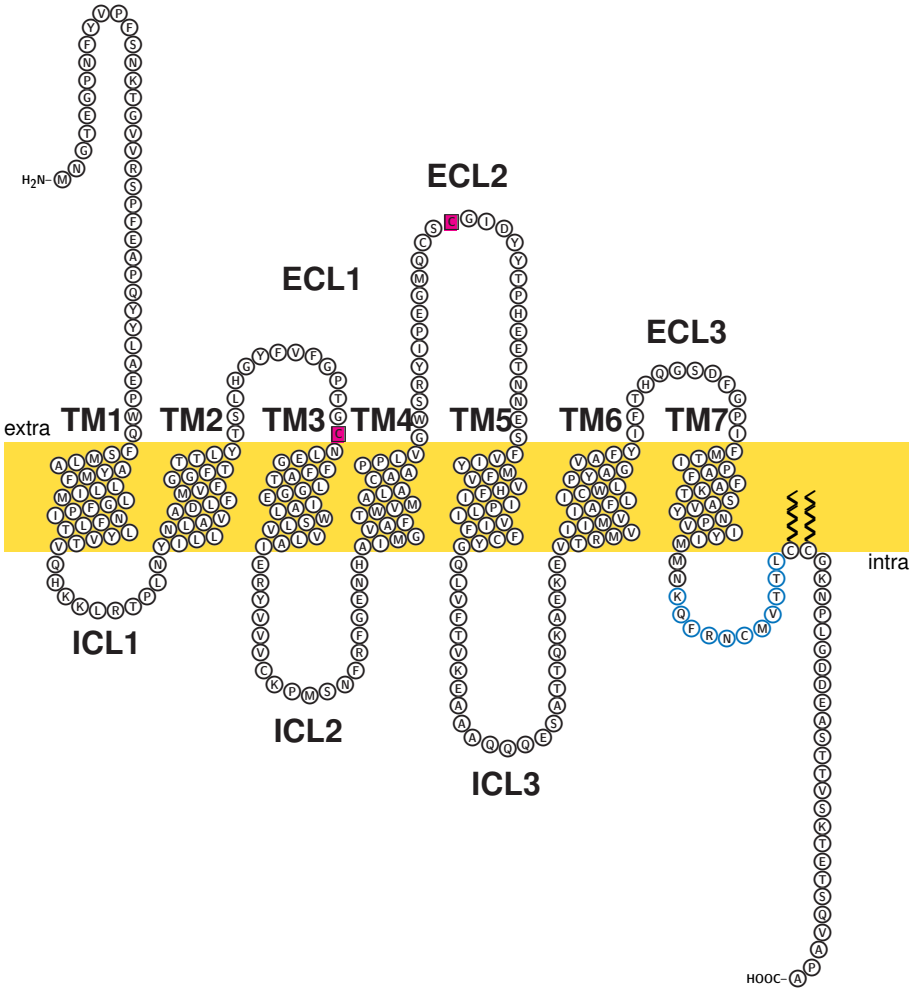

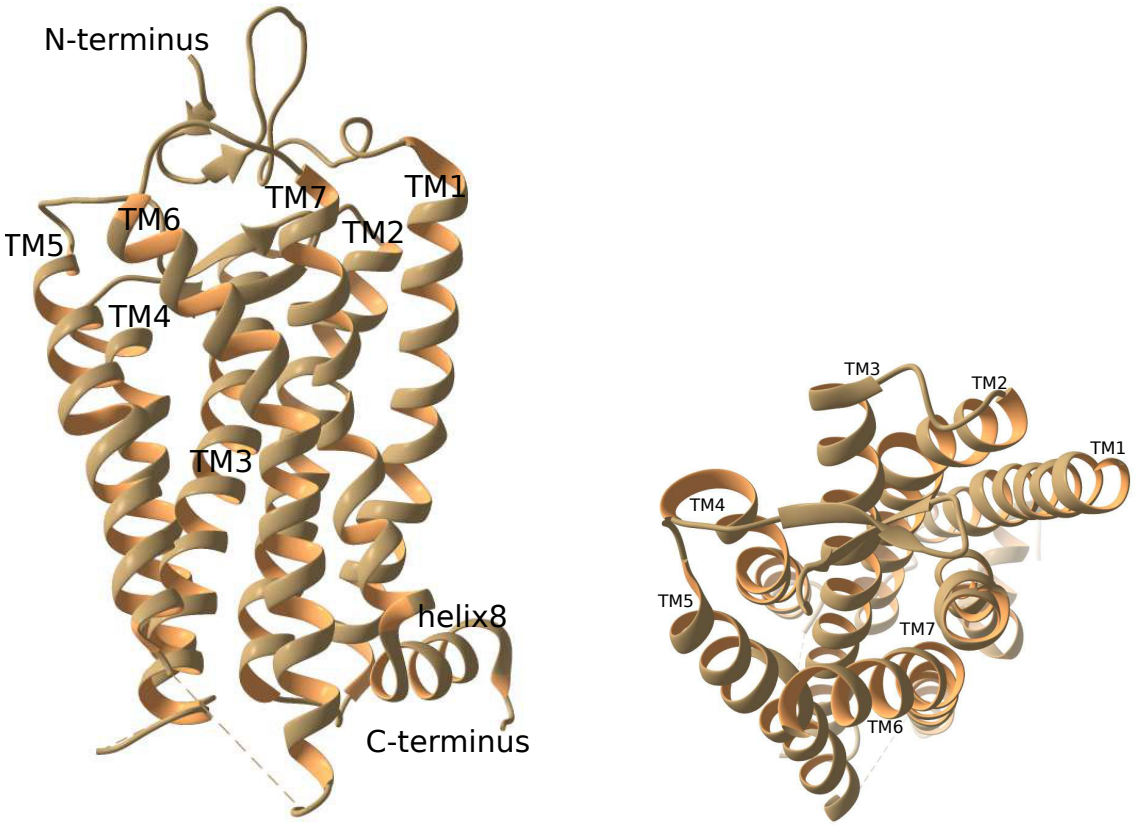

Figure 1.2: Crystal structure of bovine rhodopsin (PDB 1F88). It was the first crystal structure of a GPCR solved in 2000 [9]. The 7 transmembrane helices including helix 8 are clearly visible in the structure.

Intertransmembrane contacts, stabilising a GPCR, are mainly found in the central or cytoplasmic side of the TM bundle. The intracellular part is the interface for the cytosolic signalling. Additionally, the intracellular regions, especially the C-terminus, can be extensively post-translational modified, which can influence receptor activity and internalisation. At the extracellular site, a conserved disulphide bond near the binding regions between ECL2 and TM3 limits the conformational plasticity of the ECL2 and the conformational change near the disulphide bond upon ligand binding. At the C-terminus, a short amphipathic helix (helix 8) with a palmitoylation site, is present, which can be anchored to the membrane of a cell [10] (figure 1.2).

1.1.3 Signalling

A GPCR transmits stimuli across cell membranes and thus transmits signals from the extracellular to the intracellular environment of a cell. Its ligands bind from the extracellular side and convey conformational changes resulting in the activation of the GPCR. This conformational activation increases the affinity for a heterotrimeric G-protein, which consists of a α, β, and γ subunit [11]. Upon binding of a ligand to its GPCR, a guanosine diphosphate (GDP) is released at the α subunit, which in turn is replaced by a guanosine triphosphate (GTP). This exchange of GDP to GTP dissociates the heterotrimeric G-protein into a α subunit and a $\beta\gamma$ complex. The dissociation lasts until the GTP is again hydrolysed to a GDP and thus enabling the reassociation of the subunits and the inactivation of the GPCR complex [11].
Four different heterotrimeric G-protein families exist (G_s, G_i, G_q, G_{12}) based on the primary sequence similarities of the α subunits [12]. While some GPCRs only bind specifically to proteins of one G-protein family, others can interact with those of several G-protein families [12]. The interactions between a GPCR and several G-proteins result in a further complexity in the downstream signalling of the GPCRs.
The activated complexes may cause several downstream protein to generate a cellular response depending on the GPCR-G protein-complex. The activated intracellular signals can be quite diverse and may include cAMP, cGMP, inositol phosphate, diacylglycerol, arachidonic acid, and cytosolic ions [11]. The downstream signalling may also activate phosphorylation enzymes, which may phosphorylate the intracellular domains of the GPCRs. These phosphorylations enable the binding of arrestin proteins. Binding of an arrestin internalises the GPCR and mediates endocytosis [13]. In the endosomes, the arrestin-GPCR complex is either degraded via lysosomes or recycled and trafficked back to the plasma membrane. However, this complex does not only interrupt the signalling via internalisation, but it is also able to signal in a G-protein independent manner suspected to regulate the GPCR trafficking [13].
Activation of a GPCR can be induced by a wide range of ligands, from a single photon to ions, odorants, amino acids, fatty acids, neurotransmitters, peptides, and to prote-

olytic enzymes, which are able to cleave receptor fragments generating an activating ligand [14].

1.1.4 Classification and Residue Nomenclature

Kolakowski divided the family of GPCRs into the well-known A-F classification system in 1994 including non G protein binding receptors classifying them as O (other) [15].
In 2001, Fredriksson et al. created an additional classification system of known and predicted GPCRs according to their phylogenetic criteria, termed *glutamate, rhodopsin, adhesion, frizzled/taste2*, and *secretin* family. The *glutamate* corresponds to the C family, the *rhodopsin* to the A, the *frizzled/taste2* to the F family. The *adhesion* and *secretin* family belong in the first classification system to the family B [1]. The class D and E are not found in any vertebrates [2].
To get comprehensive site-defined properties of different GPCRs, Ballesteros and Weinstein [16] developed a common numbering scheme as residue-nomeclature for the *rhodopsin* family. The most conserved residue in each TM domain is taken as a reference residue and the number .50 is assigned to it. This arbitrarily assigned number is preceded by the TM helix number of the residue. The following and preceding residues are numbered according to their position to the reference residue [16].
Wootten et al. used the same approach as the Ballesteros &Weinstein numbering system, but for the *secretin* family. The numbering for the residue-nomenclature by Wootten uses the most conserved residue in the *secretin* family [17] (figure 1.3).
From here on, the receptors belonging to the *rhodopsin* family are numbered according to the Ballesteros & Weinstein residue nomenclature and its absolute numbers are shown in superscript. All the receptors belonging to the *secretin* family are numbered according to the Wootten numbering and its absolute numbering is also shown as superscript after the residue.

[2] www.guidetopharmacology.org

Figure 1.3: Snake plot of a sequence of a member of the *secretin* family, the mus musculus $CRF_{2\beta}R$, including the Wootten numbering scheme. The most conserved residue in a TM is given the number .50, the preceding amino acid has the number .49 and the following amino acid 0.51. The very first number is the TM helix number.

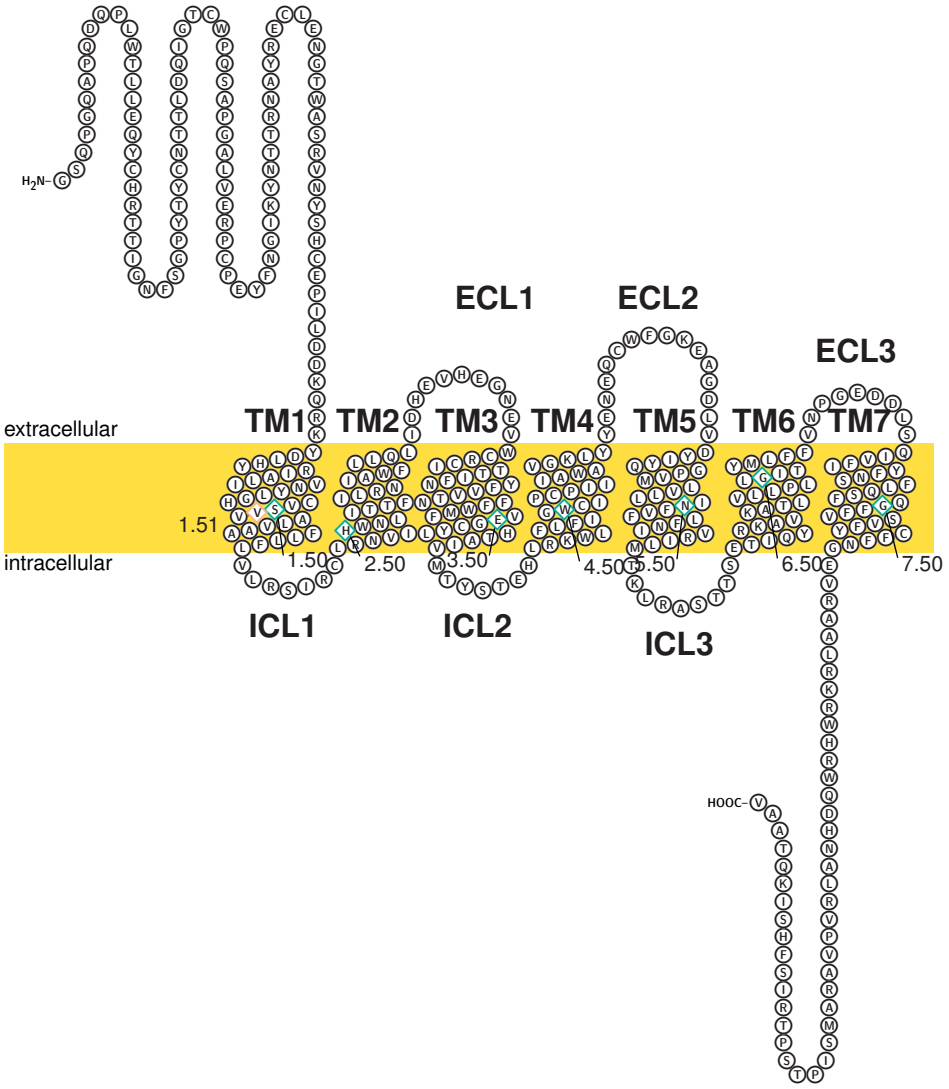

1.2 *Secretin* Family: Corticotropin-Releasing Factor Receptor

The CRF receptor belongs to the family B of the GPCRs according to Kolakowski or to the *secretin* family classification according to Fredriksson nomenclature. Only 15 members belong to the GPCR *secretin* family compared to almost 670 full length receptors belonging to the *rhodopsin* family. The *secretin* family members are:
- calcitonin & calcitonin-like receptors (CALCR, CALCRL),
- glucagone receptor (GCRR),
- gastric inhibitory polypeptide receptor (GIPR),
- glucagon-like peptide receptor (GLP1R, GLP2R),
- growth-hormone-releasing hormone receptor(GHRHR),
- adenylate cyclase activating polypeptide receptor (PAC1/ADCYAP1R1),
- parathyroid hormone receptors (PTHR1, PTHR2),
- secretin receptor (SCTR),
- vasoactive intestinal peptide receptors (VIPR1, VIPR2),
- and corticotropin-releasing factor receptors (CRF_1R, CRF_2R).

Compared to the *rhodopsin* family, whose ligands can be as diverse as photons, small molecules or ions, the ligands targeting the *secretin* family are all peptides with more than 27 amino acid residues. They are synthesised and released by endocrine, neurone, or immune cells [18] and all peptides have an important role in central homeostatic functions [8].

The CRF receptors are encoded by two genes generating CRF_1R and CRF_2R. A third CRF receptor has been found, CRF_3R, however in only one fish species, [19]. The member of the *secretin* family share between 32-67 % sequence identity with the highest variation at the N-terminal ECD [8]. Each mRNA has several exon/introns junctions, creating several splice variants, with CRF $_{1\alpha}$ R, CRF $_{1\beta}$ R, CRF $_{2\alpha}$ R, CRF $_{2\beta}$ R, and CRF $_{2\gamma}$ R being the physiological relevant membrane receptors in mammalians [20]. There are also soluble receptors as for example the corticotropin-releasing factor-

binding protein (CRF-BP) [21], which is suggested to play a modulatory role in the CRF system, and also a splice variant of the CRF_2R rendering the receptors soluble, the soluble corticotropin-releasing factor 2α ($sCRF_{2\alpha}R$) [22], whose exact role has yet to be determined in the CRF system.

1.2.1 Ligand and Ligand Binding

The ligands for GPCRs can be divided in different groups according to their influence on the activation of the receptors. Agonist fully activate the receptors, partial agonists only induce sub-maximal activation even at saturating concentrations, antagonist have no effect on basal ligand-independent activity, inverse agonists are able to decrease basal activity [23].

The endogenous agonists of the CRF receptors, the corticotropin-releasing factor (CRF) and its analogues, the urocortins I-III (Ucn I-III), are widely found throughout the human body. While CRF has a high affinity to the CRF_1R and thus being called the endogenous ligand for CRF_1R, Ucn II and III are called the endogenous ligands for CRF_2R due to their higher affinity for CRF_2R (figure 1.4 and table 1.1).

Figure 1.4: Sequences of the ligands CRF, Ucn I, Ucn II, Ucn III and antagonist astressin. All peptides are amidated at the C-terminus. X stands for D-Phe, B for NIe. The italic residues in the astressin sequence participate in a lactam bridge.

```
r/hCRF      SEEPPISLDLTFHLLREVLEMARAEQLAQQAHSNRKLMEEII..   42
rUcn        .DDPPLSIDLTFHLLRTLLELARTQSQRERAEQNRIIFDSV...   40
hUcn        .DNPSLSIDLTFHLLRTLLELARTQSQRERAEQNRIIFDSV...   40
hUcnII      ...IVLSLDVPIGLLQILLEQARARAAREQATTNARILARVGHC   41
hUcnIII     ...FTLSLDVPTNIMNLLFNIAKAKNLRAQAAANAHLMAQI...   38
Astressin   ...........XHLLREVLEBARAEQLAQEAHKNRKLB.EII..   30
```

X non conserved
X similar
X ≥50% conserved
X ≥80% conserved

An agonist in the *secretin* family can be converted into an antagonist by deleting ca. the first 10 amino acid residues of the N-terminus of an endogenous ligand [24]. This

implies that the N-terminusis responsible for inducing structural changes to its corresponding receptor and thus activating the receptor for signalling. The ligand alone has already a low α-helical propensity and therefore no well defined structure in an aqueous environment. However, the binding of the ligand to its receptor induces an α-helical structure [18]. The truncation of the N-terminus decreases the α-helical propensity of the ligand. Therefore many antagonists, whose N-terminus has been truncated, have a lactam bridge to stabilise the α-helical content and induce an α-helical structure even in the absence of a receptor. This is the case, for example, for the antagonist astressin, which has been created by deleting the N-terminus of the CRF ligand and introducing a lactam bridge between the residues Glu30 and Lys33 (table 1.4).

If the C-terminus of the ligand of the *secretin* family is truncated, the ligands show a decreased affinity to the receptors. This indicates that the C-terminus is responsible for the affinity of the ligand to its corresponding receptor [25]. The C-termini of all endogenous ligands of the *secretin* family are amidated. If the C-terminus has no amid group, the ligand loses affinity to the receptors as is shown in a study with the antagonist astressin [26]. The deamidation of astressin decreased the affinity of astressin to the receptors about 100 times. The two amide protons of the amideted C-terminus are found to be important by Grace et al. in the NMR-derived structure of $CRF_{2\beta}R$ [27] since they hydrogen bond intramolecular with the carbonyl group of Glu39 and intermolecular with the hydroxyl group of Tyr115 of the first extracellular domain (ECD). In the deamidated astressin, the intramolecular hydrogen bond to Glu39 is disrupted. An irregular helical conformation from Arg35 on is the result, which rearranges the side chains of the amino acid residues Leu37, Nle38 and Ile41 of astressin differently, which are involved in the regular receptor binding [26]. However, the equivalent Tyr115 in the ECD of the CRF_1R-structure derived from crystallisation is found to form a hydrogen bond to the equivalent Asp65 and Thr69 and thus an interaction between Tyr115 to Glu39 would disrupt the first mentioned hydrogen bond [28]. Additionally, the C-terminal amide nitrogen of the ligand binds via in-

tramolecular hydrogen bond to Met38 and not to Glu39, as found by Grace et al. Considering that the set of natural ligands for the *secretin* family is remarkably homogenous and that the ECDs of the *secretin* family have a conserved fold despite of their low homology, a common activation mechanism for the *secretin* family has been proposed. This mechanism is a 'two domain model', where in the first step the ECD captures the C-terminus of the ligand [20]. The captured ligand moves its N-terminus near the TM domain of the receptor. This facilitates an interaction between the receptor and the N-terminus of the ligand and the receptor is activated [20].

Ligand	$CRF_{1\alpha}R$ [nM]	$CRF_{2\beta}R$ [nM]	ECD-$CRF_{1\alpha}$ [nM]	ECD-$CRF_{2\beta}R$ [nM]
r/hCRF	1.0	6.2	NSD	97
hUcn I	0.4	0.5	150	6.5
hUcn II	> 100	0.5	NSD	73
hUcn III	> 100	14	NSD	> 300
Astressin	2.0	0.62	27	10.7

Table 1.1: Inhibitory binding constant K_i for the CRF receptors for different ligands. NSD: no significant displacement of the ligand using ^{125}I-sauvagine as radioligand [29] .

1.2.2 Stuctural overview of CRF receptors

The GPCR *secretin* family has the well known 7 transmembrane domains, which are organised in an anti-clockwise fashion, when looking from the extracellular domain down on the membrane protein [30]. Common for the *secretin* family is its long N-terminal extracellular domain (ECD), which consist of about 120 amino acids having six conserved cysteine residues (Cys, C) involved in three disulphide bridges. Additionally two conserved Cys residues are present in the ECL1 and ECL2 forming another disulphide bond [12]. The sequence identity between CRF_1R and CRF_2R is approximately 70 % with the N-terminus having the highest divergence and the TM regions the least [20].

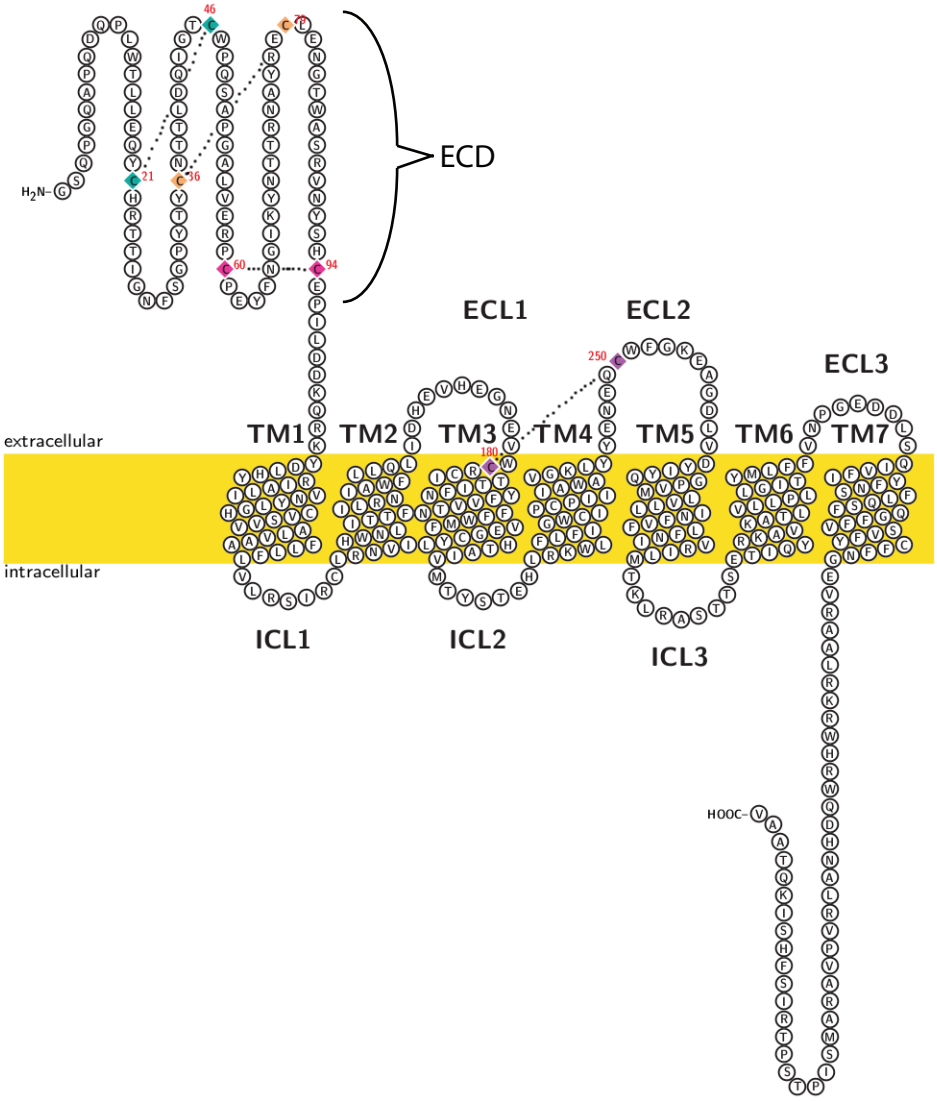

Figure 1.5: An example for a *secretin* family member, the mus musculus $CRF_{2\beta}R$. The coloured cysteine pairs participate in disulphide bridges. The first extracellular domain (ECD) is indicated.

Extracellular Domain of CRF Receptor 2β

The main binding site for the ligands of the *secretin* family is on the ECD as shown by site-directed mutagenesis and cross-linking experiments of the *secretin* family [12, 31–33].

Due to their importance, various ECDs of the *secretin* family receptors have been crystallised without [28, 34] or with ligand [28, 35–37] or studied by NMR without [38] or with ligand [26, 39, 40]. All the structures show a conserved fold, despite their low homology [24].

The ECDs of the *secretin* family have 2 central antiparallel β-sheets stabilised by 3 disulphide bridges with the pattern 1-3, 2-5, 4-6; this fold is known as short consensus repeat (SCR) or sushi domain. For mus musculus $CRF_{2\beta}R$, the 2 antiparallel β-sheets include the regions 63-64 (β1), 70-71 (β2), 79-82 (β3), and 99-102 (β4), which are stabilised by the three disulphide-bridges Cys45-Cys70, Cys60-Cys103, Cys84-Cys118. The central core of the fold consists of a possible salt bridge between Asp65-Arg101 sandwiched by the aromatic rings of Trp71 and Trp109 [38]. If the Asp65 is mutated to an alanine or if Asp65 is mutated to an argenine, while Arg101 is mutated to an aspartic acid, the canonical disulphide arrangement is lost. Mutating only Arg101 to alanine retains the disulphide bond arrangements and induces only a small effect on ligand binding. Mutating Arg101 to alanine disrupts solely the salt bridge, which does not however interfere with the local geometry and disulphide formation [41].

Asp65 hydrogen bonds with Trp71 and stabilises the ligand-binding loop. This hydrogen bond appears to be important for the local arrangement of the β1-sheet and is responsible for the correct formation of adjacent loops as well as the residues Glu66 and Glu67, which are involved in ligand binding (figure 1.6) [41].

Two disordered loops are found on the ECD, loop 1 consists of the residues 48-58, which is very flexible and has a high sequence variability in the CRF receptor family. Loop 2 consists of the residues 84-98, which has a slow conformational exchange. Loop 2 is highly conserved in the CRF receptor family and its slow dynamics are suppressed upon antagonist binding. For Pro83 and Pro85, each having two equal intensities indicating a cis/trans isomerisation. Upon ligand binding, the prolines are pushed into the trans conformation. Additionally, the regions 65-69, 84-95 of loop 2, and 111-115 undergo conformational changes upon ligand binding [29].

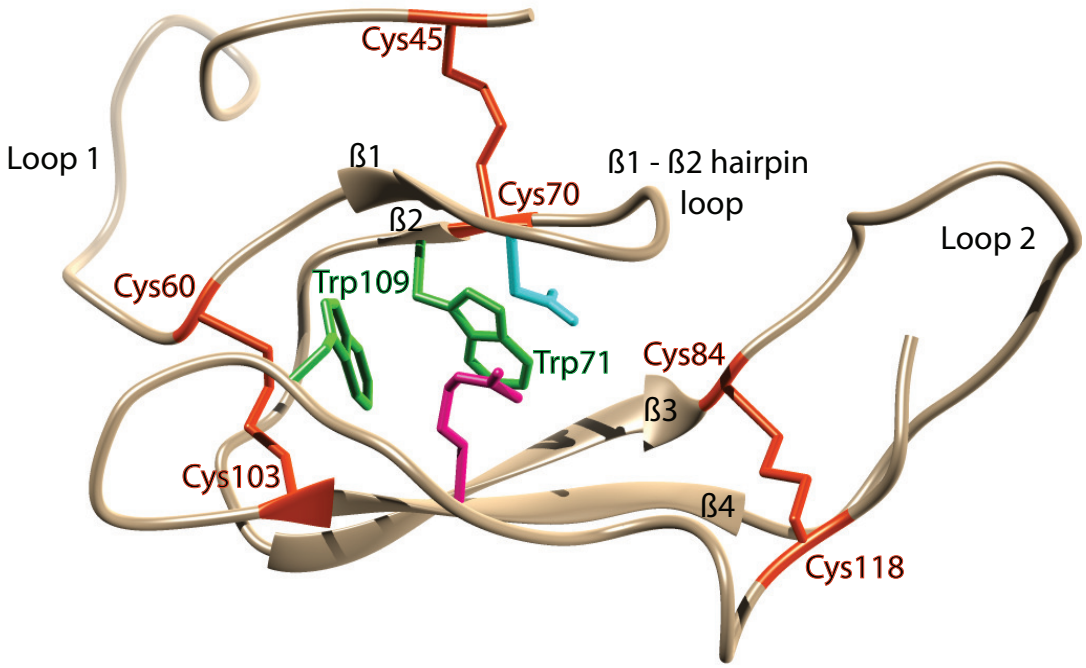

Figure 1.6: Extracellular domain of $CRF_{2\beta}R$ showing visibly the short consensus repeat. Pink is Arg101 and cyan Asp65, which might participate in a salt bridge, green is Trp71 and Trp109, orange are the cysteines participating in disulphide bridges Cys45-Cys70, Cys60-Cys103, Cys84-Cys118.

The antagonist astressin binds to the ECD via its hydrophobic face of its helix. The C- and N-terminus of astressin are amphipathic, its hydrophobic residues are on the concave and the hydrophilic residues on the convex face of the helix [26].The most crucial hydrophobic interactions are for astressin: Leu37, Nle38, Ile40, Ile41, and for the ECD: Glu66, Ile67, Cys84, Phe88, Val113, Tyr115, and Cys118. The amino acid residues Leu27 and Ala31 of astressin interacts with Ile91 of the ECD and Asn34 of astressin to Phe88 of the ECD. There is a hydrogen bond between Ile42 of astressin to Val113 of the ECD and a hydrophobic interaction of Ile41 of astressin to Tyr115 and Val113 of the ECD [26]. The C-terminus of astressin binds between the 2 β-sheets of the ECD [42].

Tramsmembrane domain of CRF Receptor

A crystal structure of a human CRF_1R has been published in 2013 [43] with the ECD truncated and lacking the C-terminus including helix 8, and having an insertion of T4 lysozyme into ICL2. Additionally the receptor has been thermostabilised according to Serrano-Vega et al [44]. With all these modifications the structure is pushed into an inactive conformation, which however facilitates an easier purification and crystallisation.

The structure of the receptor shows a pronounced V-shape having a large cavity on the extracellular site. This large cavity is presumed to be the peptide-binding site. The ECL1 has a short α-helix parallel to the membrane and the ECL2 is anchored to the TM3 via a disulphide bond. The TM7 is kinked and its extracellular end is shifted away from the axis of the helical bundle by ca. 10 Å. The TM7 is rotated by 25° compared to the dopamine D_3 receptor, a member of the *rhodopsin* family [42]. It is not clear whether this rotation is induced by the truncation of helix 8 or if this rotation is also found in the native structure. TM1 is slightly bend and its EC end packed against TM7 and thus TM1 is also shifted similarly away from the axis as TM7. The kink in TM7 is stabilised by hydrogen bonds between the highly conserved $Ser^{1.50}$ to $Phe^{7.51}$ and $Ser^{7.47}$. TM6 is shifted away from TM5 and outwards from the axis. Its cytoplasmic end points to TM3. The residues $His^{2.5}$ and $Glu^{3.5}$, which have been shown to be involved in activation of the receptors with biochemical methods [45–47], are in hydrogen bond distance in the crystal structure. On the TM4, a highly conserved GWGxP motif is present in the *secretin* family. This motif reveals a network of interaction. The $Trp^{4.50}$ protrudes to TM2 and TM3 caused by the unwinding nature of $Gly^{4.49}$. The hydrogens of the side chain of $Trp^{4.50}$ bond to $Asn^{2.52}$ and facilitate an edge-to-face interaction with $Trp^{3.46}$. The TM4 is bound to TM3 by a hydrogen bond from the side chain of $Tyr^{3.38}$ to the carbonyl of $Trp^{4.50}$ and by hydrophobic interactions of $Gly^{4.49}$ to $Trp^{3.46}$ as well as $Pro^{4.53}$ to $Tyr^{3.38}$. It is not immediately clear from the crystal structure if this highly conserved motif is involved in the function of the receptor.

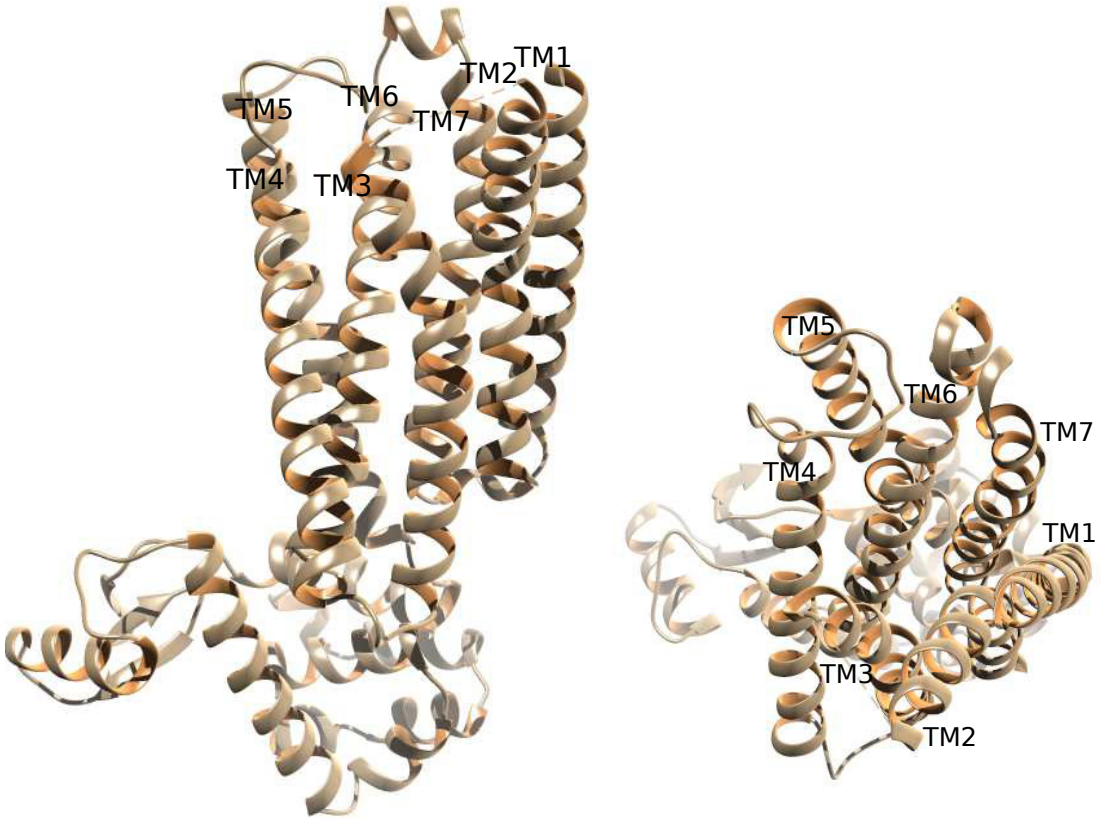

Figure 1.7: Crystal structure of CRF_1R stabilised with an insertion of T4 lysozyme instead of ICL2 (PDB 4K5Y).

To stabilise the receptor further, an allosteric antagonist binding to the TM region was added during the purification. The antagonist is highly selective for CRF_1R but not for CRF_2R. A high sequence identity is found in the binding cavity of the allosteric antagonist comparing the homology of CRF_1R to CRF_2R. Especially the residues interacting with the ligand are conserved. Only in the second shell within 5 Å of the binding cavity, two residues differ, $His^{3.40}$ and $Met^{5.43}$ in CRF_1R correspond to $Val^{3.40}$ and $Ile^{5.43}$ in CRF_2R. Mutating the residues of CRF_2R to CRF_1R, the affinity of the antagonist for CRF_1R is reduced to that of CRF_2R [48].

Another crystal structure of the *secretin* family, the human glucagon receptor (GCGR), has been published the same year [49]. The receptor is also thermally stabilised [44], the ECD and the C-terminus after helix 8 are truncated. Helix 8 is in the crystal struc-

ture 25° tilted from the membrane axis. Whether this tilt is induced by the crystallisation or is also found in native structures of the *secretin* family, is not sure, as helix 8 is missing in the crystal structure of CRF_1R. But there are hydrogen bondings between Glu406 in helix 8 with $Arg^{2.46}$ and $Arg^{6.37}$ in the crystal structure of GCGR, which are conserved among the *secretin* family. Another common motif in the *secretin* family is $FQG^{7.50}xxVxxxY^{7.57}CF$. The $Gly^{7.50}$ induces a bend in the TM helix 7 and is stabilised by a hydrophobic interaction with $Phe^{2.57}$.

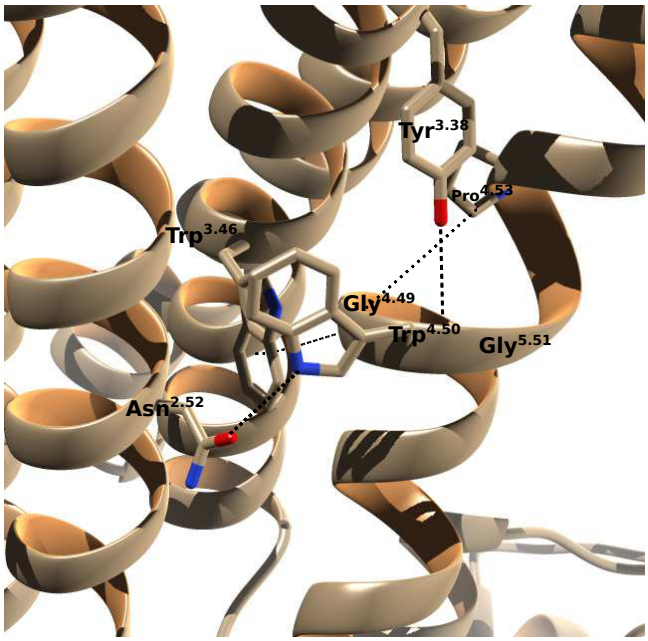

Figure 1.8: The GWGxP motif with their connections drawn as dotted lines.

GCGR and CRF_1R have overall 30 % sequence identity. Both crystal structures have a pronounced V-shape, one arm consists of TM2-TM5, the other of TM1, TM6, and TM7. With this shape, a solvent filled cavity is produced, which is accessible from the extracellular side. When both structures are superimposed, the best agreement is given for TM1-TM5, with TM4 overlaying imperfectly. Both structures have a common set of motifs, as for example the before mentioned GWGxP motif, giving a network to link the TM domain 2, TM domain 3 and TM domain 4, the $Ser^{1.50}$-$Ser^{4.74}$/$Gly^{7.50}$/Phe/$Leu^{7.51}$ motif, which stabilises the kink in the TM7. The extracellular halves of

TM 6 and TM 7 and the ECL 3 point away from the centre in both structures. On the intracellular side, $His^{2.50}$ and $Glu^{3.50}$ are conserved.
In the GCGR, $Tyr^{7.57}$-$Tyr^{6.42}$ hydrogen bond to $Glu^{3.50}$ and in the *rhodopsin* family this hydrogen bond is linked to activation and interaction to a G-protein. In the CRF_1R structure, the $Tyr^{7.57}$ is mutated to an alanine and shifted into the inactive state giving a different conformational state. Whether this different conformation is induced by the mutation or due to the absence of helix 8, is not clear. $Arg^{2.46}$ has a comparable position in both structures, but in GCGR it makes a salt bridge to Glu406 in helix 8 and $Arg^{6.37}$ [42].
The ligands for CRF receptors have a longer N-terminus than other ligands in the *secretin* family. The solvent exposed cavity is wider in the crystal structure of CRF_1R than of GCGR, which might accommodate the longer N-terminus of its ligands [42].

Comparison between *Rhodopsin* and *Secretin* Family

Despite the vast range of ligands including hormones, neurotransmitters and light, the conformational changes induced upon activation, due to ligand binding, are highly conserved in the GPCR *rhodopsin* family [23], like the (D/E)RY motive in TM3 (known as ionic lock), WxP in TM6, and NPxxY in TM7 [50]. The family B does not have the DR(Y) motif nor the ionic lock.
Nevertheless, common motifs are found between the *rhodopsin* and *secretin* family, as for example the disulphide bond between ECL 2 and $Cys^{3.29}$, and similar regions of contacts between helices TM1-TM2, TM1-TM7, TM3-TM6, and TM3-TM4 (figure 1.2) [49]. Due to the similar pattern of interactions between the helices, the orientations and positions of the TM helices are conserved. However, the distances between TM2-TM7 and TM3-TM7 in the *secretin* family are the largest observed in the GPCR family. Their orthosteric pocket is wider and deeper than for any member of the *rhodopsin* family [42].

Nevertheless superimposing CRF_1R with human dopamine D3 receptor from the *rho-*

Interaction	*secretin* [Wollenstein]	*rhodopsin* [Ballesteros & Weinstein]
TM1-TM2	$Leu^{1.54}$-$Phe^{2.57}$ (hydrophobic)	$Asn^{1.50}$-$Asp^{2.50}$ (polar)
TM1-TM7	$Ser^{1.50}$-$Ser^{7.47}$ (hydrogen bond)	-
TM3-TM4	$Trp^{4.50}$-$Trp^{3.46}$	$Trp^{4.50}$-$Trp^{3.38}$
TM3-TM6	$Tyr/Phe^{3.44}$-$Leu/Phe^{6.49}$ (hydrophobic)	$Ile/Val/Leu^{3.40}$-$Phe^{6.44}$
	$Tur^{3.44}$-$Gly^{6.50}$ (close contact)	
TM3-TM5	$Asn^{5.50}$-$Leu^{3.47}$ (hydrogen bond)	-

Table 1.2: Common contacts in *secretin* and *rhodopsin* family between helices TM1-TM2, TM1-TM7, TM3-TM6, and TM3-TM4, but with family specific interaction pattern [49].

dopsin class shows a resemblance in the cytoplasmic region, especially at the cytoplasmic halves of TM 3 and TM 5. This similar conformation might be responsible for binding to the G_α protein [43].

1.2.3 Soluble $CRF_{2\alpha}$ receptor

This 143 amino acid residues long, soluble variant of the $CRF_{2\alpha}$ receptor ($sCRF_{2\alpha}R$) is produced by a deletion of an exon shortly after the ECD, followed by a frame shift resulting in a 38 amino acid residues long hydrophilic C-terminus. The $sCRF_{2\alpha}R$ has been found in the olfactory bulb, the cerebral cortex, and the midbrain region in mice using a reverse transcription polymerase chain reaction. A synthetic peptide fragment specifically binding to the unique C-terminus of the $sCRF_{2\alpha}R$ shows a close distribution of $sCRF_{2\alpha}R$ and CRF_1R in mice brains. The $sCRF_{2\alpha}R$ has a higher affinity for CRF and Ucn 1 suggesting a modulatory role for the ligands in the CRF family [22].
However, the role of $sCRF_{2\alpha}R$ is not conclusive yet. Evans et al showed [51] that $sCRF_{2\alpha}R$ is translated but not trafficked for secretion and degraded proteosomically, which is in disagreement with the study of Chen et al [22]. Evans et al also showed that the first 16 amino acid residues of the $sCRF_{2\alpha}R$ have a high propensity to encode a signal peptide. However, they do not secret the soluble receptor. The same sequence of amino acid residues is found in the $CRF_{2\alpha}R$. There, it is not the signal peptide secreting $CRF_{2\alpha}R$ but the TM helix 1, which is used as anchor-signal peptide. Therefore,

the 16 amino acid residues long sequence is called a pseudo-signal peptide. Nevertheless the pseudo signal peptide can be converted to a signal peptide by mutating Asn13 to an hydrophobic or positive charged amino acid residue and thus the signal propensity of the signal peptide can be restored.

1.2.4 In Medicinal Chemistry

The expression levels of the ligands, CRF and urocrotins I-III (Ucn I-III) and of the corticotropin-releasing factor receptors (CRF Rs) vary in different body parts like the brain, skin, skeletal muscle, immune system, heart, genitourinary system, and gastrointestinal system. While CRF is mainly responsible for the activation of the hypothalamic pituitary adrenal axis (HPA) activated under stress conditions, the Ucns play an important role in the peripheral stress responses [52].
Whereas CRF_1R is found throughout the human brain, such as for example in the olfactory bulb, the cortex, the septum, the hippocampus, the amygdala, and the cerebellum, CRF_2R is found in stress-related areas in the human brain as, for example, in the bed nucleus of the stria terminalis (bond of fibrils between amygdala to septal nuclei, hypothalamic and thalamic areas; correlates with anxiety in response to threat monitoring), the medial amygdala (almond shaped nuclei located within medial temporal lobes, part of the limbic system; formation and storage of memories associated with emotional events as fear stimulations) and the hypothalamus and is additionally distributed in peripheral tissue as skin, skeletal and smooth and cardiac muscles [20, 53].
CRF_1R initiates endocrine stress responses and mediates anxiety related behaviour upon activation via stressors [54]. CRF_2R knock out mice are hypersensitive to stress and have significant elevation in anxiogenic-like and depression-like behaviour [55]. It is hypothesized that CRF_1R and CRF_2R have complementary roles in controlling the HPA-axis [56], as CRF_1R agonists induce catecholamine secretion in dose-dependent manner in rat and human adrenal neuroendocrine cells, while activating CRF_2R sup-

presses those secretions. The effects can be blocked via the addition of the corresponding antagonists [57]. Nevertheless the role of CRF_2R in stress adaptation is still discussed controversially. However, $CRF_{2\beta}R$ has many regional specific effects, as discussed below.

- CRF_2R deficient mice have a reduced intestinal inflammation and a reduced mRNA expression of potent chemoattractants (agents that induce a leucocyte to migrate towards something). Thus CRF_2R mediates intestinal inflammatory responses via release of pro-inflammatory mediators [58].
- Examination of skeletal muscle of mice showed that in myoblasts solely CRF_1R is expressed, while in myotubes solely CRF_2R is expressed. The different expression levels are already seen during myogenic differentiation. The transcription of CRF_2R in myotubes is promoted by physiological stress, such as high fat diet and psychological stress. Interestingly, only after physiological stress, $CRF_{2\beta}R$ and leptin (being responsible for the satiety feeling) are increased, while after psychological stress only $CRF_{2\beta}R$ levels are increased and leptin levels are decreased in the ventromedial hypothalamus [59].
- In contrast, in the cardiac myocytes, mRNA of $CRF_{2\beta}R$ is decreased under stress and after injection of lipopolysaccharide. For $CRF_{2\beta}R$ itself, a cardioprotective role is associated. Activating $CRF_{2\beta}R$ via the Ucn system by exogenously administrated Ucn I can increase the cardiac contractility, increase the coronary blood flow, conductance, cardiac out put and heart rate. Ucn I- III have a protective effect against ischemic and reperfusion injuries [60].
- CRF_2R deficient mice are hypervascularized postnatally. CRF_2R activation reduces vascular endothelial growth factor release from smooth muscle cells, inhibiting smooth muscle cell proliferation, and capillary tube formation in collagen gel in-vitro. Thus via CRF_2R a tonic inhibition of adult neovasculerisation is induced. It might be a potential target for the modulation of angiogenesis in cancer cells [61].
- The CRF system modulates the feeding in mice [62]. While infusion of CRF_1R agonists, Ucn I and $astressin_1$ A increased the anorexic effect and induced interocep-

tive stress, such as conditioned taste aversion and diarrhoea/defecation, the infusion of Ucn II suppressed feeding via CRF_2R-dependent mechanism without inducing malaise.

- Addiction might be regulated by the CRF receptor system especially in the central nucleus of amygdala, which encodes the stimulus-reward association [63]. It is widely accepted that stress situations induce a relapse, seeking addicting substances. CRF induces long term potentiation of glutamatergic transmission in vitro in the lateral- to central-amygdala pathway in a dose dependent manner [63]. Wang et al [64] could show that stress triggered glutamate/dopamine release and cocaine seeking in drug experienced rats could be blocked by CRF_2R, but not CRF_1R selective antagonists.

- CRF is expressed more in females than in males in the paraventricular nucleus of the hypothalamus (PVN), amygdala, and the bed nucleus of the stria terminalis. Interestingly, Weathington et al. [56] showed in rats that the expression of CRF_1R and CRF_2R changes in a sex and age specific pattern. They measured the receptor binding in the amygdala in prepuberty and adult rats and showed, that the binding increases far more for the CRF_2R in males than in female and CRF_1R increased far more for female than male rats across the puberty (see fig 6.1).

across puberty	CRF_1R		CRF_2R	
	male	female	male	female
Basolateral amygdala	$\Downarrow$	$\Uparrow$	$\Uparrow$	$\downarrow$
Posteroventral medial amygdala	$\Downarrow$	$\Uparrow$	$\Uparrow$	-
Posterodosal medial amygdala	-	-	$\Uparrow$	$\uparrow$
central amygdala	-	-	$\Uparrow$	$\uparrow$

Table 1.3: The changes of age and sex specific binding pattern measured across of prepuberty and adult rats.

1.3 NMR Structure of Membrane Proteins

Membrane proteins are often expressed weakly in cells [65]. Depending on the biochemical method used for analysis, the final yield might be too low for measurements, as it is often the case for nuclear magnetic resonance (NMR) spectroscopy measurements, which demand mg-quantities. Therefore over-expression is a common step to increase the very low yield. Heterologous expression has been accomplished in many different host cells such as prokaryotes (*E. coli*), yeast (*P. pastors*, *Saccharomyces cerevisae*), insect cells (*Drosphila*, *Lepidoptera*), *Bacchulo virus* infecting insect cells, and mammalian cells (CHO, HEK, etc) [65]. After the expression, the membrane proteins are solubilised with detergents either from folded receptors in the membrane of the host cell or from refolding of initially inactive forms from inclusion bodies [66]. Purifications of active GPCRs from inclusion bodies has been very difficult and thus most purification protocols start with the folded receptor in the membrane using detergents [67]. Often, the protein has a specific tag to enable its purification using the corresponding affinity columns or a specific ligand affinity column is generated [67]. It is important to assess the activity of the membrane protein via biochemical assays to ensure its correct fold and native characteristics. Possible biochemical methods are for example radio active binding assays, where a ligand is radioactive labeled and added to the receptor. Excess of ligand is washed of, and the bound fraction of the ligand is measured via its radioactivity counting [68].

1.3.1 Importance of Detergents

Detergents are amphipathic molecules with a polar head group and a hydrophobic tail. They spontaneously form micelles in an aqueous solution, when a certain threshold of a concentration is exceeded, the critical micelle concentration (cmc). Detergents can be divided into ionic, having a positive or negative charge on the head group, non-ionic, having a non-charged head group, and zwitterionic detergents, hav-

ing chemical groups with a positive and a negative charge [69]. There are also bile acid salts, which are ionic detergents, but have a rigid steroidal group resulting in a polar and apolar face. The longer the alkyl chain of a detergent the lower the cmc; and the more double bonds and branch points, the higher the cmc [70].
Generally, zwitterionic detergents tend to deactivate membrane proteins more than non-ionic detergents [71]. However not only the potency to solubilise the protein is important, also protein stability is an important factor, as the presence of detergents might disturb membrane protein structures and ligand binding, as it is the case for GPCRs [69].
Extraction and purification of GPCRs is still cumbersome because no general purification protocol exists. No buffer conditions can be transferred from one to another membrane protein system and the solubilisation is influenced by various parameters such as buffer composition, initial protein concentration, detergent concentration, temperature, pH, salt concentration etc. [69]. An additional complication is that membrane proteins such as GPCRs tend to aggregate even in the presence of detergents [71]. Additionally, the detergent used for purification should be compatible with the methods chosen for structural studies. Thus either the detergent used for extraction is already compatible with the structural studies or the detergent has to be exchanged during the purification.

Another system recently introduced are nanodiscs, a very promising tool to stabilise GPCRs and membrane proteins in a lipid mimetic membrane [72–74]. A nanodisc is a self-assembled phospholipid bilayer encapsulated by two copies of a membrane scaffold protein (MSP) derived from apolipoprotein A-1 scaffold protein [75]. The scaffold protein has been modified in length by varying the number of helices resulting in different diameters of the nanodisc [76]. The incorporation of membrane proteins into nanodiscs is not an easy tasks, as the exact lipid:protein ratio has to be found and a purification protocol needs to be established, where empty nanodiscs can be separated from membrane protein containing nanodiscs. So only few GPCR have been incorporated into nanodiscs so far, as for example the β2-adrenergic receptor, which

has been shown to still be able to bind its agonist after being incorporated into nanodiscs [77]. The parathyroid hormone 1 receptor of the *secretin* family incorporated into nanodiscs was used to show that a receptor in nanodiscs is still able to activate the G-protein [78]. Nanodiscs can also inhabit one or two receptors depending on the ratio of lipid:protein as was shown with the rhodopsin receptor [79].

1.3.2 Isotope Labelling

To facilitate structural studies of membrane proteins, they are commonly labelled with NMR-active nuclei such as ^{13}C or/and ^{15}N or/and ^{2}H. As mentioned, different expression systems are available, but not all are able to produce labelled proteins in high amounts. *E.coli* is usually preferred due to its inexpensiveness, ease of culturing, and flexibility for isotope labelling strategies; its drawbacks are the absence of post-translational modification and the lack of some eukaryotic membrane components such as cholesterol. Another popular expression system is yeast, whose advantages are as well the inexpensiveness, ease of culturing, but additionally having the advantage of eukaryotic post-translational modifications; the disadvantage is that its endogenous GPCRs might interfere with the expression and purification [80]; yeast has quite thick cell walls, which might be hard to destroy, and labelling strategies are more limited than for *E.coli* [80]. *Baculovirus* infected insect cells have more similar post-translational modification to mammalian cells, thus most of the GPCRs are expressed active [80]; insect cells have a disadvantage requiring a high amount of virus titre, the culture is only stable up to 1 month, and its limited labelling strategies [80]. Mammalian cells have the advantages of its native cellular environment for GPCRs, their correct trafficking and folding and post-translational modification, therefore most GPCR are expressed in an active conformation [80]; disadvantages are they are costly, difficult to scale, and their few labelling strategies [80].
Another recently developed strategy for protein expression is the so-called cell-free expression. As the name indicates, no cells are used in this expression system and

therefore only the desired protein is expressed. Thus, even highly toxic protein can be produced. Additionally, it is possible to completely control the labelling. Drawbacks are a poor scalability, their relatively high expenses and low success rate for GPCRs to date and limitations in detergents due to interferences with the protein-production-machinery [80] .

1.3.3 GPCRs studied by NMR

For NMR measurements, quite large amounts of protein are needed (about 0.1 mg to 5 mg of protein in 100 µL to 300 µL). Therefore an expression system is chosen where high amount of protein and an ease for labelling is assured [80]. Due to the low success rate for GPCR in cell free expression, *E.coli* is very often a preferred labelling system [81, 82].

GPCRs are quite large, especially when they are in a detergent buffer, creating a protein-micelle complex. Due to their increased tumbling times, which is proportional to the molecular radius and viscosity and temperature, line broadening is inevitable. This can be overcome by a transverse relaxation optimised spectroscopy (TROSY)-sequence [83]. This sequence can be used for proteins even exceeding molecular sizes of 100 kDa [83]. Additionally, perdeuteration can enhance the resolutions of a spectrum of large membrane proteins reducing transverse relaxation rates by decreasing the dipole-dipole relaxation [84]. Conformational-based line broadening might occur as well due to their inherent flexibility and looser structure in a micelle [84].
The poor chemical shift dispersion of GPCRs renders a structure assignment more difficult due to the high α-helical content in membrane proteins. Therefore selective labelling is a wide spread method to decrease the amount of peaks and spectral crowding, as was for example applied for a chemokine receptor [85]. Selective labelling was also used for the β adrenergic receptor, however not for structural assignment but for dynamical analysis of the receptor via NMR spectroscopy [86].
Sensory rhodopsin II was measured and its structure determined by liquid NMR spec-

troscopy [87]. Even though the receptor is composed of 7TM helices, it does not belong to the GPCR family as it does not bind to a G-protein but acts as a photoreceptor converting light into a proton gradient avoiding blue light and thus escaping conditions of oxidative stress [88].

Solid state NMR seems to be the preferable technique to measure GPCRs due to its feasibility to measure samples even with slow tumbling rates. In 2012, a three-dimensional structure has been reported by Park et al. of a chemokine receptor by solid-state NMR. Not only a fully ^{13}C-, ^{15}N-labelled receptor was expressed, but also a selectively ^{13}C-, ^{15}N-Phe labelled receptor to facilitate assignment [85]. The human cannabinoid type 2 receptor NMR spectrum was predicted by computational analysis and then measured by solid state NMR spectroscopy [89].

Another approach to study GPCR by NMR is to fragment GPCRs thus cutting down the size of a GPCR instead of expressing and measuring a whole GPCR. As was already mentioned, structural analysis by NMR spectroscopy was done for the N-terminal domain of *secretin* family members [38]. There is also a structural study performed by NMR spectroscopy on the helix 8 of a human β2 adrenergic receptor showing that helix 8 is random coiled in a water solution and only forms a α helix if α-helical inducing agents are added as for example detergents or DMSO [90]. A fragment consisting of the TM helix 7 and the helix 8 was studied by NMR as well [91], showing that there are distinct interactions between the fragment and membrane protein lipid molecules, indicating that the fragment itself might alter the membrane structure and dynamic. The ICL 3 is also a fragment highly investigated because of its importance of binding to G proteins [92, 93]. Even though this approach sheds light into the structure of those fragments, the fragment might behave differently in the presence of the full receptor.

One important tool of NMR spectroscopy is to study dynamics. A ^{13}C-methionine labelled β2-adrenergic receptor was expressed and measured with liquid NMR. The receptor was studied under different conditions, such as without ligand, with inverse agonist, agonist, and a G-protein mimicking nano body showing different conforma-

tional states for each additive. This suggest a conformational heterogeneity, which is not reported in crystal structures [86]. Another study was performed to elucidate the activation of rhodopsin receptor by light induction with solid state NMR. The influence of the ligand rhodopsin isomerisation on the rhodopsin receptor was investigated and how specific residues shifted upon isomerisation [94].

1.4 Nogo-A-Δ20

1.4.1 Physiological Role

The Nogo membrane protein belongs to the reticulon protein family because of its C-terminal 200 amino acid residues long sequence, which is jointly responsible for the membrane curvature [95]. Nogo has three isoforms: A, B and C [96]. Nogo-A is found in the endoplasmatic reticulum and on the cell surface of myelin sheaths. It hinders regeneration of neuronal tissues after a central nerve system injury as a growth inhibitory molecule [97]. The dissected neuronal axons are inhibited to regrow and reconnect. Blocking Nogo-A enhances regeneration of axonal extension in vivo [97, 98]. The exact physiological role of Nogo-A has not been studied extensively yet. One hypothesis proposes that Nogo-A might prevent abnormal sprouting of axons and regulate dynamics of the synapsis during learning processes [98].
Nogo-A is the largest protein in the family with 1192 amino acid residues [95]. It has two major binding sites, one is the extracellular 66 amino acid residuers long loop at the C-terminal region called Nogo-66 and a segment in the middle of the Nogo-A protein called Nogo-A-Δ20. It is not uncommon for a protein to have two active sites within a sequence as for example the proteins neurotrophic factors or netrin are also known for having two binding sites [99].
Nogo-66 binds to the Nogo receptor 1 and its complexation blocks neurite extension. Nogo-A-Δ20 binds to the GPCR sphingosine 1-phosphate receptor 2 (S1PR2) [100] and neurite growth inhibition has been found for Nogo-A-Δ20 just as for Nogo-66.

The two active sites may contribute to acute and chronic impairment of axonal plasticity [101].
S1PR2 might bind via its ECLs to the structurally disordered segment Nogo-A-Δ20. The residues participating in the interaction between Nogo-A-Δ20 and S1PR2 and whether the structurally disordered Nogo-A-Δ20 establishes a well-ordered structure upon binding are unknown yet.

1.4.2 Intrinsically Disordered Protein and NMR spectroscopy

Intrinsically or natively disordered proteins (IDPs) are either entire proteins or regions in proteins, which do not adopt a well-defined three dimensional structure. In contrast, there are numerous folded proteins or enzymes, which need to have precisely positioned functional groups for stabilisation or to carry out their functions. Nevertheless, IDPs are important in cellular functions and altered expression might result in many diseases such as cancer or Alzheimer [102]. The advantages of lacking a well-defined structure might provide a larger interaction surface than in folded proteins. Also having a higher conformational flexibility might give IDPs the chance to sample vast and heterogeneous conformations enabling to bind several binding partners at the same time. Short linear peptide motifs could facilitate interactions with many different proteins [103].
Upon ligand binding, many IDPs tend to fold as for example the already discussed CRF ligand [26]. Due to the folding, they often interact with relatively high specificity and low affinity [103]. Therefore, signalling proteins are often enriched with intrinsically disordered regions, as was proposed for the IC loops of the GPCRs [104].
X-ray crystallography is one of the most utilised tools in structural biology but not useful for examining the dynamical changes in IDPs. NMR spectroscopy on the other hand, is a powerful tool to investigate structural and dynamical features in proteins and especially in the flexible IDPs [105]. But it is important to keep the environmental parameters constant as IDPs are highly pH and temperature sensitive [106].

1.5 Motivation for Dissertation

Most of the crystallised GPCR are heavily engineered. They are, for example, thermally stabilised or a T4 lysozyme is included in the receptors or bind specific camelid antibody fragments (nanobodies). It is also common to use high affinity and very low-off-rate synthetic antagonists and to cleave off the C- or N-termini. All of these techniques are non-natural forced stabilisation of the GPCRs. Furthermore, crystal structures only show a snapshot of a certain conformational state and provide only a static view of a highly dynamic protein. Although these structures give a basic understanding of the structure-function relationship, they do not show any dynamical features, which might be important for ligand binding or affinity and conformational change upon ligand binding. NMR spectroscopy could be used as a complementary technique to x-ray crystallography, as with NMR it is possible to study dynamical features in a protein.

However, to be able to study a membrane protein by NMR spectroscopy, expression and purification must be optimised in order to obtain high yields of protein. Additionally, it must be expressed in a medium, where it can be labelled to ensure its feasibility for NMR measurements. This is still a challenging task, as GPCRs are known for giving very low yields ($< 1\,\mathrm{mg\,L^{-1}}$ expression culture). Also choosing an ideal detergent for extraction, which does not unfold the protein, cannot be underestimated. Additionally, a purification tool has to be chosen for separating folded from unfolded receptor.

As a GPCR, the $CRF_{2\beta}R$ is chosen, because of its relevance in physiology and its promising assistance in drug development if structural or dynamical features are known. Thus a purification protocol is attempted to obtain a functionally active $CRF_{2\beta}R$ with a native sequence and if possible measuring NMR spectroscopy experiments. Additional information of the $sCRF_{2\alpha}R$ might be valuable to understand its role in the CRF system and thus a purification protocol is established and NMR spectroscopy measurements attempted.

The Nogo-A-Δ20 segment is an interesting system for NMR spectroscopy, as IDPs are disordered and thus hardly feasible to crystallise. IDPs normally give high yields (> $20\,\mathrm{mg\,L^{-1}}$ bacteria culture) and are readily labelled in *E.coli*. Of interest is the interaction of Nogo-A-Δ20 to its binding partner S1PR2. Thus a labelling protocol is attempted to establish followed by NMR spectroscopy experiments, first for the assignment of Nogo-A-Δ20 and then for investigating of possible ligand-protein interactions.

Chapter 2

Expression and Purification of CRF Receptor Isoforms

2.1 soluble $CRF_{2\alpha}$ Receptor

In 2004, Chen et al. found a soluble splice variant of the corticotropin-releasing factor receptor in mice ($sCRF_{2\alpha}R$) [22]. This splice variant was expressed primarily in the olfactory bulb, cortex, and midbrain region, having a distribution close to that of CRF_1R. The splice variant originated by the deletion of exon 6 from the gene encoding $CRF_{2\alpha}$ receptor. This created a frame shift of the following amino acid residues, which resulted in a unique hydrophilic C-terminus (figure 2.1). The first extracellular domain (ECD) of $sCRF_{2\alpha}R$ is the same as in $CRF_{2\alpha}R$ with the first 19 amino acid residues belonging to a pseudo-signal peptide. The pseudo-signal peptide has a high propensity to be a signal peptide on the basis of its sequence; however, these amino acid residues are unable to mediate secretion at the Golgi apparatus into or out of the membrane in the early biogenesis [107]. Additionally the pseudo-signal peptide is not removed after secretion, as it is usually the case for signal peptides; thus it was defined as pseudo-signal peptide. Instead, it is the first transmembrane domain that acts as an anchor-signal for $CRF_{2\alpha}R$ and guides the receptor towards the secre-

tory pathway, which is typical for G-protein coupled receptors (GPCRs) [107]. Since $sCRF_{2\alpha}R$ has no transmembrane region, it is efficiently translated but not trafficked to the secretory pathway and neither secreted [51], resulting in proteosomal degradation. Interestingly, mutating the Asn13 residue in the pseudo-signal sequence to a hydrophobic or positively charged amino acid, it rescued the signal peptide propensity of $sCRF_{2\alpha}R$ [51, 107]. Thus in certain cases, the pseudo-signal peptide might serve again as a conventional signal peptide [107].
For this study, a fusion protein that lacks the peudo-signal peptide was expressed in *E.coli* and purified from the soluble cell lysate.

2.1.1 Expression and Purification

$sCRF_{2\alpha}R$ has six cysteine residues (Cys or C) forming at least two disulphide bonds. An oxidising environment is needed in order to form disulphide bridges. However, the cytoplasm of *E.coli*, where proteins are expressed, has a reducing environment. A thioredoxin-tag, which can catalyse disulphide bond formation even in a reducing environment, was therefore utilised in our fusion construct [108]. This was achieved using a plasmid (pET 32a) that includes a thioredoxin-tag and a His_6-tag at the N-terminus (figure 2.1). The thioredoxin- and His_6-tag are removed from the expressed fusion protein via a thrombin cleavage site.
Additionally, the reducing environment in the cytoplasm can be altered by mutating the thioredoxin (*trxB*) and glutaredoxin (*gor*) pathways that normally ensure the negative potential [109, 110]. The commercially available Origami^{TM} (DE3) *E.coli* cell strains have a mutation in the cytoplasmic reductases (*trxB* and *gor*) that ensures the alteration of the reducing environment. Thus this cell strain was appropriate for expressing $sCRF_{2\alpha}R$.

HLTDDSFDTD VLKADGAILV DFWAEWCGPC KMIAPILDEI ADEYQGKLTV AKLNIDQNPG

TAPKYGIRGI PTLLLFKNGE VAATKVGALS KGQLKEFLDA NLAGSGSGHM *HHHHHH*SSGL

10 20 30 40 50

VPR GSG*MKETAAA KFERQHMDS*P DLGTEELLLD GWGVPPDPEG PYTYCNTTLD

60 70 80 90 100 110

QIGTCWPQSA PGALVERPCP EYFNGIKYNT TRNAYRECLE NGTWASRVNY SHCEPILDDK

120 130 140

EYPLPEECDP LEPHHHLHSE KHRVVPAATH RPRSARGQ

Figure 2.1: Amino acid sequence of the fusion protein of $sCRF_{2\alpha}R$. The underlined amino acid residues belong to the $sCRF_{2\alpha}R$ sequence, the bold amino acid residues belong to the thioredoxin-tag, and the amino acid residues in italics belong to either the His_6-tag or the S-tag. The scissors indicate the site at which thrombin cleaves the N-terminal His_6-tag, between the Pro-Arg and Gly-Ser residues. Additionally, the double underlined amino acid residues indicate the hydrophilic C-terminus unique for $sCRF_{2\alpha}R$ formed after exon 6 deletion in the gene encoding $CRF_{2\alpha}$ receptor [22].

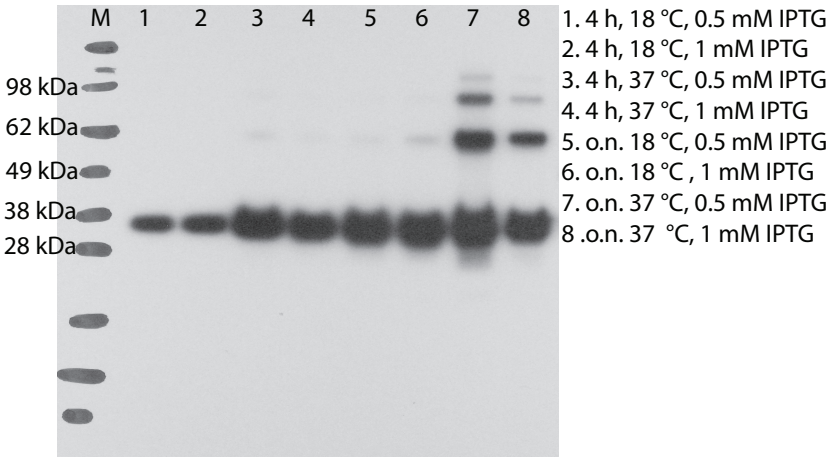

Figure 2.2: Western blot of the expression test of $sCRF_{2\alpha}R$ fusion protein in Terrific Broth. An anti-His_6-tag antibody was used for illumination. The cells were grown at 37°. Upon obtaining an optical density of 0.7 at 590 nm, the bacteria culture was transferred either to 18° or kept at 37°. After induction with either 0.5 mM or 1.0 mM IPTG, samples were taken at different time points, either after 4 h or over night expression (o.n. ca 16 h). The band at 33 kDa represents $sCRF_{2\alpha}R$ (theoretical molecular weight is 29.9 kDa).

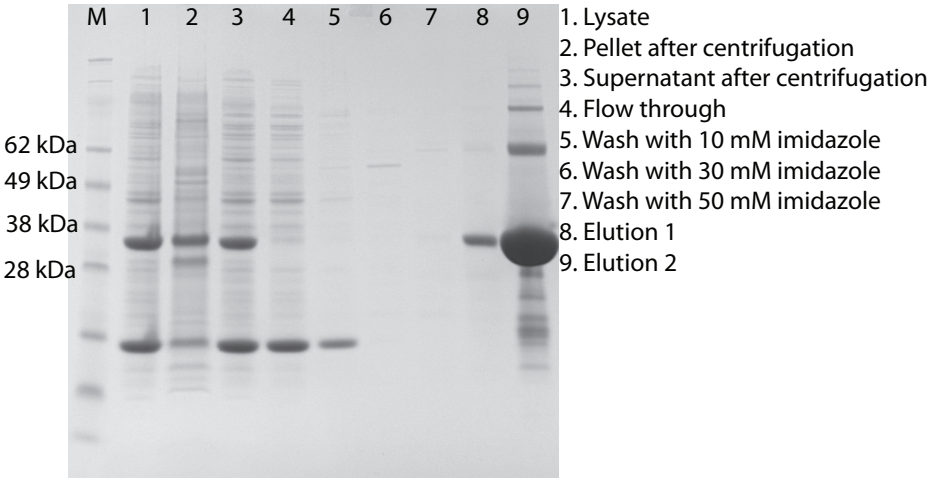

Figure 2.3: A NuPAGE® 4 % to 12 % Bis-Tris gel of sCRF$_{2\alpha}$R purification. Lane 1 is the entiry cell lysate; lane 2 represents the insoluble fraction and lane 3 is the soluble fraction; lane 4 is the flow through of Ni-NTA resin; lanes 5 to 7 correspond to the wash of the Ni-NTA resin with different imidazole concentrations; lane 8 and 9 are the elution of the Ni-NTA resin with 500 mM imidazole. In the elution of the Ni-NTA resin are high molecular species present, which might be multimers of sCRF$_{2\alpha}$R. For instance, the band at 65 kDa could be a dimer of sCRF$_{2\alpha}$R.

An expression test was performed on the fusion construct using different temperatures during induction and different isopropyl β-D-1-thiogalactopyranoside (IPTG) concentrations. Samples were taken at different time points (figure 2.2). The fusion construct was expressed in Terrific Broth. The band at 33 kDa represented the fusion protein, which theoretical molecular weight was 29.9 kDa. The maximal intensity of this band, in absence of high molecular weight species, was obtained from samples that were either expressed for 4 h and induced with 0.5 mM IPTG at 37° or over-night induced with 0.5 mM IPTG at 18°.

To obtain isotopically labelled sCRF$_{2\alpha}$R for nuclear magnetic resonance (NMR) spectroscopy measurements, the Terrific Broth medium was replaced by minimal medium with NMR active isotopically labelling reagents, as for example ^{13}C-D-glucose and/or ^{15}N-ammonium chloride. The cells were expressed over night at 20° induced with 0.5 mM IPTG. The temperature was slightly increased as in minimal media the expression yield is lower. Additionally, the media was supplied with Hutner's salts as trace metal supply [111].

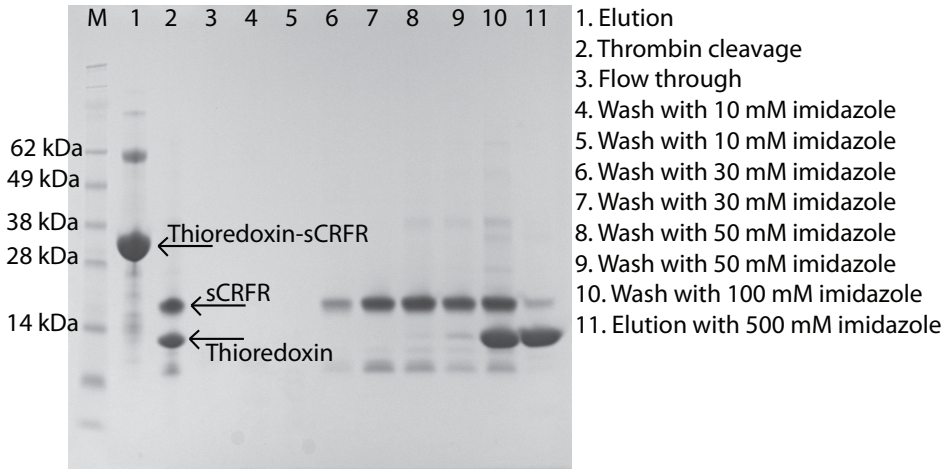

Figure 2.4: A NuPAGE® 4 % to 12 % Bis-Tris gel of $sCRF_{2\alpha}R$ upon thrombin cleavage and further purification by nickel affinity chromatography. Lane 1 shows the elution of the fusion protein of the first Ni-NTA resin; lane 2 is the thrombin cleaved fusion protein. The band at 20 kDa represents $sCRF_{2\alpha}R$ (theoretical molecular weight 16.7 kDa) and the band at 12 kDa represents the thioredoxin-tag (theoretical molecular weight is 13.2 kDa); lane 3 is the flow through of the second Ni-NTA resin; lane 4 and 5 are the wash of Ni-NTA resin with 10 mM imidazole, lane 6 and 7 is the wash with 30 mM imidazole, lane 8 and 9 with 50 mM imidazole, and lane 10 with 100 mM imidazole; lane 11 is the elution with 500 mM imidazole. It is visible, that $sCRF_{2\alpha}R$ still elutes at 100 mM imidazole.

After expression, the bacteria were centrifuged and the resulting pellet was either shock frozen with liquid nitrogen and stored at $-80°$ or immediately used for purification.

The cells were resuspended, later lysed by a Microfluidizer and loaded on Ni-NTA resin. For nickel affinity chromatography, the resin was equilibrated in 50 mM Tris, 500 mM NaCl, 10 mM imidazole at pH 8. The bound fusion protein was eluted with 500 mM imidazole (figure 2.3). The elution from Ni-NTA resin had some minor impurities at lower molecular weight and some major impurities at high molecular weight. The latter might be multimers of $sCRF_{2\alpha}R$, as their molecular weights are multiples of that of a monomer of $sCRF_{2\alpha}R$ (33 kDa).

Subsequently, the fusion protein was cleaved with the human thrombin enzyme overnight at ca. 22 °C. The cleaved fusion protein was loaded again on a Ni-NTA resin to bind the cleaved thioredoxin-tag including the His_6-tag and collect the $sCRF_{2\alpha}R$ in the flow through and wash. Surprisingly, even the cleaved $sCRF_{2\alpha}R$ had a certain affinity

to Ni-NTA resin since the flow through did not contain it and 30 mM to 100 mM imidazole is needed to fully elute $sCRF_{2\alpha}R$ (figure 2.4). This unusual behaviour could arise from the three consecutive histidines in the C-terminal tail of $sCRF_{2\alpha}R$ (figure 2.1), as those might have a certain affinity for the Ni-NTA resin. Thus separating the thioredoxin-tag from the cleaved $sCRF_{2\alpha}R$ is not feasible by nickel affinity chromatography.

Thus size exclusion chromatography (SEC) was performed with $sCRF_{2\alpha}R$ using a Superdex 200 10/300 GL column. This column has a separating range for protein with molecular weights between 10 kDa to 600 kDa. The size exclusion chromatogram showed two monodispers but overlapping peaks at 14.5 mL, with a shoulder at 13.5 mL, and at 16 mL, with a small shoulder at 17.5 mL, implying that a wide range of different molecular weight species were present after thrombin cleavage.

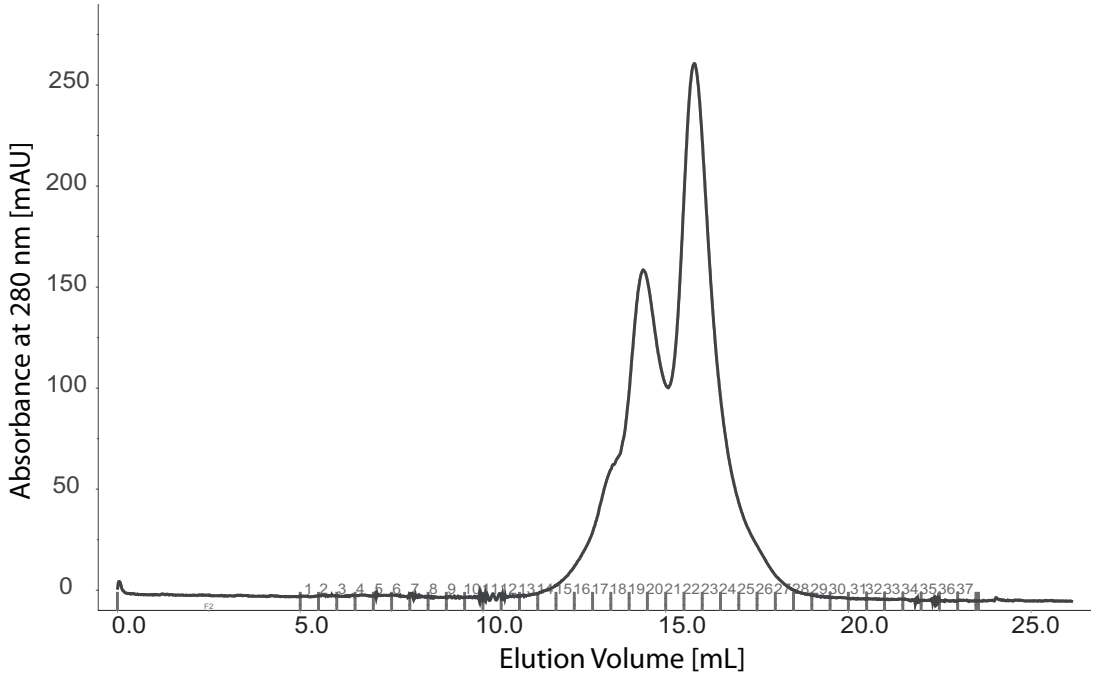

Figure 2.5: Size exclusion chromatogram of Superdex 200 elution profile of cleaved $sCRF_{2\alpha}R$. Two major overlapping peaks were obtained at around 14.5 mL and 16 mL including shoulders.

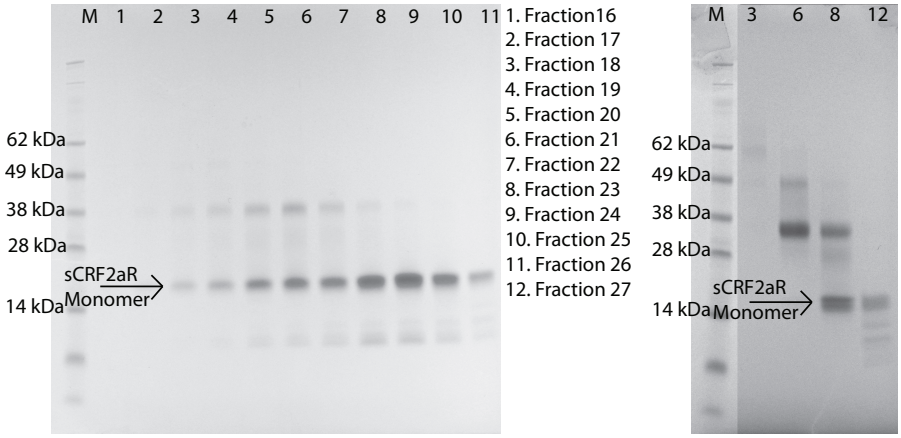

Figure 2.6: A NuPAGE® 4 % to 12 % Bis-Tris gel of fractions of $sCRF_{2\alpha}R$ after size exclusion chromatography. Left: with β-Mercaptoethanol in the loading buffer for SDS gel; right: without β-mercaptoethanol in the loading buffer.

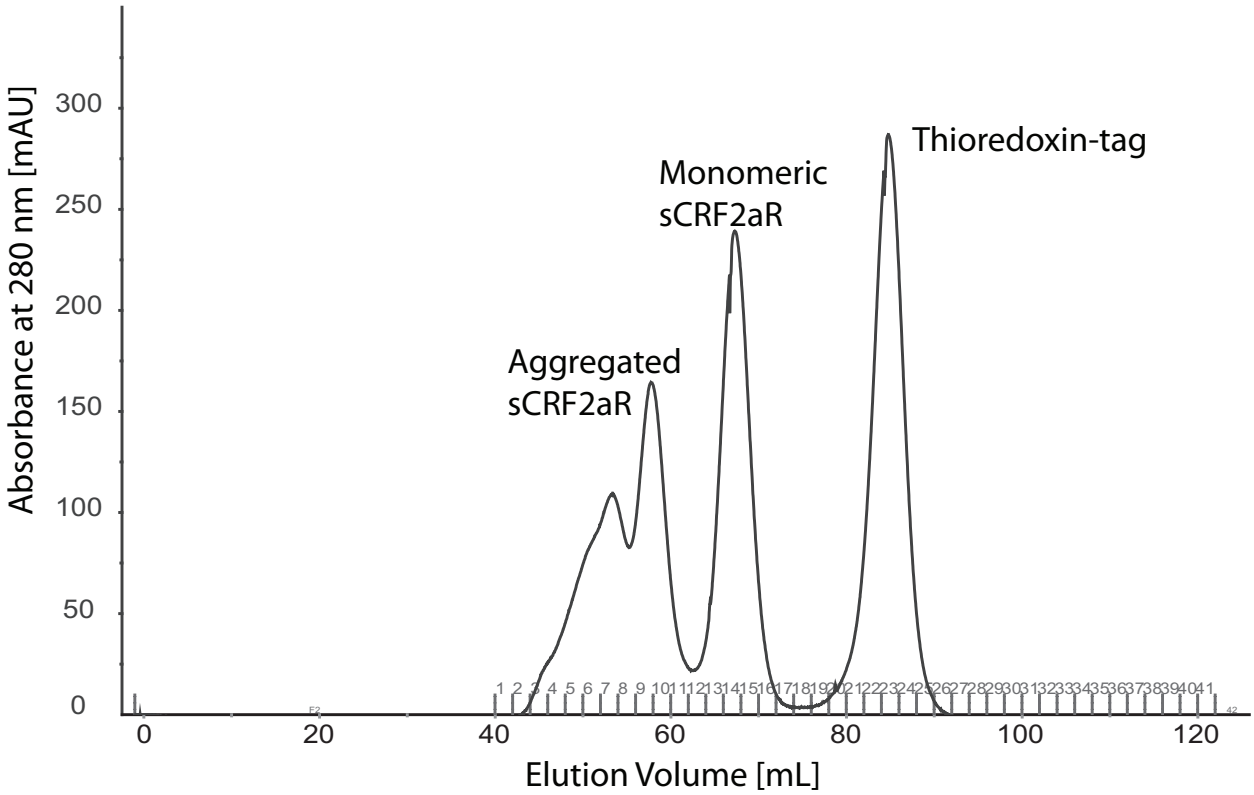

Figure 2.7: Size exclusion chromatogram of a Superdex 75 high load chromatography of cleaved $sCRF_{2\alpha}R$. The sample was directly loaded on the size exclusion after thrombin cleavage. Multimer and dimer eluted at around 50 mL and 58 mL, the monomer at around 69 mL, the thioredoxin-tag at around 85 mL.

Loading the fractions on a NuPAGE® $4\,\%$ to $12\,\%$ Bis-Tris gel in presence of a reducing agent in the loading buffer indicated a poor separation from high molecular weight species and $sCRF_{2\alpha}R$ monomer. Omitting the reducing agent β-mercapthoethanol in the loading buffer for the Bis-Tris gel, showed that the high molecular weight species in the SEC profile are multimers of $sCRF_{2\alpha}R$, probably due to the formation of intermolecular disulphide bridges (figure 2.6). The monomeric species of $sCRF_{2\alpha}R$ was found in the peak eluted at around $16\,$mL, the higher molecular weight species were found at $14.5\,$mL and $13.5\,$mL. However, adding a reducing agent during the purification is not feasible due to the presence of disulphide bridges within the $sCRF_{2\alpha}R$ protein, which would get reduced, too.
Using a Superdex 75 10/300 GL column instead of a Superdex 200 10/300 GL improved the separation (figure 2.7) as this column is able to separate proteins in the molecular range of $3\,$kDa to $70\,$kDa. The multimer and dimer eluted at around $50\,$mL and $58\,$mL, respectively, the monomer at around $69\,$mL, and the thioredoxin-tag at around $85\,$mL. Thus, the monomer was separated from the bulk of proteins of *E.coli* and from high molecular weight species with a Superdex 75. However, still some inhomogeneities might have been present in the monomer fraction due to conformers that might have different disulphide bridge connections, which is often the case for disulphide bridged proteins [37, 112]. The monomeric fraction from Superdex 75 was loaded on a reverse phase HPLC C4 column. An acetonitrile gradient was used for the elution of $sCRF_{2\alpha}R$ similar to the established reverse phase HPLC purification for the ECD of $CRF_{2\beta}R$ by Perrin et al. [112]. The chromatogram of $sCRF_{2\alpha}R$ shows many overlapping peaks having similar retention times indicating that different conformers of $sCRF_{2\alpha}R$ are present (figure 2.8).

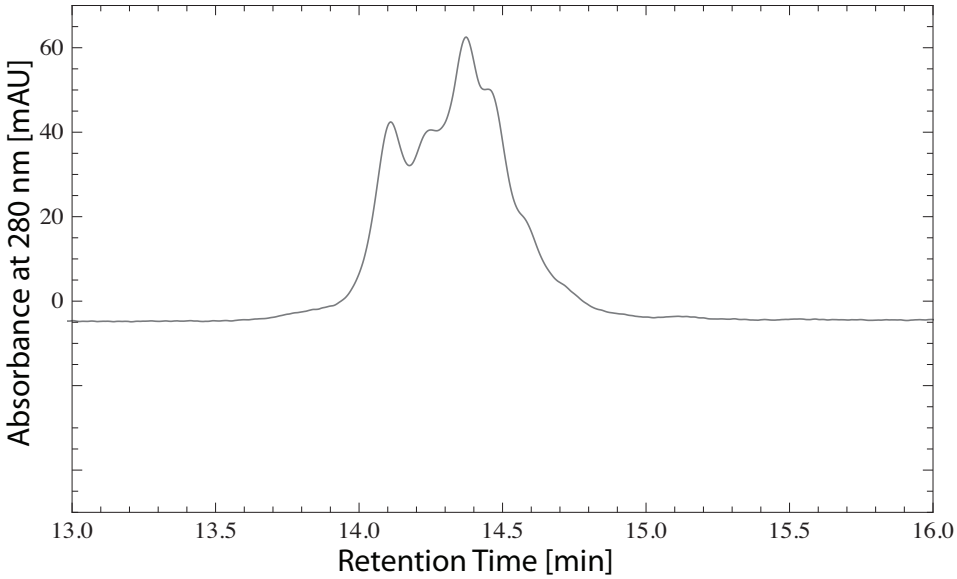

Figure 2.8: Reversed-phase HPLC chromatogram of $sCRF_{2\alpha}R$ running a gradient with acetonitrile. The elution profile of $sCRF_{2\alpha}R$ shows many overlapping peaks indicating that different conformers are present.

In order to verify the folding of the protein, NMR spectroscopy measurements were performed. Since [^{15}N, ^{1}H]-HSQC spectra are published for the folded and unfolded ECD of $CRF_{2\beta}R$ [38] and due to the sequence similarity of the ECD of $CRF_{2\beta}R$ and $sCRF_{2\alpha}R$ and their similar fold, as is found for all receptors belonging to the *secretin* family, similar spectra are expected for $sCRF_{2\alpha}R$ and the ECD of $CRF_{2\beta}R$.

When the ECD of $CRF_{2\beta}R$ was unfolded, the tryptophan peaks were found at a chemical shift of 10 ppm, when the protein was proper folded, they appeared at around 11 ppm [38].

Thus similar measurements were performed with ^{15}N-labelled $sCRF_{2\alpha}R$, either after SEC with Superdex 75 or after reverse phase HPLC purification. Measuring the labelled protein after Superdex 75 showed mainly an unfolded species indicated by the shift of tryptophans (figure 2.9).

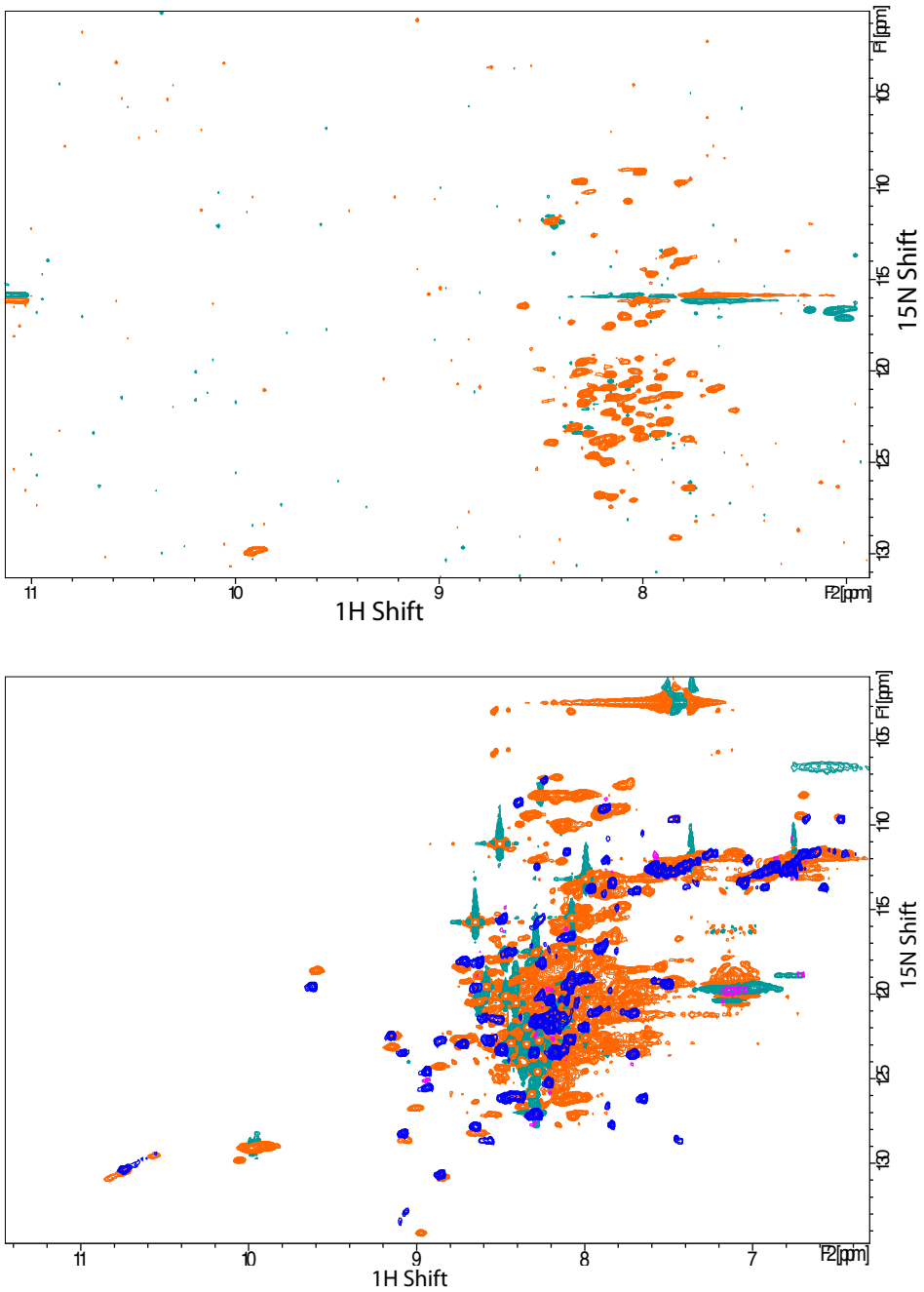

Figure 2.9: [^{15}N, ^{1}H]-spectra of sCRF$_{2\alpha}$R. Top: [^{15}N, ^{1}H]-TROSY spectrum of 100 µM sCRF$_{2\alpha}$R purified only on SEC with Superdex 75 recorded at pH 4.93; bottom: orange spectrum is a [^{15}N, ^{1}H]-HSQC of 200 µM sCRF$_{2\alpha}$R purified with HPLC and blue spectrum is a [^{15}N, ^{1}H]-HSQC of a 15 µM correctly folded ECD of CRF$_{2\beta}$R at pH 6.5. Good indication of correctly folded ECD is the shift of the tryptophans in the region of 10-11 ppm. If the tryptophans are around 11 ppm and not 10 ppm, the ECD is folded. The same is expected for sCRF$_{2\alpha}$R due to its sequence similarity. sCRF$_{2\alpha}$R after SEC just showed unfolded receptor, but some higher amount of folded species after HPLC. All spectra were recorded at 25° on a 600 MHz NMR spectrometer.

The sample measured after HPLC already consisted of a higher concentration of folded species. This is probably due to the separation of some unfolded from the folded species. However, still some unfolded $sCRF_{2\alpha}R$ was present in the sample, which might result from the overlapping peaks in the HPLC chromatogram. Unfortunately, changing HPLC conditions, such as gradient or elution time, did not improve the resolution further. // It was therefore clear that it was not possible to obtain properly folded samples with standard chromatographic techniques. Thus alternative strategies such as specific ligand-affinity chromatography should be used. This method might help isolate folded $sCRF_{2\alpha}R$ from the unfolded species as the folded protein should bind to the ligand attached to a resin, while the unfolded protein should be found in the flow through (see chapter 3: 'Ligand Affinity Chromatography').

2.2 $CRF_{2\beta}$ Receptor

Even though G protein-coupled receptors (GPCRs) are an important membrane protein class and they are often targeted for new drug developments [6, 8, 113], few receptors of this class can be expressed and purified in quantities high enough for biochemical analysis. Many GPCRs are expressed in rather low yields (< 1 mg per of litre culture [114]). Not only the expression system itself seems to be a challenge, but also many GPCRs are known for being hard to extract in a stable way. Finding a good detergent for extracting and purifying them is therefore demanding and time consuming.
The *E.coli* expression system was chosen for the production of the corticotropin-releasing factor receptor 2β ($CRF_{2\beta}R$) due to its ease of handling and its non-post-translational modification giving uniform non-glycosylated samples. It is also possible to isotopically label the protein in *E.coli*, which is crucial for heteronuclear NMR spectroscopy measurements.
The expression protocol for $CRF_{2\beta}R$ by Japelli et al. [115] was taken as starting point in this thesis for establishing an expression and purification protocol for an uniformly folded sample that could be applied to the production of isotopically labelled protein.

The established expression protocol by Jappelli et al. is shortly summarised:
E.coli bacteria were grown carrying the (pelB-)$CRF_{2\beta}R$ plasmid in Terrific Broth (TB) medium up to an OD_{600} of 0.9 and expressed at 18 °C with 1 mM IPTG for approximately 24 h. The centrifuged cells were resuspended in 50 mM Tris, 300 mM NaCl with lysozyme and protease inhibitor tablets (Complete EDTA-free protease inhibitor (PI) cocktail tablets from Roche Diagnostics). The cells were then stirred for 30 min at 4 °C. The lysate was passed twice through a microfluidizer, and centrifuged for 15 min at 10 krpm. The supernatant was centrifuged again for 1.5 h at 40 krpm. The resulting pellet was resuspended in 50 mM Tris, 300 mM NaCl, 25 % glycerol and stirred over night at 4 °C. The next day, an extraction trial was performed with different detergents. The highest yields were obtained for FC14. However,it was considered that FC14 might be a very harsh detergent for purification and a different detergent or a detergent mixtures might be a better solution for the purification of $CRF_{2\beta}R$.
Jappelli et al extracted the $CRF_{2\beta}R$ just in detergents without adding any cholesterol. However, cholesterol was shown to bind to GPCRs and render them more stable resulting in higher yields at the end of a purification [116–119]. Cholesterol can change physical properties of membranes as for example curvature, lipid order, and membrane fluidity and it is present at high concentrations in eukaryotic cellular membranes [120]. Therefore, in this thesis, cholesterol was added in every purification step as soon as a detergent was used.

So far, many published crystal structures of GPCRs are obtained from biological engineered receptors [9, 43, 49]. One technique is for example the thermostabilisation of the receptors with either systematic scanning mutagenesis, [44, 121, 122] or random mutagenesis as used in evolution-biased strategies [123]. These point mutations serve to lock the receptor in a certain conformational state [121]. This procedure, normally done on detergent-solubilised receptors, renders the GPCRs easier to purify and crystallise due to their higher stability [124]. The CRF_1 receptor was also thermostabilised for its crystallisation [43].

Therefore, some point mutations were considered to be introduced into the $CRF_{2\beta}R$ in this thesis. However, the CRF_1 receptor was engineered into an inactive state and since the aim of this thesis is to purify $CRF_{2\beta}R$ in an active state, not all point mutated residues can be introduced into the $CRF_{2\beta}R$. To maintain an active conformation, only one or two point mutations should be introduced to render the receptor easier to purify. This is possible since the inactivation of a GPCR is not obtained just by one point mutation but just increases the propensity for an inactive state, however does not lock it there.
Taking the expression protocol of Jappelli et al as starting point, each step was examined to increase the yield of the protocol. Additionally, a purification protocol was attempted to yield an active $CRF_{2\beta}R$ in mg-quantities.

2.2.1 Expression

Three constructs of $CRF_{2\beta}R$ fusion proteins were tested for their yield of expression. Two were designed by Jappelli et al. Both fusion proteins had a His_6-tag at the C-terminus and a small linker to connect it to the C-terminus of $CRF_{2\beta}R$. At the N-terminus, one construct contained a pelB-signal peptide sequence from *E.carotovora* [125], whereas the other did not (figure 2.10). This signal peptide sequence should ensure the secretion via the Sec-dependent pathway [126]. The pelB-$CRF_{2\beta}R$ fusion protein expressed in lower yields than the no signal peptide $CRF_{2\beta}R$, which is consistent to the observation of Jappelli et al [115].
The third fusion protein of $CRF_{2\beta}R$ had a Mistic-sequence at the N-terminus. The Mistic (Membrane-Intergrating Sequence for Translation of Integral membrane protein Constructs) is a membrane protein from *Bacillus subtilis* [127]. Mistic can autonomously translocate itself into membranes skipping the rate determining step of the cellular translocon machinery. The usefulness of the Mistic-sequence has been shown in a prove of principle by Roosild et al in 2005 [127] improving considerably the yields of membrane proteins. Additionally, they proved that the C-terminal part

of Mistic is exposed to the periplasm in *E.coli*. Thus attaching the Mistic-sequence to the N-terminus of a protein ensures its translocation to the periplasm.

```
                                        10         20         30
MKYLLPTAAA GLLLLAAQPA MA MVAQPGQAPQ DQPLWTLLEQ YCHRTTIGNF

         40         50         60         70         80         90
SGPYTYCNTT LDQIGTCWPQ SAPGALVERP CPEYFNGIKY NTTRNAYREC LENGTWASRV

        100        110        120        130        140        150
NYSHCEPILD DKQRKYDLHY RIALIVNYLG HCVSVVALVA AFLLFLVLRS IRCLRNVIHW

        160        170        180        190        200        210
NLITTFILRN IAWFLLQLID HEVHEGNEVW CRCITTIFNY FVVTNFFWMF VEGCYLHTAI

        220        230        240        250        260        270
VMTYSTEHLR KWLFLFIGWC IPCPIIIAWA VGKLYYENEQ CWFGKEAGDL VDYIYQGPVM

        280        290        300        310        320        330
LVLLINFVFL FNIVRILMTK LRASTTSETI QYRKAVKATL VLLPLLGITY MLFFVNPGED

                   to Ala, A
        340        350        360        370        380        390
DLSQIVFIYF NSFLQSFQGF FVSVFYCFFN GEVRAALRKR WHRWQDHHAL RVPVARAMSI

        400        410        420
PTSPTRISFH SIKQTAAVNS SSVDKLAAAL EHHHHHH
```

Figure 2.10: Amino acid sequence of the fusion protein encoded by the (pelB-)$CRF_{2\beta}R$ plasmid. The underlined residues belong to the $CRF_{2\beta}R$ sequence, the bold residues belong to the prokaryotic signal peptide pelB-tag, which is present in the pelB-$CRF_{2\beta}R$ fusion protein and not in the $CRF_{2\beta}R$ fusion protein. The amino acid residues in italics belong to the His_6-tag. The letter in grey shows the point mutation introduced to (pelB)-$CRF_{2\beta}R$.

The Mistic-sequence was also attached to the N-terminus of the $CRF_{2\beta}R$. Roosild et al. expressed the receptor and purified it with a nickel affinity column in the detergent LDAO. The Mistic-tag was removed later via thrombin cleavage.

Expressing and purifying the Mistic-$CRF_{2\beta}R$ in FC14 resulted in an increased yield by a factor of 3 to 4 compared to the no signal peptide construct of $CRF_{2\beta}R$ (data not shown). Therefore, Mistic-$CRF_{2\beta}R$ was used for further expression and purification.

MK*HHHHHHHH* GGLVGGGSHG **MFVTFFEKHH RKWDILLEKS TGVMEAMKVT**

SEEKEQLSTA IDRMNEGLDA FIQLYNESEI DEPLIQLDDD TAELMKQARD MYGQEKLNEK

10

LNTIIKQILS ISVSEEGEKE GSGSGHM*HHH HHH*SSGGSST SLYKKAGSLV PR GSGSQPGQAP

20 30 40 50 60 70

QDQPLWTLLE QYCHRTTIGN FSGPYTYCNT TLDQIGTCWP QSAPGALVER PCPEYFNGIK

80 90 100 110 120 130

YNTTRNARE CLENGTWSR VNYSHCEIL DDKQRKYDLH YRIALIVNYL GHCVSVVALV

140 150 160 170 180 190

AAFLLFLVLR SIRCLRNVIH WNLITTFILR NIAWFLLQLI DHEVHEGNEV WCRCITTIFN

200 210 220 230 240 250

YFVVTNFFWM FVEGCYLHTA IVMTYSTEHL RKWLFLFIGW CIPCPIIIAW AVGKLYYENE

260 270 280 290 300 310

QCWFGKEAGD LVDYIYQGPV MLVLLINFVF LFNIVRILMT KLRASTTSET IQYRKAVKAT

to Ala, A Stop Codon

320 330 340 350 360 370

LVLLPLLGIT YMLFFVNPGE DDLSQIVFIY FNSFLQSFQG FFVSVFYCFF NGEVRAALRK

Stop Codon

380 390 400

RWHRWQDHNA LRVPVARAMS IPTSPTRISF HSIKQTAAV

Figure 2.11: Amino acid sequence of the fusion protein encoded by the Mistic-CRF$_{2\beta}$R plasmid. Compared to the (pelB-)CRF$_{2\beta}$R construct, Mistic-CRF$_{2\beta}$R has a Mistic-sequence at the N-terminus indicated by bold and two His-tags indicated by letters in italics. The scissor show the thrombin cleavage site, between the Pro-Arg and Gly-Ser residues. The letters in grey show the point mutation introduced to Mistic-CRF$_{2\beta}$R.

Additional to the OverExpress™ C43(DE3) and Rosetta 2 (CE3) cell strains examined by Jappelli et al, Origami™B(DE3), BL21 Star ™(DE3) co-expressed with DsbC, SHuffle®T7 and OverExpress™ C41(DE3) cells were tested. Origami™B(DE3) was chosen, as it has point mutations in his genome to decrease the reducing environment of *E.coli* in cytoplasm to facilitate easier disulphide bond formations. Additionally, CRF$_{2\beta}$R was co-expressed with DsbC isomerase in BL21 Star ™ as this protein is able to reshuffle disulphide bridges. The SHuffle®T7 strain has a mutation in its genome to express

DsbC automatically in the cytoplasm. The OverExpress™ C41(DE3) strain was chosen due to their larger membranes which may increase the membrane protein concentration. BL21 Star ™(DE3) cells were used as a control. After induction at 18 °C and over night expression, samples were taken and a Western blot was performed. The $CRF_{2\beta}R$ was detected with an anti-His_6-tag antibody (figure 2.12).
BL21 Star ™(DE3) was the only cell strain giving $CRF_{2\beta}R$ in high yields, as indicated by a band on a NuPAGE® 12 % Bis-Tris gel at the molecular weight expected for Mistic-$CRF_{2\beta}R$ W375Stop. $CRF_{2\beta}R$ co-expressed with DsbC gave a weaker band at a lower molecular weight than when $CRF_{2\beta}R$ was expressed alone. It was not investigated if the lower band was $CRF_{2\beta}R$. On the basis of this test, BL21 Star ™(DE3) cells were used for further expression.

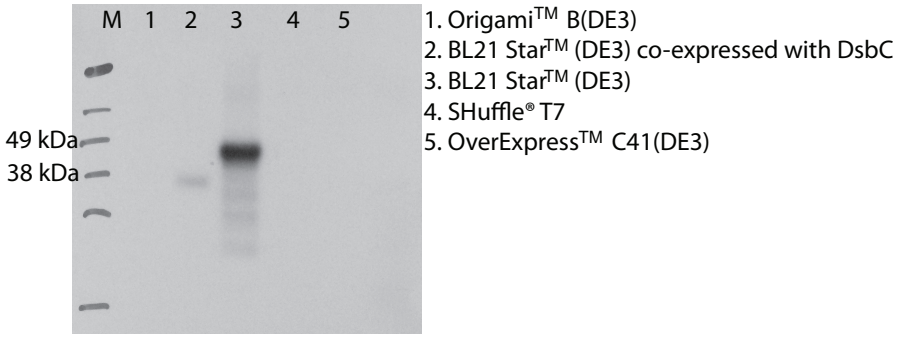

Figure 2.12: Western blot of an expression trail with different cell strains using the plasmid Mistic-$CRF_{2\beta}R$ W357Stop. The primary antibody was specific for His_6-tag.

Expression Medium

Besides the TB medium, which was utilised by Jappelli et al, an auto induction medium was examined as alternative expression system [128]. This is an expression system, where no induction with IPTG is needed due to the addition of glucose and lactose. As long as glucose is present in the medium, the cells use glucose as a carbon source instead of lactose; therefore, no expression is induced by lactose. However, when the glucose is depleted, the cells start to produce the desired protein [128]. This expression system had been shown to work for some GPCR proteins fused N-terminally with

the Mistic-sequence yielding mg-quantities [129]. However, in our case, even though different time points and temperatures were investigated for the auto-induction for the expression of the Mistic-$CRF_{2\beta}R$, no condition yielded higher amounts of $CRF_{2\beta}R$ than for the established TB-medium (data not shown). Thus, TB medium was used for expressing unlabelled $CRF_{2\beta}R$ as described by Jappelli et al [115].

2.2.2 Preparation of the Membrane for Extraction

There are different methods to extract membrane proteins. Either the membrane protein fraction is separated from the soluble protein fraction and subsequently the membrane proteins are extracted from the host membrane [43] or the membrane proteins are extracted from the whole cell lysate [67].
Before the extraction of $CRF_{2\beta}R$ from the membrane protein fraction, the *E.coli* lysate was centrifuged twice, first to remove the inclusion bodies and cell debris and then to separate the membrane fraction from the soluble one. The former one was resuspended over night and subsequently extracted with a detergent. The Mistic-tag was then cleaved off with thrombin.
Purification of the protein from the whole cell extraction was faster compared to the one from membrane fraction. *E.coli* cells were lysed and the membrane protein was then immediately extracted. Since GPCRs are known to be unstable, a fast purification protocol is preferred.
No difference in the purity of $CRF_{2\beta}R$ was observed when comparing the membrane protein fraction and the whole cell extraction (data not shown). Thus the whole cell extraction was preferred due to its shortening of time for the purification.

2.2.3 Cell Disruption

To disrupt *E.coli* cells, the cell lysate was passed twice through a microfluidizer before the extraction with detergents. Microfluidizers use high shearing forces to break the

cells. Due to heat development, the system should be cooled with ice water.
A Western blot of a purification of Mistic-CRF$_{2\beta}$R, using a microfluidizer for cell disruption, exhibited several bands in the nickel-affinity chromatography elution. For the illumination of the band, an anti-His$_6$-tag antibody was used. The bands collapsed to one band upon thrombin cleavage corresponding to the His-tagged Mistic. Thus, it was assumed that the bands, found in the nickel-affinity elution on the Western blot, correspond to Mistic-CRF$_{2\beta}$R and might represent differently truncated receptors. The truncation of the receptor was thought to be induced by the shearing forces of the microfluidizer. Thus a bounce homogeniser was used for lysing instead of the microfluidizer. However, the yield of purified Mistic-CRF$_{2\beta}$R was reduced, when the bounce homogeniser was used, probably due to decreased efficiency of cell disruption (data not shown).

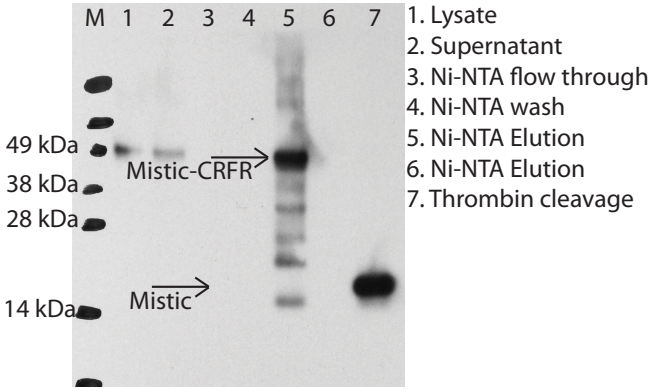

Figure 2.13: Western blot of a purification of Mistic-CRF$_{2\beta}$R using a microfluidizer to disrupt *E.coli* cells. Lane 1 is the lysate of the purification; lane 2 is the supernatant of a centrifugation after the membrane proteins have been solubilised with the detergent FC14; lane 3 is the flow through of a nickel affinity chromatography; lane 4 is the wash of the nickel-resin; lane 5 and 6 are the elution of the affinity chromatography with 500 mM imidazole; lane 7 is the elution cleaved with human thrombin. The elution after the affinity chromatography has several bands, which all collapse to one band upon thrombin cleavage, corresponding to the His-tagged Mistic.

However, when a Western blot was performed with different dilution ratio between a receptor sample and a SDS-loading buffer, the amount of bands varied as well. When the *E.coli* lysate, containing the receptor, was diluted 1:1 with loading buffer, again several bands were visible in the Western blot, using an anti-His$_6$-tag antibody for

analysis. When the cell lysate was diluted 1:9 with loading buffer, only one strong band remained.
The different bands found after Ni-elution might not have been only truncated, but also not well solubilised receptors. Thus, microfluidizer was used again as a cell disrupter, just at a lower pressure, *e.g.* 25 PSI instead of 40 PSI, to decrease the shear forces generated on the receptor.

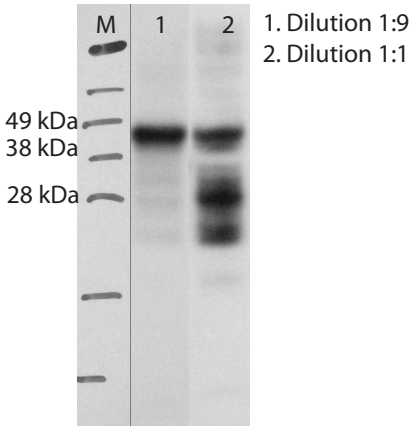

Figure 2.14: Western blot of lysed *E.coli* cells with different dilution ratios. While the 1:1 dilution of the lysate with loading buffer contained several bands illuminated with an anit-His_6-tag antibody, the bands collapsed to one band, when the lysate was diluted 1:9 with loading buffer.

2.2.4 Extraction

Due to the fact that Jappelli et al. used the membrane fraction for extraction, a detergent trial examination was performed with different detergents using the whole cell extraction method (figures in 'Extraction, Mistic-$CRF_{2\beta}$R'). Since the detergent FC14 at $0.5\,\%$ concentration gave the highest yield in the extraction protocol of Jappelli et al, FC14 was taken as a control to estimate the efficiency of other detergents.

Mistic-CRF$_{2\beta}$ Receptor

Different detergents were investigated, some being mild, as for example DDM or FC12, and some being harsher but more suitable for NMR spectroscopy measurements due to their small-micelle sizes, as for example LMPG or FC14.
It is not possible to extract Mistic-CRF$_{2\beta}$R in higher yields with $1\,\%$ DDM compared to $0.5\,\%$ FC14 (figure 2.15), even after $2.5\,$h.
The same applies to $0.5\,\%$ LDAO (figure 2.16). Only after $24\,$h, a band appeared at around $20\,$kDa. However, its molecular weight is too small to be the $68.5\,$kDa fusion protein. In figure 2.16, the intensities of the visualised bands for the FC14 extraction varied with time, probably due to pipetting mistakes. Nevertheless, it was assumed that after $3\,$h, no more receptor was extracted.
Additionally, LMPG and DMPC, either alone or in combination with FC14, were investigated (figure 2.17). $0.5\,\%$ LMPG was able to extract the same amount of fusion protein after $8\,$h as FC14. Also the mixture between FC14 and LMPG was capable to extract the fusion protein in higher amounts.
In contrast, other detergents such as FC12 and DHPC7 did not extract the fusion protein (figure 2.18).

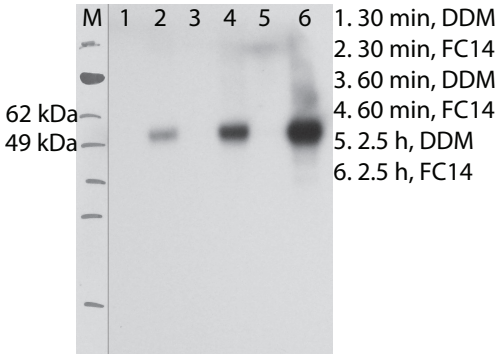

Figure 2.15: Western blot of a whole cell extraction of Mistic-CRF$_{2\beta}$R with $0.5\,\%$ FC14 and $1\,\%$ DDM using an anti-His$_6$-tag antibody. After $2.5\,$h of extraction, only FC14 was able to extract Mistic-CRF$_{2\beta}$R in high yields.

Different mixtures of FC14 and DDM were examined, too (figure 2.19). Remarkably, a

mixture of $0.25\,\%$ FC14 and $0.25\,\%$ DDM extracted $CRF_{2\beta}R$ as well as FC14 alone. Interestingly, detergents that were able to extract $CRF_{2\beta}R$ using the membrane protein fraction (even though at low yields) such as FC12, DDM, and LDAO [115] were not capable anymore to extract the receptor using the whole cell extraction method.

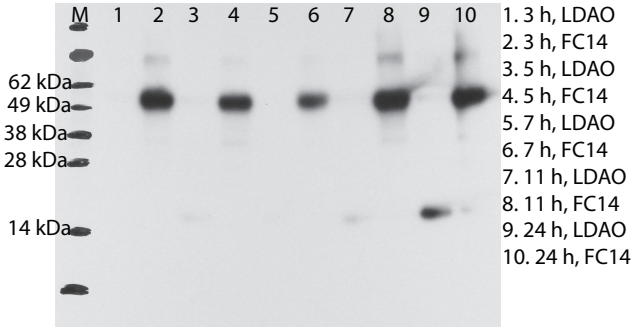

Figure 2.16: Western blot of a whole cell extraction of Mistic-$CRF_{2\beta}R$ with $0.5\,\%$ LDAO and $0.5\,\%$ FC14 using an anti-His_6-tag antibody. LDAO was not able to extract Mistic-$CRF_{2\beta}R$, only a band at around $20\,$kDa after $24\,$h appeared. FC14 was able to extract Mistic-$CRF_{2\beta}R$; the fluctuations of the intensity of the bands are probably due to pipetting mistakes.

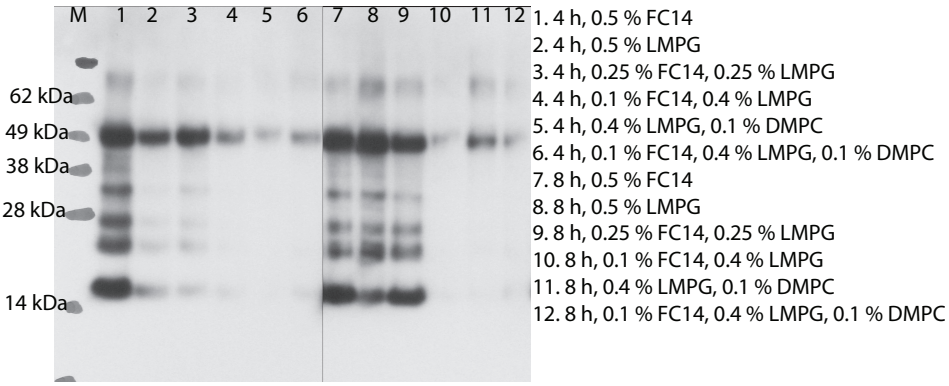

Figure 2.17: Western blot of whole cell extraction of Mistic-$CRF_{2\beta}R$ with different concentrations of FC14, LMPG, DMPC using an anti-His_6-tag antibody. No differences are visible between $4\,$h and $8\,$h using FC14. For LMPG alone and in mixture with FC14, higher yields of extraction resulted after $8\,$h than after $4\,$h. Mixture of LMPG and DMPC or of all three detergents gave smaller yields of extraction.

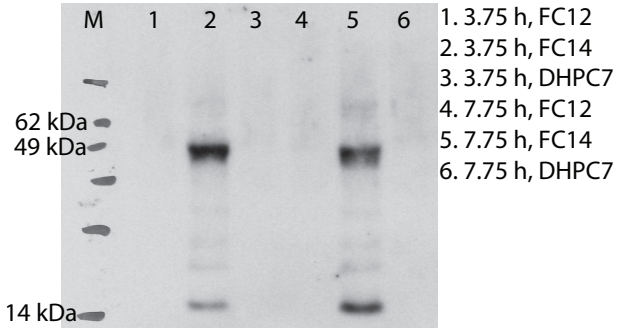

Figure 2.18: Western blot of whole cell extraction of Mistic-CRF$_{2\beta}$R with $1\,\%$ FC12 or $0.5\,\%$ FC14 or $1\,\%$ DHPC7 using an anti-His$_6$-tag antibody. Only FC14 extracted the receptor.

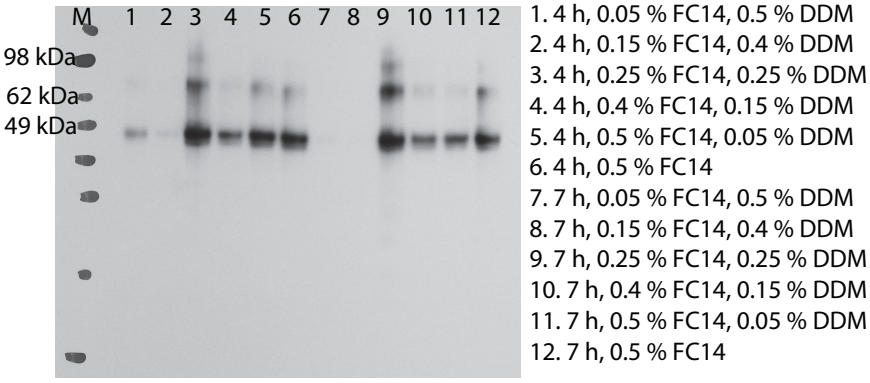

Figure 2.19: Western blot of whole cell extraction of Mistic-CRF$_{2\beta}$R with different ratios between FC14 and DDM using an anti-His$_6$-tag antibody. The highest yields were obtained for $0.25\,\%$ FC14 and $0.25\,\%$ DDM after $4\,$h.

Summarised, the highest yield for the extraction of Mistic-CRF$_{2\beta}$R was with the detergents FC14 or LMPG or a mixture of FC14 and DDM (figure 2.1).

To compare the yields and feasibility of purification, Mistic-CRF$_{2\beta}$R was extracted and further purified in the presence of these three detergents. In each buffer, cholesterol hemisuccinate (CHS) was added. When the receptor was extracted with FC14, the protein was purified with FC14; when it was extracted with FC14/DDM mixture, it was purified with DDM; when it was extracted with LMPG, it was further purified with LMPG (table 2.2). The yield after the Ni-NTA column was ca. $5\,\mathrm{mg\,L^{-1}}$ of culture for FC14, ca. $3\,\mathrm{mg\,L^{-1}}$ for DDM/FC14, and ca. $1.5\,\mathrm{mg\,L^{-1}}$ for LMPG.

The fusion protein was cleaved over night with human thrombin protease at $22\,^{\circ}$C and

Detergent	Detergent concentration [%]	Extraction efficiency
FC14/CHS	0.5/0.06	+++
DDM/CHS	1.0/0.12	-
FC14/DDM/CHS	0.05/0.5/0.06	+
FC14/DDM/CHS	0.15/0.4/0.06	+
FC14/DDM/CHS	0.25/0.25/0.06	+++
FC14/DDM/CHS	0.4/0.15/0.06	++
FC14/DDM/CHS	0.5/0.05/0.06	+++
LMPG	0.5	+++
FC14/LMPG/CHS	0.25/0.25/0.03	++
FC14/LMPG/CHS	0.1/0.4/0.012	+
LMPG/ DMPC	0.4/0.1	+
FC14/LMPG/DMPC/CHS	0.1/0.4/0.1/0.012	+
DHPC	1.0	-
FC12	1.0	-
LDAO	0.5	-

Table 2.1: Detergents and their efficiency to extract $CRF_{2\beta}R$ compared to 0.5 % FC14 with a whole cell extraction.

the next day loaded on a SEC Superdex 200 column (figure 2.20). For each sample, several elution peaks were observed. This indicated that several species were present in each sample and not only a single one, which is preferred for biochemical analysis. Surprisingly, the peaks of each sample purified with different detergents eluted at different retention times. This most probably resulted from the fact that each detergent has a different micelle size, each being built from a distinct number of detergent molecules.

Concentration of Detergent for Extraction	Concentration of Detergent for Purification
0.5 % FC14/0.06 % CHS	0.01 % FC14/0.0012 % CHS
0.25 % FC14/0.25 % DDM/0.06 % CHS	0.025 % DDM/0.003 % CHS
0.5 % LMPG/0.06 % CHS	0.025 % LMPG/0.003 % CHS
1 % DDM/0.12 % CHS	0.025 % DDM/0.003 % CHS

Table 2.2: Concentrations of detergents used for purification of $CRF_{2\beta}R$.

In order to asses the different activities of $CRF_{2\beta}R$ extracted in the three detergents,

a radioactive ligand binding assay was executed by Dr. Marilyn Perrin at the Clayton Foundation laboratory for Peptide Biology (Salk Institute, San Diego, USA) (figure 2.21). The antagonist [125-I-DTyr1]-astressin was used as radioactive ligand. Since the ligand might also bind unspecifically to the laboratory tools used for these measurements, the obtained result is a combination of specific and unspecific binding of the radioactive ligand. The specific binding can be calculated by subtracting the unspecific binding from the total binding. The unspecific binding can be measured by adding high amounts of non-labelled ligand to the sample with radioactive ligand, displacing the radioactive ligand from the specific binding. In this experiment, $500\,\mathrm{nM}$ not-labelled astressin was used for displacement.

The results indicate that the DDM/FC14 extracted and DDM purified protein gives the highest extent of specific binding in the activity assay. The signal for the FC14 extracted and purified $CRF_{2\beta}R$ was slightly lower than for the one, which was DDM/FC14 extracted. Replacing the detergent to LMPG, decreased the signal the most. However, high amount of unspecific binding is detected in this case. Thus the most active receptor is obtained by extracting with DDM/FC14 and purifying in DDM.

When the protein samples were remeasured after one week, the signal for $CRF_{2\beta}R$ purified with DDM was reduced slightly, while the signal for FC14 purified sample decreased about one third (data not shown). Therefore DDM was preferred for the purification and storage of the receptor.

Additionally, the activity of the different peaks obtained on the SEC with the Superdex 200 of the DDM purified $CRF_{2\beta}R$ were assessed by Dr. Perrin (figure 2.20). The peak eluted as first near the void volume gave the highest signal (data not shown).

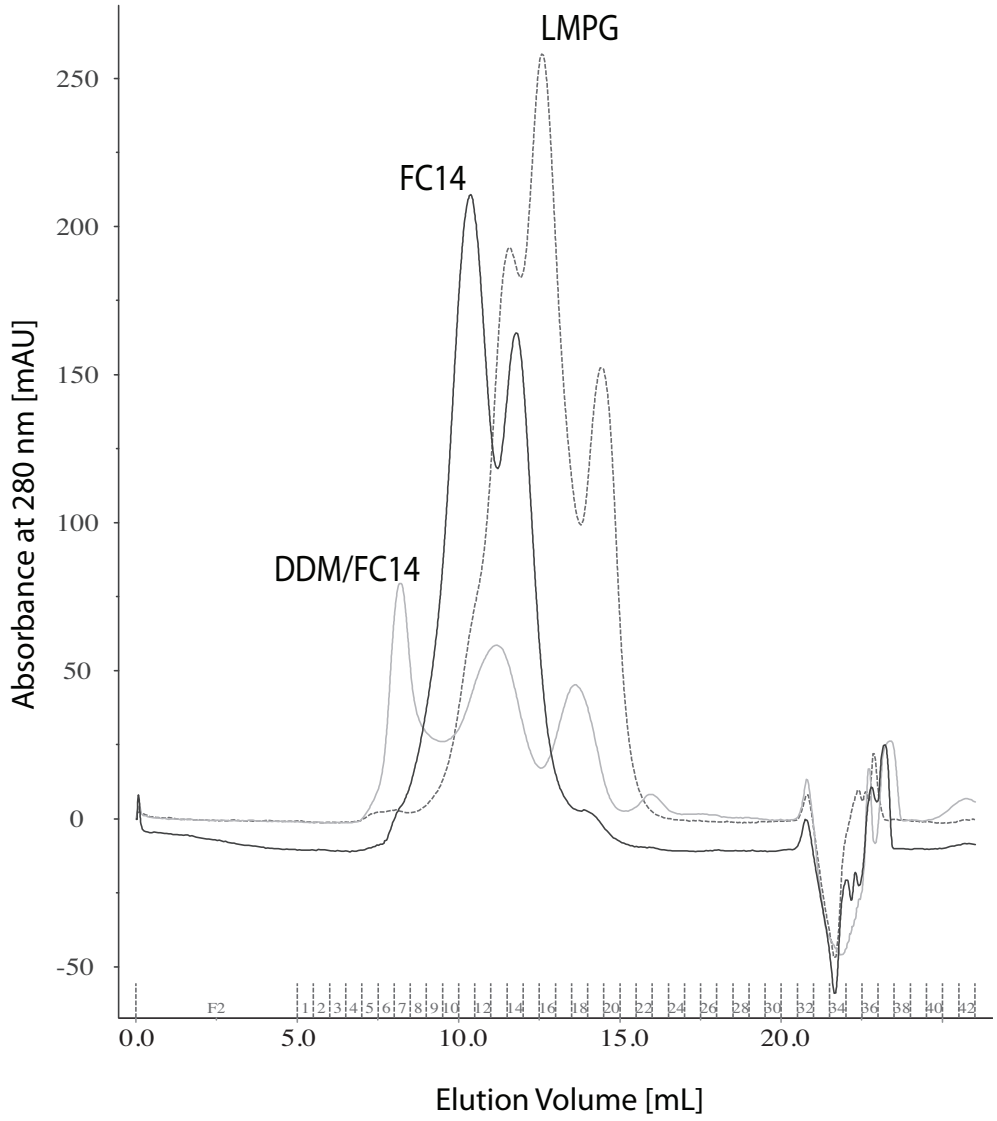

Figure 2.20: Size exclusion chromagroam of Superdex 200 of cleaved Mistic-$CRF_{2\beta}$R extracted and purified with different detergents. The chromatogram line assigned as DDM/FC14 was extracted with 0.25 % FC14/0.25 % DDM and purified with 0.025 % DDM. The line of FC14 was extracted with 0.5 % FC14 and purified with 0.01 % FC14. The line of LMPG was extracted with 0.5 % LMPG and purified with 0.05 % LMPG.

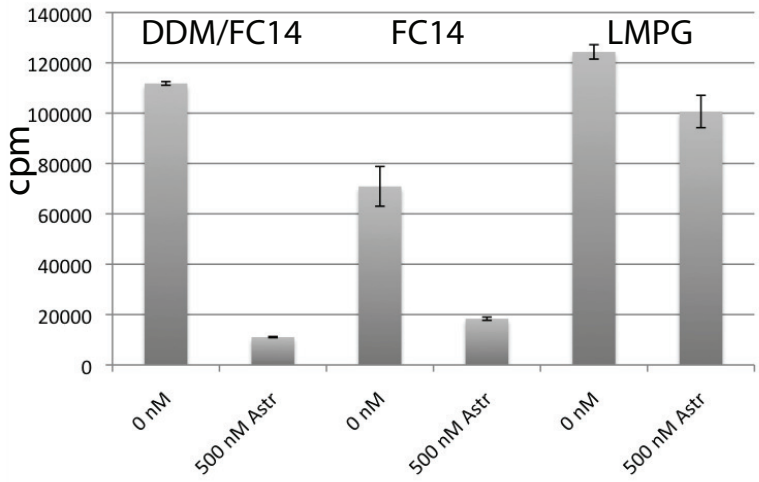

Figure 2.21: Radioactive ligand binding assay of purified samples using different detergents during extraction and purification. $CRF_{2\beta}R$ was extracted with either DDM/FC14, FC14 alone or LMPG alone and purified with DDM, FC14 or LMPG, respectively. The antagonists [125-I-DTyr1]-astressin was used as radioactive ligand. The specific binding was determined by subtracting the signal of the radioactive ligand in the presence of astressin (500 nM astressin) from the signal of the radioactive labelled ligand alone (0 nM). $CRF_{2\beta}R$ extracted with DDM/FC14 and purified with DDM resulted to have the highest activity.

Mistic-$CRF_{2\beta}$ Receptor Mutants

We considered to introduce in the $CRF_{2\beta}R$ sequence thermostabilising point mutations, which were used for the crystallisation of CRF_1R [43]. Those mutations rendered the CRF_1R more stable and thus facilitated its purification and crystallisation. Hence, they might also stabilise $CRF_{2\beta}R$ and ease its purification. The point mutations of CRF_1R were compared to the polar residues found to be important for ligand-biased signalling in the *secretin* family [17]. Mutating the polar residues may lock the receptor into a specific conformational state resulting in a biased signalling. Thus the point mutation $Y357A^{7.57}$ was chosen.

Additionally, a stop codon at the position 386 of the sequence (L386Stop) was introduced to $CRF_{2\beta}R$, as was for CRF_1R. Hollenstein et al. reported an increase of expression for the CRF_1 receptor, when the C-terminus was cleaved off [43].

The introduction of the Y357A mutation resulted in a higher yield of $CRF_{2\beta}R$ extracted with DDM, when compared to the wild type (figure 2.22 and 2.23). The highest yield of $CRF_{2\beta}R$ Y357A$^{7.57}$ extraction was achieved with $1\,\%$ DDM after $3.5\,h$. Introducing a stop codon at L386 also increased slightly the extraction yield compared to the native receptor, however, not as much as the point mutation Y357A.

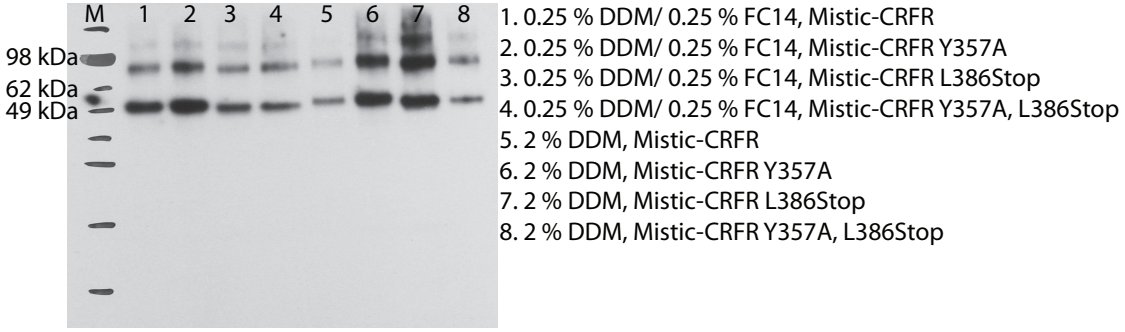

Figure 2.22: Western Blot of whole cell extraction of different mutants of Mistic-$CRF_{2\beta}R$ with either $0.25\,\%$ FC14/ $0.25\,\%$ DDM or $2\,\%$ DDM using an anti-His_6-tag antibody. Interestingly, different extraction yields were obtained for different mutants of Mistic-$CRF_{2\beta}R$. $2\,\%$ DDM gave about the same yield for the mutants as with $0.25\,\%$ FC14/$0.25\,\%$ DDM.

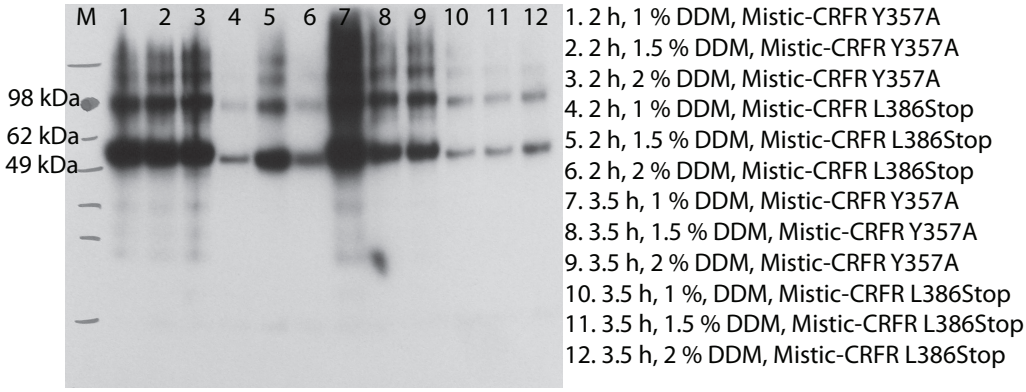

Figure 2.23: Western Blot of whole cell extraction of different mutants of Mistic-$CRF_{2\beta}R$ with different concentrations of DDM using an anti-His_6-tag antibody. Different yields were obtained for different mutants. The highest yields were obtained for Mistic-$CRF_{2\beta}R$Y357A with $1\,\%$ DDM after extracting for $3.5\,h$.

To investigate the yields and activities of the different mutants, $CRF_{2\beta}R$ and $CRF_{2\beta}R$ Y357A$^{7.57}$ were purified and examined with a radioactive ligand binding assay. Wild

type $CRF_{2\beta}R$ was extracted with DDM/FC14 as control, $CRF_{2\beta}R$ Y357A was extracted with either DDM/FC14 or DDM alone (table 2.2). All extracted proteins were further purified with 0.025 % DDM/0.003 % CHS. The mutant gave about 30 % higher yield than the wild type. If the higher yield resulted from a higher rate of expression, or a stabilisation of the receptor, was not investigated.

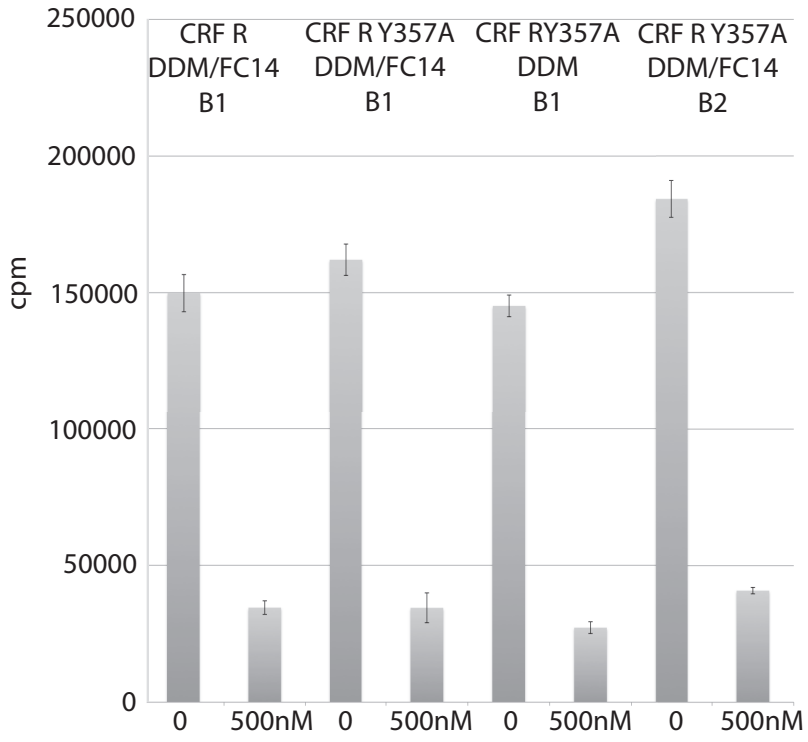

Figure 2.24: Radioactive ligand binding assay of purified $CRF_{2\beta}R$ and $CRF_{2\beta}R$ Y357A$^{7.57}$ using different detergents during extraction and purification. $CRF_{2\beta}R$ was extracted with DDM/FC14, $CRF_{2\beta}R$ Y357A$^{7.57}$ with either DDM/FC14 or DDM. The extracted fusion proteins were all further purified with DDM. The final samples were either in the buffer B1(50 mM TRIS, 500 mM NaCl, 20 % glycerol, 0.025 % DDM/0.003 % CHS) or in the buffer B2 (15 mM TRIS, 150 mM NaCl, 20 % glycerol, 0.025 % DDM/0.003 % CHS). The antagonists [125-I-DTyr1]-astressin was used as radioactive ligand. The specific binding is the subtraction of the signal of the radioactive labelled antagonists in the presence of astressin (500 nM astressin) from the signal of the radioactive labelled antagonist alone (0 nM).

The activities of the differently purified proteins were examined by Dr. Perrin. For the radioactive ligand binding assay, antagonists [125-I-DTyr1]-astressin was used. Specific binding was obtained by subtracting the unspecific binding (the displacement

of labelled from non-labelled astressin) from the specific and unspecific binding (the labelled radioactive ligand binding alone) (figure 2.24).
No difference in ligand binding was observed for the wild type and mutant. Furthermore, no difference was observed between the receptor extracted with the mixture of the detergents of DDM and FC14 or DDM alone. Additionally, a sample was measured with only 150 mM NaCl instead of 500 mM NaCl. The decreased salt concentration did not influence the stability of the receptor, either, as it was the case, for example, for apelin G protein- coupled receptor ([130]).

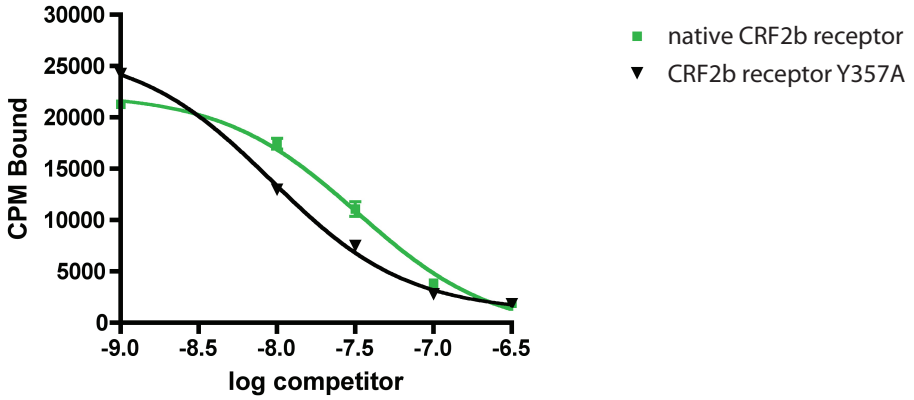

Figure 2.25: Estimation of inhibitory binding constant of astressin. The different concentrations of unlabelled astressin in the presence of a constant concentration of radioactive labelled astressin were plotted against the radioligand binding measured in counts per minute (cpm). Astressin had an affinity of 35 nM to the native $CRF_{2\beta}R$ and 11 nM the mutant $CRF_{2\beta}R$ Y357A.

Additionally to the activity test, the inhibitory binding constant K_i was measured by Dr. Perrin. K_i was examined for the native and mutated $CRF_{2\beta}R$ extracted with DDM/ FC14 (figure 2.25). Different concentrations of unlabelled antagonist astressin were measured in the presence of a constant concentration of radioactive labelled astressin [68]. The total radioligand binding measured in counts per minute (cpm) were plotted against the log of the unlabelled astressin concentration. The K_i value for the native $CRF_{2\beta}R$ was found to be 35 nM and 11 nM for the mutant $CRF_{2\beta}RY357A^{7.57}$. Thus the point mutation Y357A stabilises the receptor as was observed for CRF_1R by Hollenstein et al. [43].

2.2.5 Immobilised Metal Ion Affinity Chromatography

To purify a protein with a His_6-tag, different kinds of resin for affinity chromatography can be used. For example a Ni-NTA resin having nickel or a Talon® resin having cobalt as metal ion. His-tagged proteins should bind with higher specificity but lower affinity to the cobalt-resin than to the nickel-resin. Therefore the eluted sample from a cobalt resin should be purer. However, in the case for $CRF_{2\beta}R$, the nickel-resin could be washed with higher imidazole concentration due to its higher affinity to nickel, giving about equally pure receptor from nickel or cobalt resin (data not shown).
Additionally, batch resin binding was compared to normal gravity flow binding. In order to decrease the detergent concentration for the affinity binding, the sample was diluted, which resulted in large volumes. This was difficult to handle in batch mode. Additionally, higher amounts of resin was used for the batch binding in order to ensure a certain density of resin in the solution and thus an efficient binding. However, higher amount of resin also meant that more impurities could bind to the resin. Using different incubation times (e.g. 2h, 4h, over night) did not increase the concentration of eluted receptor. Therefore normal gravity flow binding was preferred with a drop wise flow of $1.5\,\mathrm{h}$ per litre of bacteria culture.

2.2.6 Thrombin Cleavage

Thrombin cleavage trials were performed to investigated conditions for a fully cleaved fusion protein. Different enzyme to substrate ratios were investigated, as well as different durations of cleavage, different additives ($MgCl_2$ or $CaCl_2$) and different detergents.
Full cleavage of the fusion protein at low ratio ($1\,\mathrm{mg}$ fusion protein to 7 NIH units of thrombin) was obtained only at $22\,^{\circ}\mathrm{C}$ (figure 2.26). When higher ratios were examined (*e.g.* 1:40, 1:60), the cleavage also occured at $4\,^{\circ}\mathrm{C}$ (figure 2.27). Adding $CaCl_2$ or $MgCl_2$ during the thrombin cleavage did not improve the efficiency (figure 2.27).
No difference in yields of cleaved receptor was observed in the presence of different

detergents.

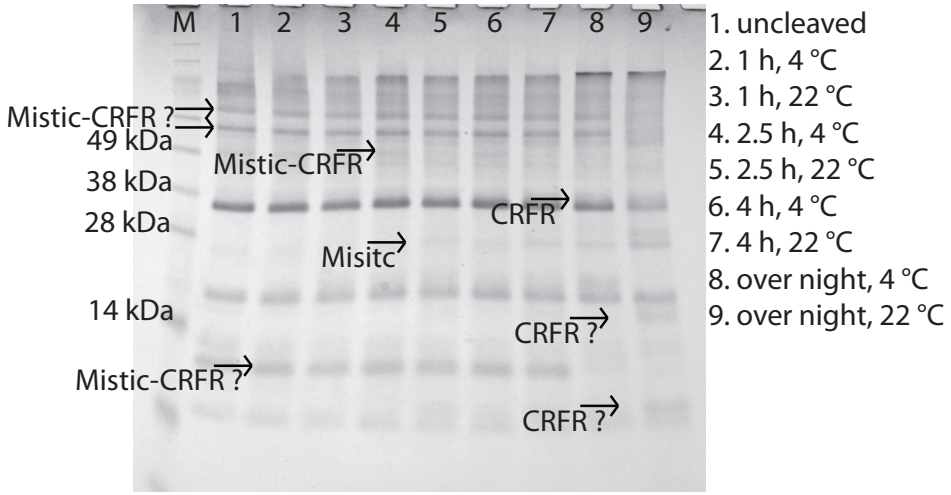

Figure 2.26: A NuPAGE® 12 % Bis-Tris gel of a thrombin cleavage trial of Mistic-CRF$_{2\beta}$R in FC14. The ratio between human thrombin and receptor was 1:7. Samples were taken at different time points. They were additionally incubated at different temperatures, 4° or ca. 22°. Many bands disappeared and appeared during the cleavage. When uncertain, what kind of protein represented a band due to its unusual molecular weight, a question mark was added. However, the highest amount of cleaved bands were obtained after an over night cleavage (ca 16 h) at RT. The cleavage trial was performed in the presence of 0.01 % FC14.

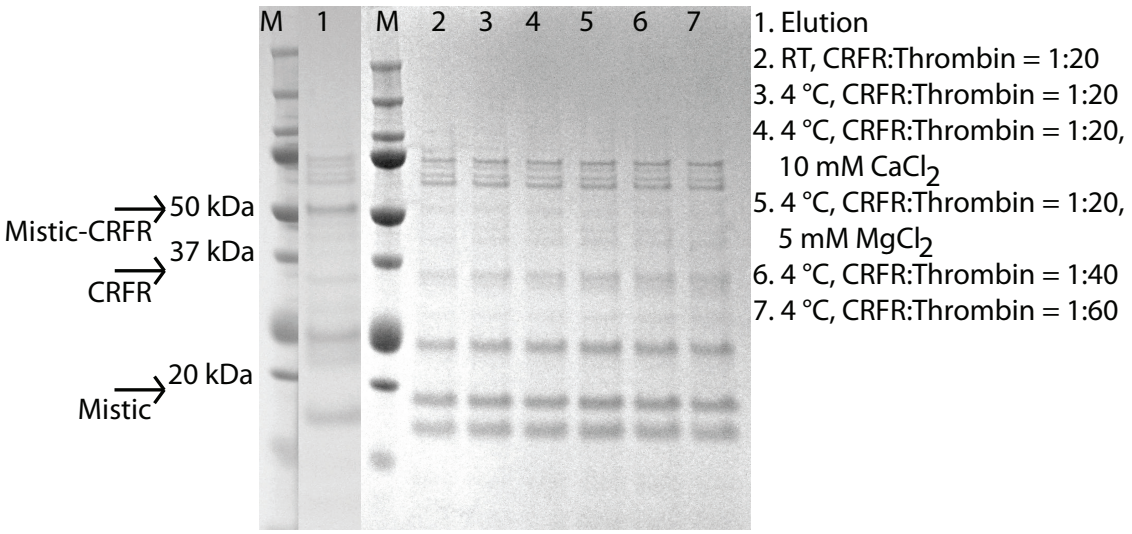

Figure 2.27: A NuPAGE® 12 % Bis-Tris gel of a thrombin cleavage trial of Mistic-CRF$_{2\beta}$R Y357A$^{7.57}$ in DDM. Different ratios between the receptor and thrombin were investigated at two temperatures, at 4° and ca 22°, including different additives. The additives did not increase the cleavage. With the ratio 1:40 almost all Mistic-tag was cleaved. Cleavage trail was performed in the presence of 0.025 % DDM.

2.2.7 Labelling of $CRF_{2\beta}$ Receptor for NMR Spectroscopy

Expressing $CRF_{2\beta}R$ in minimal medium for NMR-active isotopic labelling decreased the yield drastically. Depending on the extracting detergent, the yield of the purified receptor differed remarkably. For example for the extraction and purification with DDM, the final yield was about few ng of receptor per litre culture, while for the detergent FC14, few μg receptor per litre of culture were obtained. Therefore alternative expression conditions were explored.

A common way to increase the yield in minimal medium is to first grow the cells in a rich medium and, after reaching a certain cell density, transfer them to the minimal medium. Thus, $CRF_{2\beta}R$ was grown in TB up to an OD_{590} of 1, then the bacteria cells were centrifuged and resuspended in the minimal media. The cells were adapted to the new medium and induced with IPTG. Unfortunately, this method did not improve substantially the yield (figure 2.28).

Therefore, expression condition were varied for the minimal medium, as for example the induction temperature, the IPTG concentration or different durations of expression. They were analysed by Western blot using an anti-His_6-tag antibody. The optimal condition was an over night expression and induction at $29\,°C$ with $1\,mM$ IPTG (figure 2.28). However, the resulting sample of $CRF_{2\beta}R$ did not bind to Ni-NTA resin. A reason for this could be that the expressed receptor was unfolded or aggregated during the expression at higher temperature.

Thus another approach was investigated, namely the addition of Celtone® Base Powder (CBP) to the minimal medium. CBP is an hydrolysed algal powder, which contains a mixture of amino acids, peptides and vitamins. When added to a minimal medium, the minimal environment is turned into a 'rich' environment for bacterial growth and protein expression. As labelled CBP can be purchased, it can be also used for labelling proteins in minimal medium.

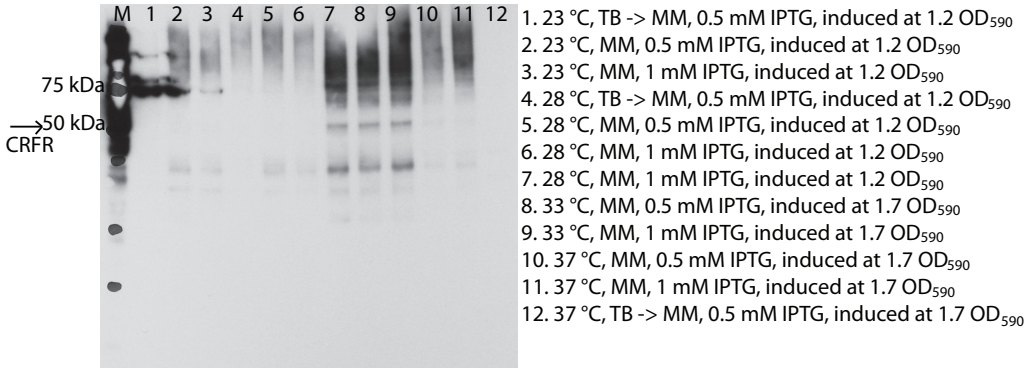

Figure 2.28: Western Blot of optimisation trial for a $50\,\%$ D_2O minimal media system with different IPTG concentrations and temperatures using Mistic-$CRF_{2\beta}R$. The primary antibody had an anti-His_6-tag specificity. The first description is the temperature at which the protein was expressed. The second description is the media used, where TB -> MM means that the cells were first grown in TB to a certain OD_{590}, centrifuged slowly at room temperature and resuspended in minimal media (MM). The third is the IPTG concentration and as last the OD_{590} at which the system was induced. Apparently, the highest yield is obtained inducing either at $28\,°C$ or $33\,°C$ using either $0.5\,mM$ or $1\,mM$ IPTG.

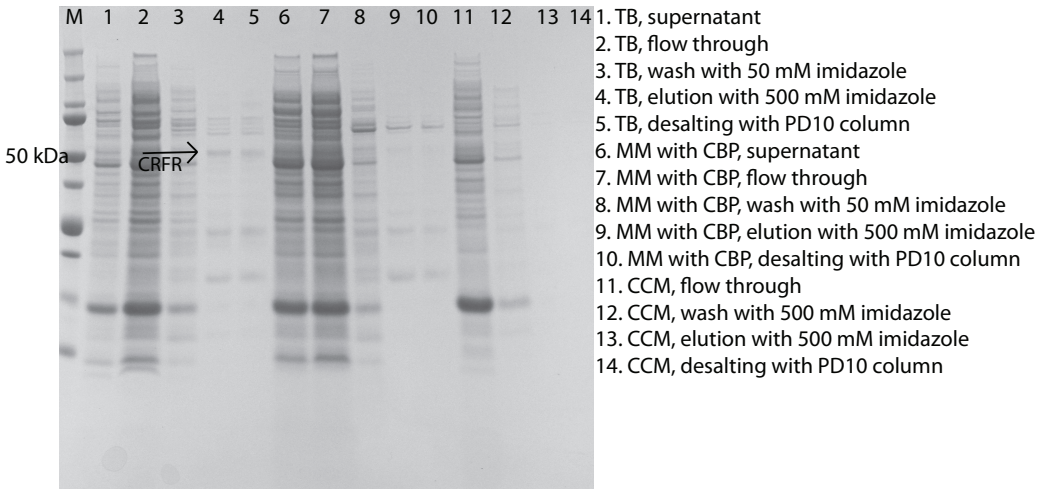

Figure 2.29: A NuPAGE® $12\,\%$ Bis-Tris gel of the purifications after expression in different media as for example Terrific Broth (TB), minimal media (MM) with $3\,g$ CBP or a ready to use bioexpress cell growth media (CCM) purchased from Cabridge Isotope Laboratories. Supernatant refers to extracted protein remained in the supernatant after centrifugation. Flow through is the flow through of the Ni-NTA resin, which was additionally washed. The protein was eluted from the Ni-NTA resin with a high imidazole concentration and immediatly desalted using a PD10 column to reduce the amount of imidazole.

Adding this rich medium powder to minimal medium increased the yield of expressed $CRF_{2\beta}R$. In particular the addition of $3\,g$ of CBP per litre of minimal medium restored

the yield to $0.5\,\mathrm{mg}$ per litre of culture, if extracted and purified in DDM, compared to $0.8\,\mathrm{mg}$ in TB medium (figure 2.29). Growing and expressing the receptor in a Celtone® complete medium (CCM), containing CBP readily dissolved, produced only low yields of $CRF_{2\beta}R$ (figure 2.29). The reason for this was not investigated.
Therefore, the receptor was expressed in the presence of CBP in minimal medium.

In summary, a new expression protocol was established for the mouse $CRF_{2\beta}R$. The fusion protein Mistic-$CRF_{2\beta}R$ was expressed instead of the (pelB-)$CRF_{2\beta}R$ as was used by Jappelli et al [115], as it gave about 3 times higher yield than the (pelB-)$CRF_{2\beta}R$ construct. When the protein was expressed unlabelled, TB was used as expression medium. When the receptor was labelled, minimal medium supplemented with Celtone® Base Powder gave the highest yield. The receptor was extracted from the whole cell lysate. DDM/FC14 mixture or DDM alone was used for the extraction of the receptor giving the highest amount of active receptor. The receptor was purified using nickel affinity resin containing $0.025\,\%$ DDM/ $0.003\,\%$ CHS. The receptor was bound to the resin via gravity flow. The receptor was then desalted and the fusion protein was cleaved with human thrombin protease over night at $4°$ at the ratio of $1\,\mathrm{mg}$ receptor to 40 NIH unit of human thrombin enzyme.

Chapter 3

Ligand Affinity Chromatography

Affinity chromatography techniques are a common tool for protein purifications [131]. This methodology is based on the specific interactions between either a metal ion to a specific tag, or an antibody to its antigen. It is also possible to take advantage of the affinity between a protein and its ligand. Ligand affinity chromatography is used in purification of proteins similarly to affinity chromatography techniques. The affinity ligand is immobilized on a solid support as for example a resin packed in a column. The obtained column can be used for the isolation of the desired and correctly-folded receptor under native conditions. The retained receptor can be dissociated by changing the buffer composition or using a competing agent in the mobile phase that displaces the receptor from the ligand bound to the resin [132]. Choosing the proper receptor-ligand interaction is a crucial factor to achieve a pure sample.

The ligand-affinity chromatography has been already adopted for the purification of GPCRs as a purification tool [67, 114, 133–135]. It ensures the selection of the folded species and its homogeneity for further biochemical analysis.

In this chapter the preparation of an affinity ligand column and its protocol of usage are described. Astressin was chosen as ligand due to its high affinity to the $CRF_{2\beta}R$ and to the first extracellular domain (ECD) of $CRF_{2\beta}R$ ($0.62\,\text{nM}$ and$10.7\,\text{nM}$, respectively) [29]. It is an antagonist for the CRF receptors (see further in chapter 1: 'Introduction, *Secretin* family: Corticotropin-Releasing Factor Receptor, Ligand and Ligand

Binding'). First the validity of the column is ensured and a purification protocol for the astressin-affinity column is established by using a well-known system, the ECD of $CRF_{2\beta}R$. Afterwards the binding-, washing-, elution-buffer conditions are transferred to the purification for $sCRF_{2\alpha}R$ and $CRF_{2\beta}R$.

3.1 Binding and Elution of the Extracellular Domain of $CRF_{2\beta}$ Receptor

The first extracellular domain of the $CRF_{2\beta}R$ was chosen to set the method. Its purification protocol is established [112] and its structure derived from NMR spectroscopy measurements has been published in complex with and without the antagonist astressin [27, 38]. Grace et al. also showed that the ECD-ligand complex could be dissociated using low pH [38]. This discovery can be used for the dissociation of the receptor from the ligand-affinity column.
The ECD was expressed and purified as described by Perrin et al. [112]. However, instead of using S-protein-agarose for affinity, nickel affinity resin was chosen for immobilised metal ion affinity chromatography. As last purification step, reverse phase HPLC chromatography was used on the ECD of $CRF_{2\beta}R$ as described in Chapter 7 of this thesis in 'Material and Methods, purification by RP-HPLC'. The largest peak was collected and lyophilised. In order to investigate the proper binding and elution buffer compositions for the astressin-affinity chromatography, the protein powder was dissolved in the binding buffer shortly before usage.
As a first trial, isocratic elution was investigated. For binding and washing, the buffer composition was the same as used during the purification of the ECD [112]. Additional buffers were investigated by slightly changing the pH and the NaCl concentration (table 3.1). No changes in ECD binding was observed depending on the binding buffer and therefore, the buffer composition of $10\,\mathrm{mM}$ Tris and $50\,\mathrm{mM}$ NaCl at pH 8 was chosen as binding condition.

For the elution, a buffer was chosen at pH 4 (table 3.1), as a dissociation of the ligand-ECD complex was observed at this pH in the publication of Grace et al in 2007 [27]. However, the change in pH only did not result in the expected dissociation of the complex. Therefore, different salts and salt concentrations were investigated (table 3.1). High salt concentration might have an influence in the disruption of the salt bridge in the structured ECD and thus separating the receptor. However, high salt concentration did not show the expected result of eluting the protein.
Since not only electrostatic interactions are formed but also hydrophobic interactions between the amphipathic astressin and the hydrophobic residues on the ECD, DDM or glycerol was added to the elution buffer. Their hydrophobic properties might mask and thus disrupt the hydrophobic interactions between the ligand and ECD. But adding them to the elution buffer did not dissociate the complex, either.

Binding Buffer A	Elution Buffer B
25 mM Tris, 150 mM NaCl, pH 8	50 mM acetic acid, 150 mM NaCl, pH 4.0
25 mM Tris, 150 mM NaCl, pH 7.4	50 mM acetic acid, 1000 mM NaCl, pH 4.0
10 mM Tris, 50 mM NaCl, pH 8	50 mM acetic acid, 2000 mM $MgCl_2$, pH 4.0
	50 mM acetic acid, 1000 mM KNO_3, pH 4.0
	50 mM acetic acid, 50 mM NaCl, 0.5 % DDM, pH 4.0
	50 mM acetic acid, 50 mM NaCl, 0.005 % DDM, pH 4.0
	50 mM acetic acid, 1 M NaCl, 5 % glycerol, pH 4.0
	50 mM acetic acid, 50 mM NaCl, 1 M Gu · HCl, pH 4.0
	50 mM acetic acid, 50 mM NaCl, 2 M Gu · HCl, pH 4.0
	50 mM acetic acid, 4 M Gu · HCl, pH 4.0
	50 mM acetic acid, 5 M Gu · HCl, pH 4.0
	50 mM acetic acid, pH 3.5
	50 mM acetic acid, pH 3.0

Table 3.1: Different binding and elution solution compositions tested for the elution of the ECD of the $CRF_{2\beta}R$ from the biotinylated astressin ligand affinity column. Varying the pH or NaCl concentration did not influence the binding to the affinity column and thus 10 mM Tris, 50 mM NaCl, pH 8 was chosen as binding buffer. For the elution buffer composition, many different salts and salt concentration were tested. Elution of the ECD was achieved in 50 mM acetic acid, pH 3.0 or pH 3.5.

In summary, varying the salt, glycerol and DDM concentration and lowering the pH from 8.0 to 4.0 did not work either as elution buffer. Therefore a chaotropic agent was

added to the elution buffer to examine, if it was possible to disrupt the ligand-ECD complex. The ECD could only be eluted at a concentration of 5 M Gu · HCl. However, this elution condition is not desired since it might unfold the ECD and eventually the $CRF_{2\beta}R$ and it is expected to be a challenge to refold a GPCR from its unfolded state.
In the search of finding an elution buffer, it was noted that washing the column with water eluted constantly a little amount of ECD. This finding indicated that salt itself dampened the disruption of the ECD-astressin complex. Consequently, the buffer composition of 50 mM acetic acid at pH 3.0 or pH 3.5 eluted the ECD. Thus, only the combination of low pH and the absence of salt could dissociate the ECD from its antagonist.

Buffer B1	Buffer B2	Gradient of buffer B2
50 mM acetic acid, pH 4.0	50 mM acetic acid, pH 3.0	0 % to 100 % in 30 min
50 mM acetic acid, 50 mM NaCl, pH 3.5	50 mM acetic acid, pH 3.5	50 % to 100 % in 20 min

Table 3.2: The buffer conditions used for washing and elution with a gradient. The one between 50 mM acetic acid, 50 mM NaCl, pH 3.5 to 50 mM acetic acid, pH 3.5 from 50 % to 100 % in 20 min separated impurities from the ECD the best.

As a next step, a gradient elution was examined for the removal of impurities and not correctly folded ECD from the astressin-affinity column. Based on the obtained knowledge of the possible elution conditions, gradients for the washing and elution were created (table 3.2). Separation of the ECD from impurities and from the incorrectly folded ECD were obtained with a gradient between the buffers 50 mM acetic acid, 50 mM NaCl, pH 3.5 to a buffer with 50 mM acetic acid, pH 3.5 (figure 3.1).
To verify that the eluted ECD from the astressin affinity column was correctly folded, an [^{15}N, ^{1}H]-heteronuclear single quantum coherence ([^{15}N, ^{1}H]-HSQC) spectrum was recorded and compared to a published one of the ECD, which corresponded to each other. Also the eluted ^{15}N-labelled ECD was measured alone and then with the cyclo(30-33) α-helical $CRF_{(9\text{-}41)}$, an antagonist for the CRF receptors (figure 3.2). Adding the antagonist to the ECD resulted in clearly visible shifts, which were equivalent to the published [^{15}N, ^{1}H]-HSQC with an antagonist [27].
The proton shifts of the tryptophan peaks of the eluted ECD from the astressin-affinity

column were visible at around 10.8 ppm, indicating that the eluted ECD was folded. Upon addition of the antagonist the splitting of the tryptophans peaks was observed, which moved downfield (ca. 10.2 ppm) and upfield (>10.8 ppm) (figure 3.2). This is consistent with the observation of Grace et al. [27].

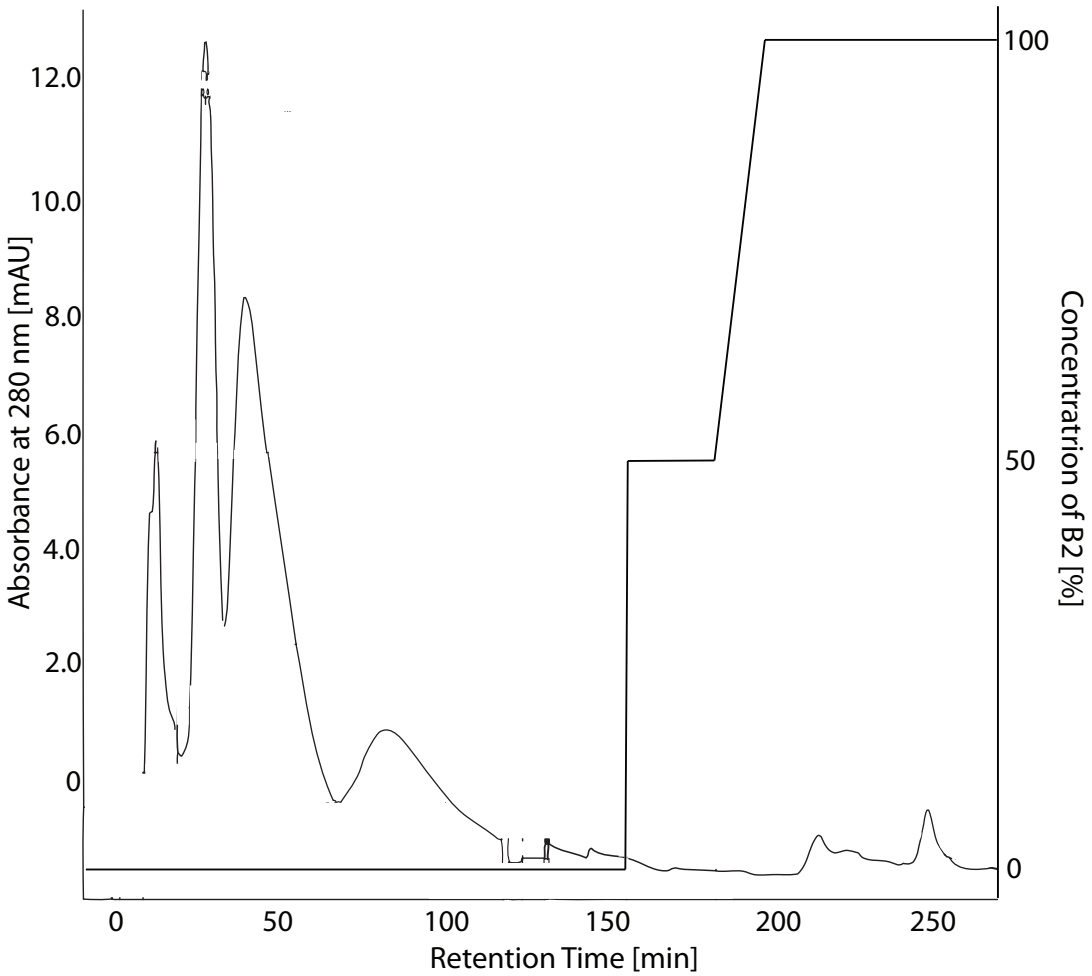

Figure 3.1: Elution chromatogram of the ECD-$CRF_{2\beta}$R using the astressin affinity column. An elution gradient was used from 50 mM acetic acid, 50 mM NaCl, pH 3.5 to 50 mM acetic acid, pH 3.5 from 50 % to 100 % in 20 min. The last peak was collected.

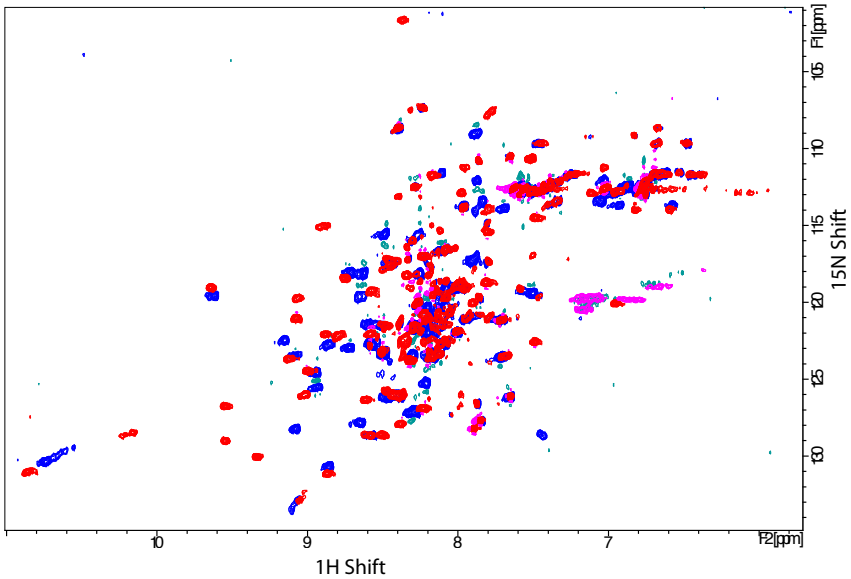

Figure 3.2: 2D [^{15}N, ^{1}H]-HSQC NMR spectrum of 40 µM ECD of CRF$_{2\beta}$R was measured on a 700 MHz Bruker NMR spectrometer at 25 °C. The ECD was measured in 50 mM acetic acid at pH 6.2. The blue spectrum is the one of ECD alone, the red spectrum is that of the ECD with the antagonist cyclo(30-33) α-helical CRF $_{(9\text{-}41)}$. In the blue spectrum, the peaks of the tryptophans are found at around 10.8 ppm indicating a folded ECD. The addition of the antagonist shifted the peaks of the tryptophans as it was observed by Grace et al upon addition of their antagonist [27].

3.2 Binding and Elution of soluble CRF$_{2\alpha}$ Receptor

The established gradient method of the ECD was then applied to sCRF$_{2\alpha}$R. The binding buffer was 10 mM Tris, 50 mM NaCl, pH 8 and washing and elution were performed with a gradient from 50 mM acetic acid, 50 mM NaCl, pH 3.5 (B1) to 50 mM acetic acid, pH 3.5 (B2) with B2 going from 50 % to 100 % in 20 min.

A similar elution profile was obtained for sCRF$_{2\alpha}$R as for the ECD of CRF$_{2\beta}$R (figure 3.3) with a difference of the elution peak. While the elution peak for the ECD always consisted of one sharp peak, in the elution profile of sCRF$_{2\alpha}$R a shoulder is visible (figure 3.3). The ratio between the first and the second peak depended on the amount of protein loaded on the astressin-affinity column. If less than 1 mg L^{-1} was loaded, two

separated peaks were eluted with the first peak being larger than the second peak. Loading the double amount of sample resulted already in a 1:1 ratio between the first and second peak (data not shown). When about 10 times the amount was loaded (> $10\,\mathrm{mg\,L^{-1}}$), the elution profile of figure 3.3 was obtained.

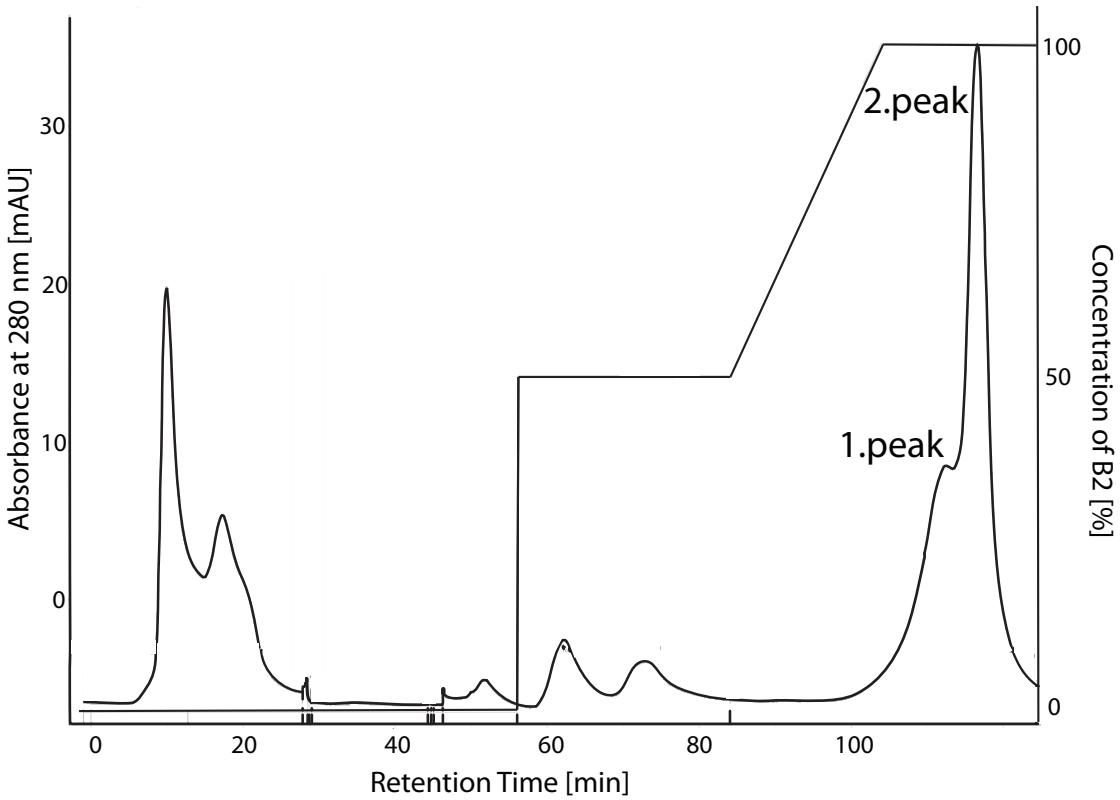

Figure 3.3: Elution chromatogram of $sCRF_{2\alpha}R$ using the astressin-affinity column. As binding buffer, 10 mM Tris, 50 mM NaCl, pH 8 is used and the washing and elution is performed with the gradient method from 50 mM acetic acid, 50 mM NaCl, pH 3.5 (A) to 50 mM acetic acid, pH 3.5 (B) starting from from 50 % to 100 % B in 20 min. In contrast to the ECD of the $CRF_{2\beta}R$, two peaks were observed labelled as peak 1 and peak 2.

Comparing the 2D [^{15}N, ^{1}H]-HSQC spectra of the first and second peak of the astressin-affinity column of a ^{15}N-labelled $sCRF_{2\alpha}R$, did not show any differences (data not shown).

If the $sCRF_{2\alpha}R$ were folded, a similar [^{15}N, ^{1}H]-HSQC spectrum would have been expected as that of the ECD of $CRF_{2\beta}R$ due to the sequence similarities between $sCRF_{2\alpha}R$

and the ECD of $CRF_{2\beta}R$ (around 60 %), and due to the same short consensus repeat fold found for all ECDs of the *secretin* family. In the 2D [^{15}N, ^{1}H]-HSQC of figure 3.4, one strong peak was found at around 10 ppm and a weaker peak at around 11 ppm indicating the eluted $sCRF_{2\alpha}R$ had very little folded species.
It was hypothesised that the unfolging of $sCRF_{2\alpha}R$ might have occurred during its elution conditions or that unfolded soluble receptor might elute simultaneously from the astressin-affinity column as folded $sCRF_{2\alpha}R$.

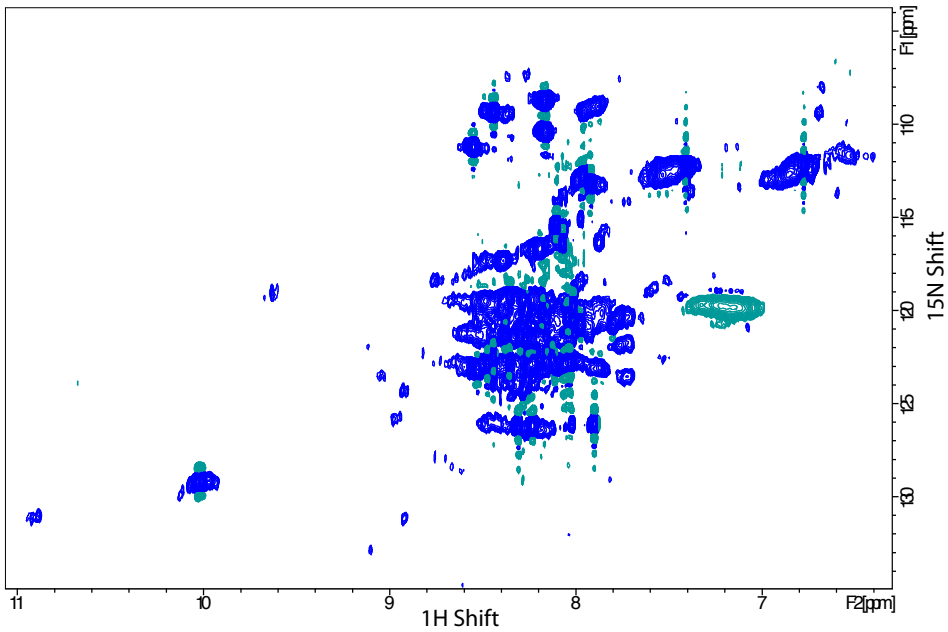

Figure 3.4: 2D [^{15}N, ^{1}H]-HSQC NMR spectrum of 270 µM $sCRF_{2\alpha}R$, collected from the first peak, was measured on a 700 MHz Bruker NMR spectrometer at 25 °C. The $sCRF_{2\alpha}R$was measured in 50 mM acetic acid at pH 6.2. A strong peak was observed at a ^{1}H-shift of 10 ppm and a waker peak at 10.8 ppm indicating that most of the $sCRF_{2\alpha}R$ is unfolded.

However, the eluted ECD of $CRF_{2\beta}R$ had no unfolded species, which was verified via 2D [^{15}N, ^{1}H]-HSQC spectrum. Therefore the elution buffer was excluded as cause for the unfolding of $sCRF_{2\alpha}R$. Measuring a [^{15}N, ^{1}H]-HSQC spectrum of an unfolded

$sCRF_{2\alpha}R$ sample in absence and in presence of astressin, did not result in any chemical shifts changes, which excludes a direct binding between the unfolded soluble receptor and astressin. However, the unfolded species might not bind directly to astressin, but unspecifically to the folded $sCRF_{2\alpha}R$ or to the resin and thus being eluted at the same time.

3.3 Binding and Elution of $CRF_{2\beta}$ Receptor Y357A

For the following experiments, the mutant Y357A was used, as it gave a higher yield than the native receptor and no differences in binding affinities were found with respect to the native protein (see chapter 2, 'Expression and Purification of CRF Receptor Related Proteins, $CRF_{2\beta}R$, Extraction, Mutants').
The established binding and elution conditions for the astressin-affinity chromatography of the ECD had to be adapted to the corticotropin-releasing factor receptor 2β ($CRF_{2\beta}R$) Y357A. First of all, $0.025\,\%$ DDM/$0.003\,\%$ CHS was added to all buffers for a membrane mimicking environment. Second, washing the bound receptor with $50\,\text{mM}$ acetic acid, $50\,\text{mM}$ NaCl, pH 3.5 already eluted the receptor in contrast to the ECD of $CRF_{2\beta}R$ and $sCRF_{2\alpha}R$. This difference was not due to the presence of DDM since ca. 20 times higher DDM concentration did not dissociate the ECD from the ligand.
Additionally, the elution at pH 3.5 with $50\,\text{mM}$ NaCl had a lot of impurities. The bound impurities might have been alpha helical membrane proteins, which also bound unspecifically to the hydrophobic properties of astressin [136].
Thus a new washing and elution buffer had to be found. Regarding the washing buffer, two approaches were investigated: either the purity of the sample was improved before loading it on the astressin-affinity column or the washing buffer had to be further optimised. To obtain a purer sample of the receptor, the thrombin cleaved elution of the Ni-NTA column was loaded again on a second nickel affinity column. While the His-tagged-Mistic and impurities, which bound to the first Ni-NTA column, should bind again to the Ni-resin, the receptor should be eluted with low imidazole

concentrations. However, the cleaved Mistic-CRF$_{2\beta}$R had a high affinity to the nickel resin. Therefore high concentrations of imidazole (> 100 mM) were needed to elute the cleaved Mistic-CRF$_{2\beta}$R. Unfortunately, this imidazole concentrations also eluted impurities. Thus improving the purity of CRF$_{2\beta}$R using a second nickel affinity column was not feasible.

Buffer B1	Buffer B2	Gradient to buffer B2
10 mM Tris, 150 mM NaCl, pH 8	10 mM Tris, pH 8	0 % to 100 % in 10 min
50 mM acetic acid, 150 mM NaCl, pH 4.0	50 mM acetic acid, 50 mM NaCl, pH 3.5	0 % to 100 % in 10 min
10 mM Tris, 150 mM NaCl, pH 8.0	50 mM acetic acid, 50 mM NaCl, pH 4	0 % to 100 % in 10 min
50 mM acetic acid, 150 mM NaCl, pH 5.0	50 mM acetic acid, 50 mM NaCl, pH 4	0 % to 100 % in 10 min
10 mM acetic acid, 150 mM NaCl, pH 3.5	10 mM acetic acid, pH 3.5	0 % to 100 % in 10 min

Table 3.3: The buffer conditions used for washing and elution with a gradient. The gradient from10 mM acetic acid, 150 mM NaCl, pH 3.5 to 10 mM acetic acid, pH 3.5 from 0 % to 100 % in 10 min separated the impurities and eluted receptor the best. 5 % glycerol was added to all buffers.

Therefore, several washing steps were examined on the ligand-affinity column. First, a washing step at pH 8 with no salt was performed. Salt can increase hydrophobic interactions and thus omitting it in the washing step, unspecific hydrophobic interactions might be decreased. Surprisingly, having no salt at pH 8 also eluted the receptor. Increasing the pH for the washing buffer from 3.5 to 4 did not eliminate impurities either, since the receptor also eluted at pH 4. Thus a gradient between pH 8 and pH 4 was performed to investigate at which pH the receptor would elute. All peaks were collected and loaded on a 12 % NUPAGE®-SDS gel to evaluate in which peaks the eluted CRF$_{2\beta}$R was present. The pH was measured from the identified samples. The CRF$_{2\beta}$R eluted at around pH 4.5 when 50 mM NaCl was present (data not shown). A washing and elution buffer were produced with the obtained knowledge of the behaviour of the CRF$_{2\beta}$R on the astressin-affinity chromatography. A 50 mM acetic acid buffer with 150 mM NaCl at pH 5.0 was used as washing buffer. The receptor was eluted with a gradient from the washing buffer to the elution buffer B2 (50 mM acetic acid including 50 mM NaCl at pH 4). The gradient was performed from 0 % to 100 % B2 in 10 min (figure 3.5). 5 % glycerol, 0.025 % DDM and 0.003 % CHS were added to all buffers. However, with this elution conditions, only a broad elution peak was ob-

tained.

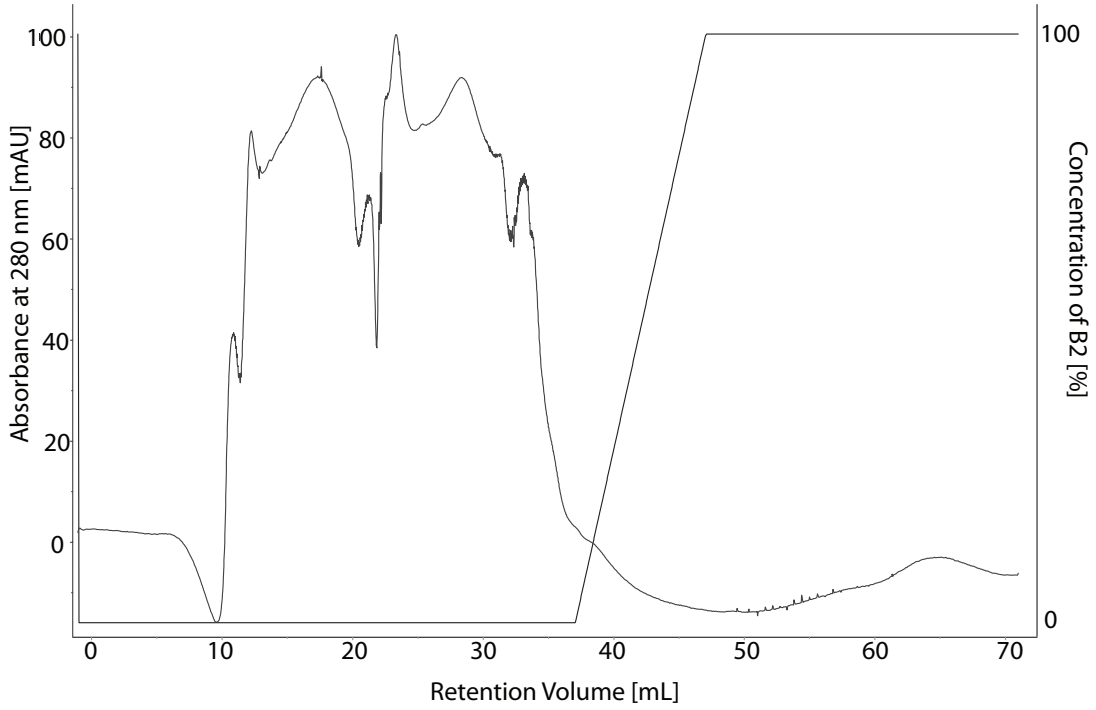

Figure 3.5: Elution chromatogram of $CRF_{2\beta}R$ Y357A using the astressin-affinity column. As a binding buffer, 10 mM Tris, 50 mM NaCl, pH 8 is used and the washing and elution is performed with a gradient from 50 mM acetic acid, 150 mM NaCl, pH 5.0 to 50 mM acetic acid, 50 mM NaCl, pH 4 from 0 % to 100 % in 10 min. 5 % glycerol and 0.025 % DDM and 0.003 % CHS were added to each buffer.

However, when the sodium chloride concentration was kept constant to 150 mM, the $CRF_{2\beta}R$ surprisingly did not elute even at pH 3.5. Only when the salt concentration was decreased the receptor dissociated from its antagonist (figure 3.6).

Also, if 500 mM NaCl was used in the binding buffer, no receptor was found in the flow through (FT). But washing the affinity column with 150 mM NaCl at pH 8 (WpH8, 150 mM NaCl), eluted some receptor, indicating that it was not fully correctly folded. Washing with a buffer at pH 5 including 150 mM NaCl (WpH5, 150 mM NaCl) did not elute the receptor. Decreasing the pH further to 3.5 with a gradient eluted impurities and also some receptor (Wgrad). When the salt concentration was lowered to zero, the receptor finally eluted completely (figure 3.6).

A radioactive ligand binding assay was performed on different washing and elution fractions of the astressin-affinity chromatography by Dr. Marilyn Perrin at the Clayton Foundation laboratory for Peptide Biology (Salk Institute, San Diego, USA) (figure 3.8). Neither of the washing fractions exhibited an activity, only the elution showed an affinity to astressin in the radioactive ligand binding assay.

Interestingly, before the ligand-affinity column, the $CRF_{2\beta}R$ is found as a monomer on a NuPAGE® 4 % to 12 % Bis-Tris gel; however, after using the astressin-affinity chromatography, $CRF_{2\beta}R$ is found as monomer, dimer and probably multimer (figure 3.7). If it is due to the elution buffer or due to the ligand-affinity column, has not been investigated yet.

The impurities in the eluted sample could be avoided, if instead of a isocratical elution, a gradient was chosen between the last washing buffer at pH 3.5 with 150 mM NaCl to a buffer at pH 3.5 without any salt (figure 3.3).

Summarised, a sample with least amount of impurities was obtained, when the buffer for the binding was 10 mM Tris, 500 mM NaCl, pH 8. Washing the ligand-affinity column was performed with 10 mM acetic acid, 150 mM NaCl, pH 3.5. The receptor was eluted with a gradient between the washing buffer and an elution buffer of 10 mM acetic acid pH 3.5 without salt in 10 min. 5 % glycerol and 0.025 % DDM and 0.003 % CHS were added to all buffers.

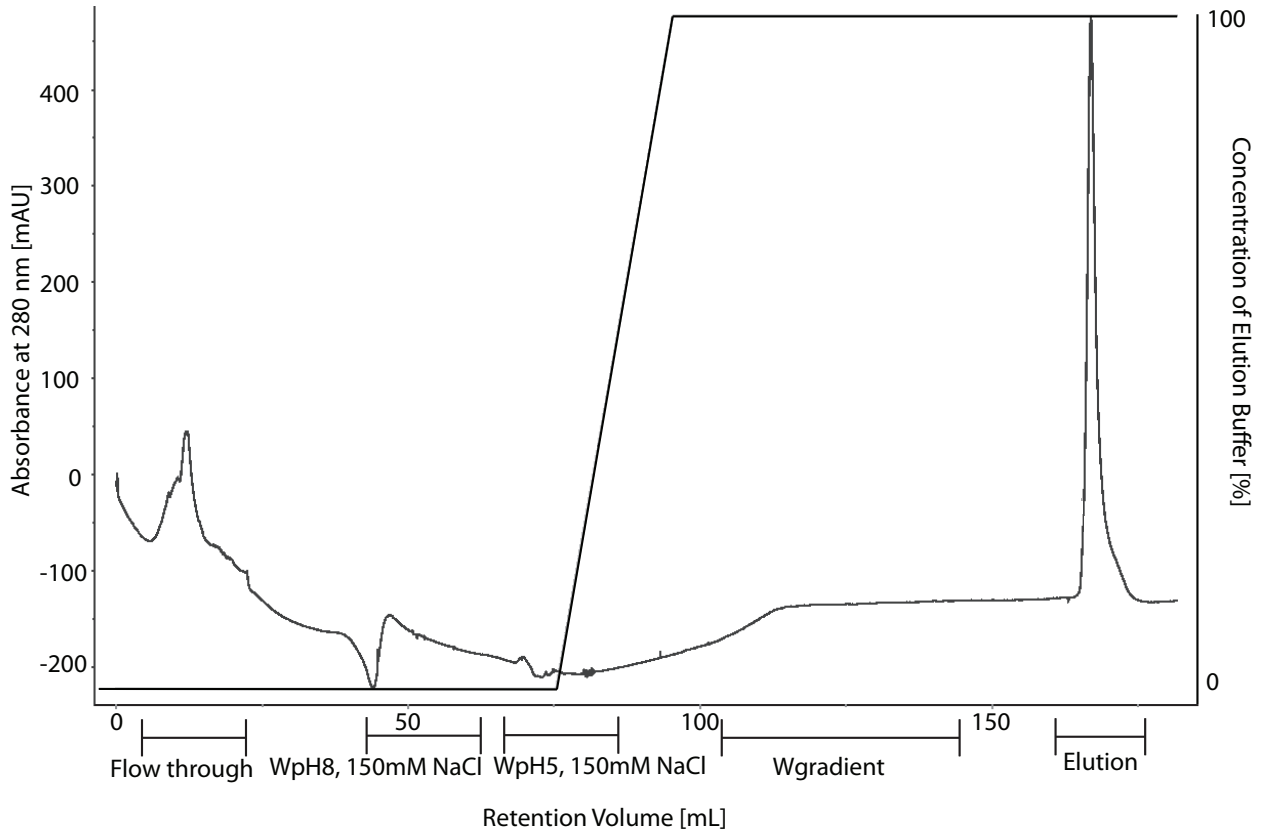

Figure 3.6: Elution chromatogram of $CRF_{2\beta}R$ Y357A$^{7.57}$ using the astressin-affinity chromatography. The flow through at pH 8, the wash with 150 mM NaCl at pH 8 (W150), the wash with 150 mM NaCl at pH 5 (WpH5), and the gradient wash from pH 5 to pH 3.5 in 20 min in the presence of 150 mM NaCl were collected in 15 ml aliquots. The buffer was exchanged from the eluted receptor at pH 3.5 without any salt to pH 8 with 150 mM NaCl and was immediately stored at 4 °C. 0.025 % DDM/0.003 % CHS and 5 % glycerol were present in all buffers.

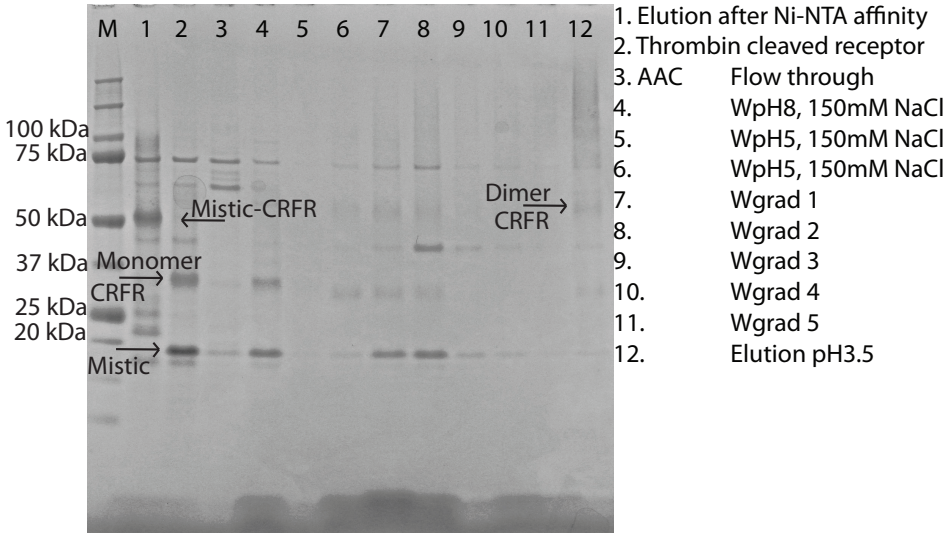

Figure 3.7: NuPAGE® 4 % to 12 % Bis-Tris gel of $CRF_{2\beta}R$ Y357A$^{7.57}$ of collected fractions from the astressin-affinity chromatography (AAC).

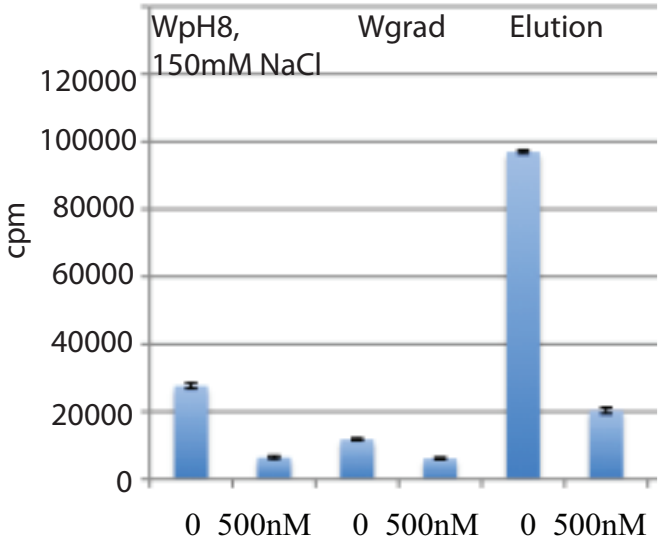

Figure 3.8: Radioactive ligand binding assay of the washing and elution fractions of the astressin-affinity chromatography of $CRF_{2\beta}R$ Y357A. The washing step with the buffer 10 mM Tris, 150 mM NaCl (WpH8, 150 mM NaCl), and the gradient fractions between the first washing buffer and the buffer of 10 mM acetic acid, 150 mM NaCl (Wgrad) and the final eluted fraction were tested. Only the elution exhibited a high ligand affinity, whereas the washes almost none. The antagonists [125-I-DTyr1]-astressin was used as radioactive ligand. The specific binding is the subtraction of the signal of the radioactive labelled antagonists in the presence of astressin (500 nM astressin) from the signal of the radioactive labelled antagonist alone (0 nM).

Chapter 4

NMR of $CRF_{2\beta}$ Receptor

Compared to the many crystal structures solved for GPCRs so far, very few NMR studies on GPCR-systems are known. There are two reasons for this, one is the large amount of protein needed for NMR spectroscopy measurements (ca. $0.1\,\mathrm{mg}$ to $5\,\mathrm{mg}$ in ca. $100\,\mu\mathrm{L}$ to $300\,\mu\mathrm{L}$) [80] and the second is that the receptor should be grown in a expression system, where isotope labelling is feasible. *E.coli* is preferred, since it is a well established expression system for uniform or selective labelling of proteins [80]. However, the expression of GPCRs are rather low in *E.coli* [80]. By far the highest obtained yield for a GPCR in *E.coli* has been for a folded triple labelled chemokine receptor CCR5 (^{2}H, ^{13}C, ^{15}N) with $10\,\mathrm{mg\,L^{-1}}$ of bacteria culture [81].
There are some successful examples of NMR spectroscopy studies on GPCRs, *e.g.* the structure determination with liquid state NMR of rhodopsin II expressed in *E.coli* [87]. Even if it does not belong to the GPCR family, rhodopsin II is also a challenging system exhibiting seven-helical transmembranes as a GPCR. NMR spectroscopy spectrum could be measured for the chemokine receptor CCR5 by Wiktor et al. in 2013, however no structure was reported [81]. Additionally to the liquid state NMR studies, GPCRs were investigated by solid state NMR, as for example for rhodopsin [94], cannabinoid type 2 receptor [89] and β2-adrenergic receptor [73,86] including a structure determination of the chemokine receptor CXCR I in phospholipid bilayers [85].
Despite all the challenges arisen from NMR spectroscopy measurements, they could

provide valuable informations, as for example informations on possible ligand-receptor interactions. Also, low affinity ligands could be studied with NMR spectroscopy [137] in contrast to crystallography, where it is a challenge to crystallise a receptor with a low affinity ligand. It would be possible to assign residues of the receptor participating in an interactions with a ligand, *e.g.* with chemical shift perturbations [138].

4.1 NMR Spectra of FC14 purified $CRF_{2\beta}$ Receptor

The first attempt of NMR measurements on corticotropin-releasing factor receptor 2β ($CRF_{2\beta}R$) are shown in this chapter.
As a first trial and before the optimisation of the purification protocol and thus without the usage of the ligand-affinity column, an initial NMR experiment was performed. The sample was prepared as followed. Mistic-$CRF_{2\beta}R$ was expressed in minimal medium in the presence of $^{15}NH_4Cl$. The receptor was extracted and purified with FC14, as it gave the highest yields (ca. $1\,\mathrm{mg\,L^{-1}}$ of ^{15}N-labelled culture). The thrombin cleaved receptor was concentrated with a $100\,\mathrm{kDa}$ molecular weight cut off concentrator. The final concentration of $CRF_{2\beta}R$ was $100\,\mu\mathrm{M}$ in the buffer $15\,\mathrm{mM}$ Tris · HCl with 50 mM NaCl and $0.01\,\%$ FC14 at the pH 6.85.
A [^{15}N, ^{1}H]-HMQC was recorded on a $700\,\mathrm{MHz}$ NMR spectrometer at either $22\,°C$ or $37\,°C$ (figure 4.1). No obvious differences can be found between the spectra of those two temperatures, only additional negative peaks were found at ca. 10.5 ppm for the spectrum at $37\,°C$.
While the spectra quality must be considered unsatisfactory, the presence of shifted tryptophan indole peaks (at 10.4 ppm) indicates a to a certain degree folded species or at least for some segments of the receptor.

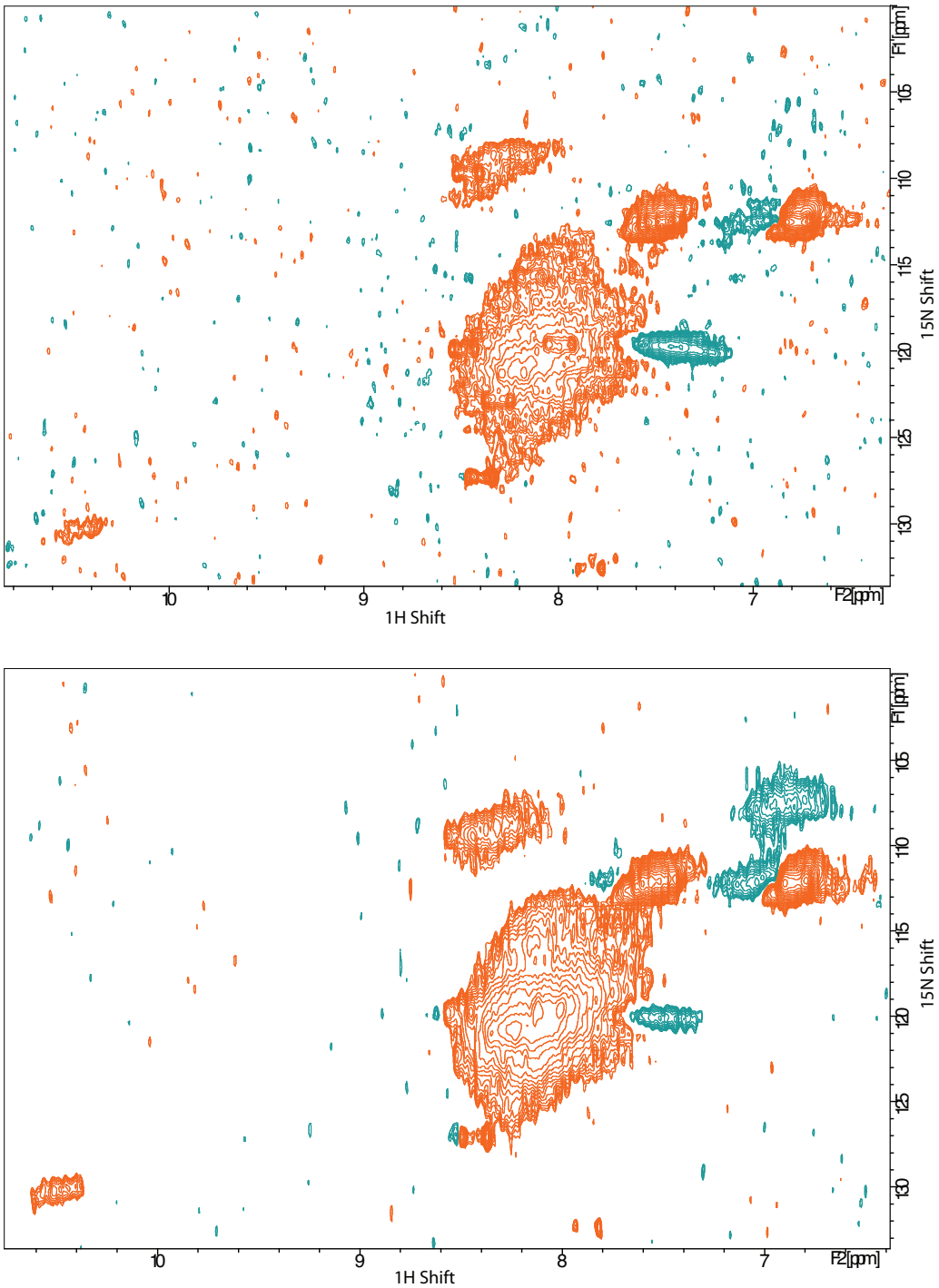

Figure 4.1: [^{15}N, ^{1}]-HMQC spectra of $CRF_{2\beta}R$ at different temperatures. Top: Spectrum at 22 °C; bottom: spectrum at 37 °C. The concentration of the receptor was 100 µM at pH 6.85. Both spectra look similar, beside the bottom spectrum having additional negative peaks at 105 ppm.

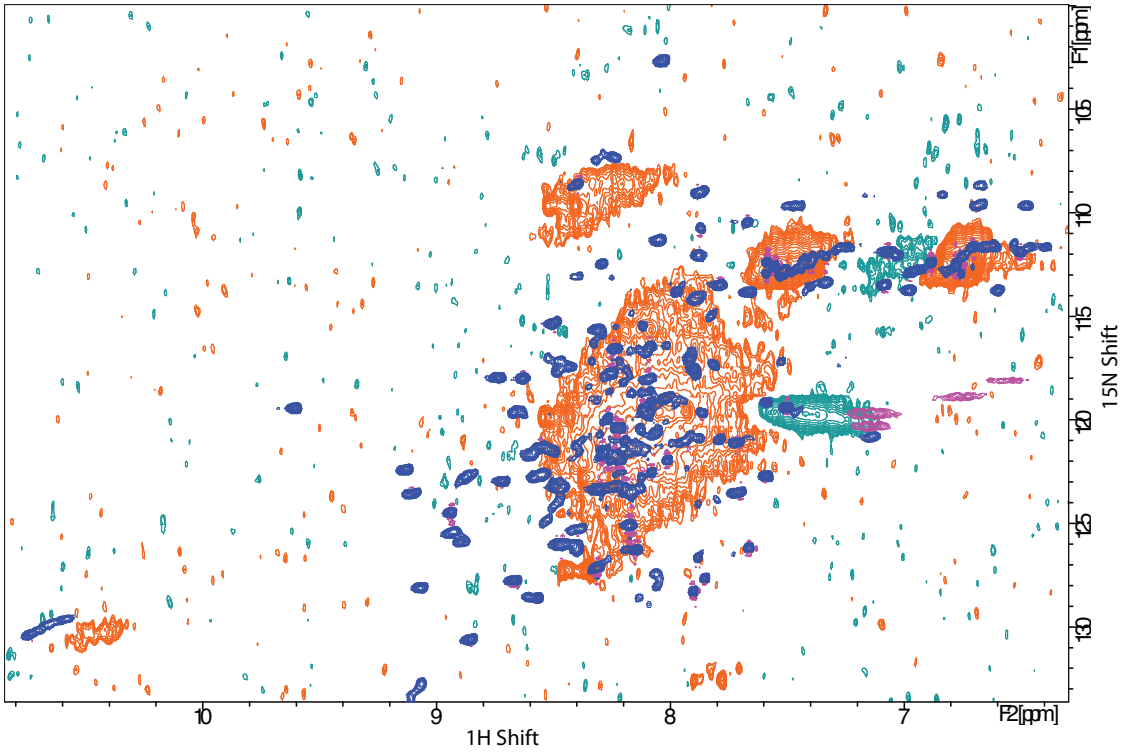

Figure 4.2: [^{15}N, ^{1}H]-HMQC of $CRF_{2\beta}R$ overlaid with [^{15}N, ^{1}H]-HSQC of the ECD of $CRF_{2\beta}R$. Orange spectrum: [^{15}N, ^{1}H]-HMQC of 100 µM $CRF_{2\beta}R$ at 21 °C pH 6.85; blue spectrum: [^{15}N, ^{1}H]-HSQC of 15 µM ECD of $CRF_{2\beta}R$ at 25 °C at pH 6.5. No peaks of the ECD can be observed in the spectrum of the full length $CRF_{2\beta}R$.

Overlaying the spectrum at 21 °C with a spectrum of the ECD of $CRF_{2\beta}R$ (figure 4.2), no peaks of the ECD were observed in the spectrum of the full length $CRF_{2\beta}R$. The peaks of the ECD did neither appear with increasing temperature (figure 4.1). The reason for the absence of the peaks of the ECD is not clear, but might be attributed to the fact that most of the receptor is not well folded, since about 60 % of the receptor is lost during the astressin-affinity chromatography.

Thus another sample was expressed in minimal medium with ^{15}N-NH_4Cl and celtone base powder (CBP) and purified with DDM over the astressin-affinity column. Unfortunately, when the receptor was concentrated with a 100 kDa molecular weight cut off concentrator at pH 6.1, the receptor precipitated.

Therefore, further investigations are needed to determine the reason of the absence of peaks of the ECD in the [^{15}N, ^{1}H]-HMQC of the $CRF_{2\beta}R$.

Chapter 5

Nogo-A-Δ20

Nogo-A isoform is an important inhibitor for axonial regrowth and reconnection. The segment Nogo-A-Δ20, located in the middle of Nogo-A, has been discovered recently in 2014 to bind to the GPCR sphingosine-1-phosphate receptor 2 (S1PR2) [100]. Blocking the Nogo-A-Δ20 region of the Nogo-A protein or blocking the S2PR1 with an antibody prevents the inhibiting characteristic of Nogo-A and thus is a promising method for reconnecting dissected spinal cords [97]. The exact residues of Nogo-A-Δ20 binding to the S1PR2 has not been elucidated yet but it is hypothesised that Nogo-A-Δ20 might bind to the extracellular loops (ECL) of S1PR2. Nogo-A-Δ20 consists of about 180 amino acid residues and thus a interaction with the transmembrane was thought to be rather difficult. Any understanding in the interaction between Nogo-A and S1PR2 or the structural features of Nogo-A-Δ20 might help develop specific peptides binding to the segment Nogo-A-Δ20.

Analysing the binding between Nogo-A-Δ20 and the ECL of S1PR2 via NMR was promising, as an expression protocol in *E.coli* and its purification was established [139] rendering isotope labelling feasible. To produce labelled Nogo-A-Δ20, the protein had to be expressed in minimal medium and an expression and purification protocol had to be established for labelled Nogo-A-Δ20.

5.1 Purification

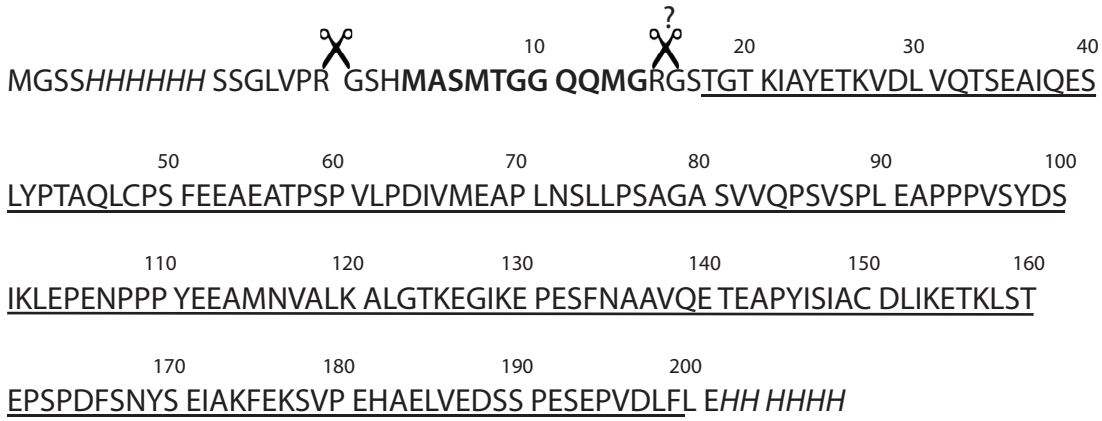

Figure 5.1: Amino acid sequence of Nogo-A-Δ20. The underlined amino acid residues belong to the Nogo-A-Δ20 sequence, the bold residues belong to the T7-tag, and the residues in italic belong to the two His_6-tags. The scissor indicates the site at which thrombin cleaves the N-terminal His_6-tag, between the Pro-Arg and Gly-Ser residues. A second cleavage site might be present indicated by an scissor with a question mark. A proline is missing to generate a native thrombin cleavage site. However even without a proline, the thrombin could cut at this place, just 20 times slower than if there were a proline [140].

The published purification from Oertle et al in 2003 [139] was modified to fit the needs for NMR measurements, such as cleaving off the fusion tag to decrease the number of amino acid residues to facilitate an easier assignment due to less overlays of peaks and a size exclusion chromatography (SEC) for an homogeneous sample.

The fusion protein for Nogo-A-Δ20 consisted of a His_6-tag and a T7-tag at the N-terminus and an additional His_6-tag at the C-terminus (figure 5.1). The two His_6-tags enable the purification with nickel affinity chromatography to separate Nogo-A-Δ20 from impurities. The T7-tag is an epitope tag for detection with T7-tag specific antibody and not directly useful for the purification itself.

Expressing Nogo-A-Δ20 in minimal medium for $8\,\mathrm{h}$ for labelling purposes resulted just in a slightly decreased final yield of Nogo-A-Δ20 compared to the commonly used media for $4\,\mathrm{h}$ at $30°$. Further, the protein was purified using the buffer composition $20\,\mathrm{mM}$ NaH_2PO_4, $500\,\mathrm{mM}$ NaCl, $20\,\mathrm{mM}$ imidazole, pH 7.4, just as described by Oertle et

al. The protein was bound to nickel affinity chromatography and eluted with 500 mM imidazole (figure 5.2).

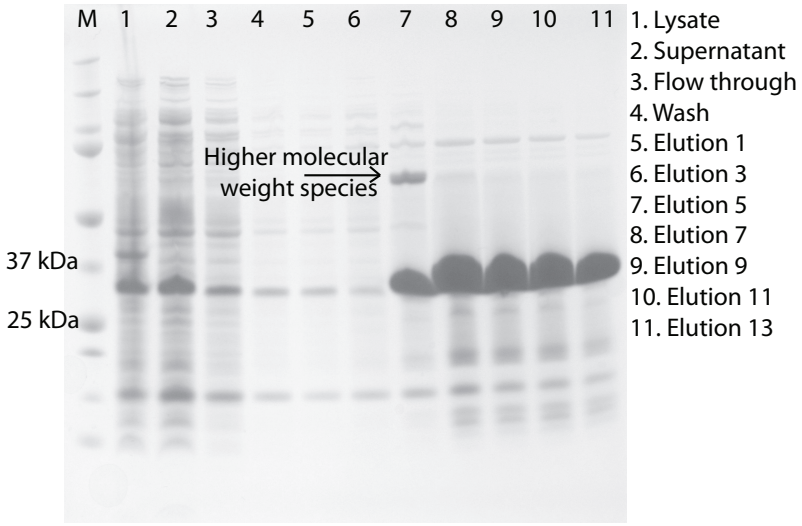

Figure 5.2: A NuPAGE® 4 % to 12 % Bis-Tris gel of the Nogo-A-Δ20 purification. The supernatant originated from the centrifugation of the lysate. The supernatant was applied on a Ni-NTA resin giving the flow through. The resin was washed with 20 mM imidazole and Nogo-A-Δ20 was eluted with 500 mM imidazole and collected as 1.5 ml aliquots. The uncleaved Nogo-A-Δ20 has a molecular weight of 24.2 kDa but is found at around 33 kDa on a Bis-Tris gel.

As was observed by Oertle et al, the fusion protein Nogo-A-Δ20 is found at a higher molecular weight compared to the estimated molecular weight. Since it was hypothesised that high molecular species of Nogo-A-Δ20 were responsible for the inhibition of regrowth of axons, only the aliquots were merged after the Ni-NTA elution, which contained high molecular weight species. An activity test was performed on the eluted and buffer exchanged Nogo-A-Δ20 by Michael Arzt (Group of Prof. Schwab, Laboratory of Neuronal Regeneration and Repair, University of Zurich), to verify if the produced protein was active (figure 5.3).

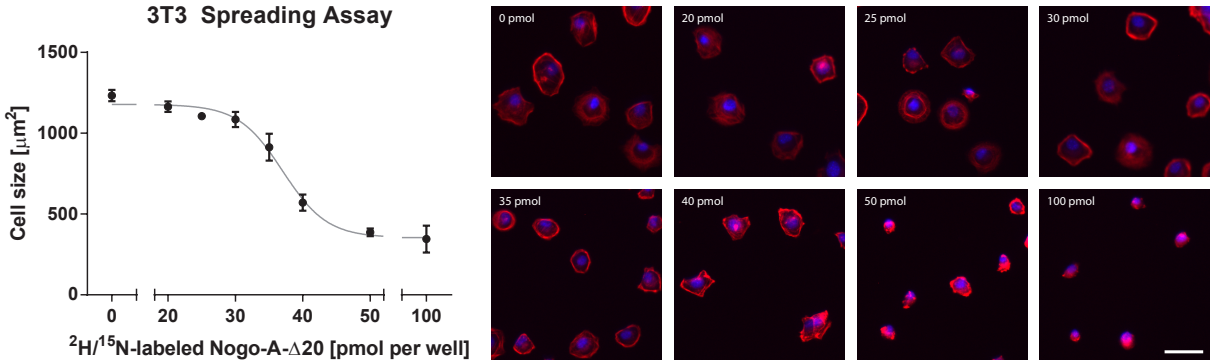

Figure 5.3: Spreading assay test of Δ20 measured by Michael Arzt (Group of Prof. Schwab, University of Zurich). A ^{2}H-, ^{15}N-labelled Nogo-A-Δ20 was expressed and purified with Ni-NTA and an activity test was performed. Right: spreading assay using different concentrations of Nogo-A-Δ20, the different cell size of 3T3 fibroblasts due to the inhibition of growth induced by Nogo-A-Δ20 are visible. Scale bar corresponds to 50 μm; left: graph of cell size vs Nogo-A-Δ20 concentration was plotted resulting in a IC_{50} of 37 pmol per well.

The activity test consisted of a spreading assay, where Nogo-A-Δ20 was spread on a hydrophobic surface at different concentrations and mammalian fibroblasts 3T3 were added. The higher the Nogo-A-Δ20 concentration, the smaller the fibroblasts should be, as the Nogo-A-Δ20 inhibited the spreading of the fibroblasts. The cell sizes of the fibroblasts were automatically evaluated for each concentration of Nogo-A-Δ20. The cell size were plotted against the concentration of Nogo-A-Δ20 used for the spreading assay and the IC_{50} was evaluated. The IC_{50} resulted in 37 pmol per well, as was commonly found for Nogo-A-Δ20 in the group of Prof. Schwab.

After verifying the activity of the labelled Nogo-A-Δ20, a thrombin cleavage test was performed. Different temperatures (4 °C, 22 °C), different time points and different ratios between bovine thrombin and Nogo-A-Δ20 were investigated (figure 5.4). The ratio of 2 NIH units of bovine thrombin per 1 mg Nogo-A-Δ20 at 4° for 1 h was sufficient to cleave the fusion protein. To get rid of the bovine thrombin, a benzamidine sepharose was added, as IDPs are easily prone for degradation with proteases due to their lack of a structure. Benzamidine resin binds selectively to trypsin or trypsin-like serine proteases such as thrombin.

After thrombin cleavage, a faint band below the cleaved Nogo-A-Δ20 was observed,

which might correspond to the additional cleavage site at Nogo-A-Δ20, as is indicated in figure 5.1 by a question mark.

To separate the additional lower band from the cleaved Nogo-A-Δ20, the cleaved sample was loaded on a size exclusion chromatography (SEC) with a Superdex 75 preparative grade column. Aliquots of the peaks were collected and analysed by NuPAGE® 4 % to 12 % Bis-Tris gel (figure 5.6). The peaks without the lower band were pooled and shock frozen with liquid nitrogen and stored at −80° until further usage.

Again, an activity assay, consisting of a spreading assay, was performed by Michael Arzt. The obtained IC_{50} was around 40 pmol per well (data not shown). Thus, the activity of the cleaved Nogo-A-Δ20 is about the same as of the non-cleaved. However, the cell sizes did not decreased as much for the cleaved than for the not-cleaved Nogo-A-Δ20. The exact meaning of the less-decreased cell sizes is not clear.

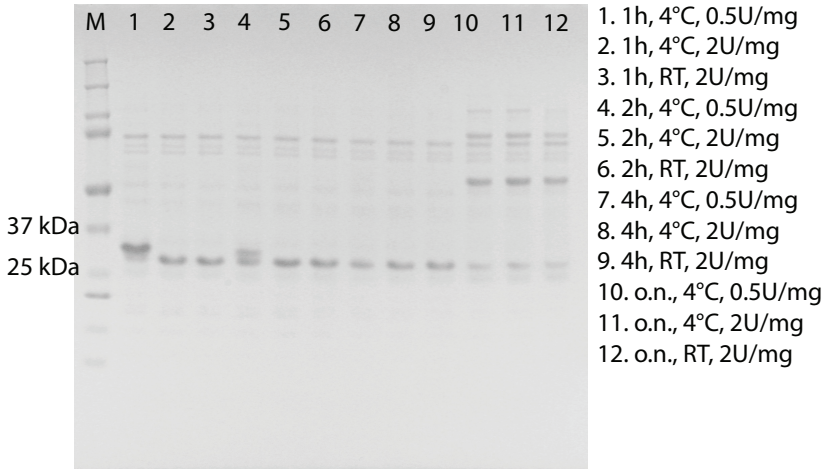

Figure 5.4: NuPAGE® 4 % to 12 % Bis-Tris gel of the thrombin cleavage trial with Nogo-A-Δ20. Three different conditions were tested with either 0.5 U thrombin per 1 mg protein at 4° or 2 U thrombin per 1 mg at 4° or 2 U thrombin per 1 mg at room temperature (RT, ca. 22.5°). Samples were taken after 1 h, 2 h, 4 h, and over night (o.n. ca. 16 h). The uncleaved species corresponded to the band at around 33 kDa, cleaved Nogo-A-Δ20 represented the band at around 30 kDa even though having an effective molecular weight of 22.3 kDa. An additional band appeared with time during thrombin cleavage at around 28 kDa, which might have been arising from the additional thrombin cleavage site. All Nogo-A-Δ20 seemed to be cut after 1 h at 4° and thus this thrombin cleavage conditions were taken for further purifications.

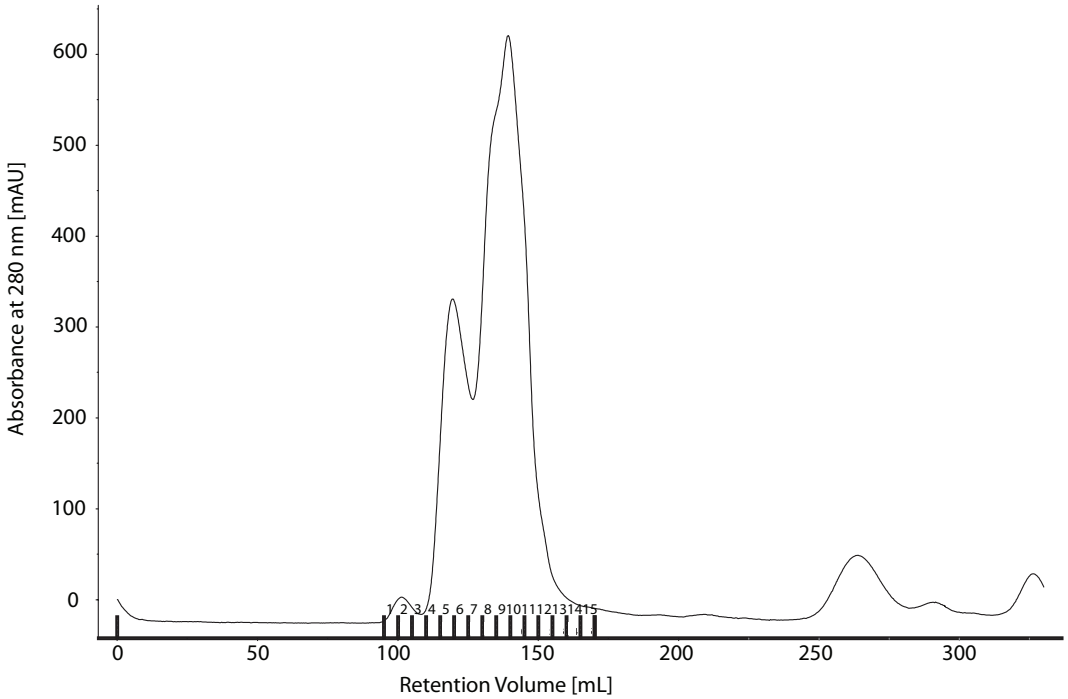

Figure 5.5: Size exclusion chromatogram of ^{15}N-labelled Nogo-A-Δ20 after thrombin cleavage on a Superdex 75 high load. The low-weight impurity after the thrombin cleavage was attempted to remove via a size exclusion chromatography. 2 mL fractions were collected and loaded on a NUPAGE® 4 % to 12 % Bis-Tris gel for analysis.

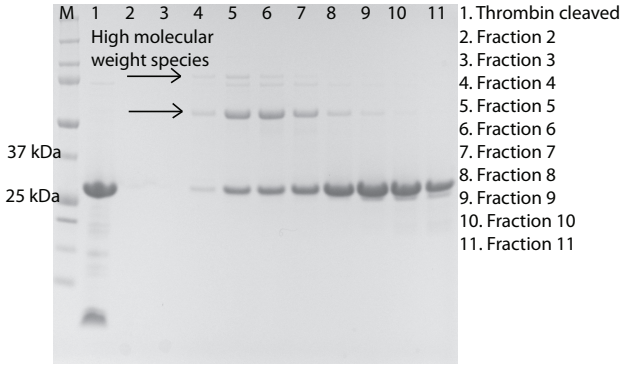

Figure 5.6: A NUPAGE® 4 % to 12 % Bis-Tris gel of the fractions of a size exclusion chromatography using Superdex 75 high load. In the first lane is the thrombin cleaved Nogo-A-Δ20. The thrombin cleaved Nogo-A-Δ20 was flash frozen for the night and thawed again next morning for the size exclusion chromatography. High molecular weight species might have been produced during the freezing or thawing cycle. The fractions 2 to 8 have been collected, merged and flash frozen to store them at −80° until they were used for an experiment.

5.2 Structural Analysis using NMR Spectroscopy

For the structural analysis of Nogo-A-Δ20, a ^{13}C-, ^{15}N-labelled sample was prepared. The triple resonance experiments HNCA, HNCACB and HNN [141] were measured on a 600 MHz or 700 MHz NMR spectrometer at 6° at pH 7.4. In HNCA, the ^{1}H and ^{15}N are correlated with $^{13}C_{\alpha}$ [142]. $^{13}C_{\alpha,i}$ and $^{13}C_{\alpha,i-1}$ are visible as both transfers occur due to similar coupling constants. $^{13}C_{\alpha,i}$ has a stronger intensity than $^{13}C_{\alpha,i-1}$ due to the chosen transfer time. In HNCACB, the ^{1}H and ^{15}N are correlated with $^{13}C_{\alpha}$ and $^{13}C_{\beta}$ [143]. Since the chemical shifts for $^{13}C_{\alpha}$ and $^{13}C_{\beta}$ evolve at the same time, they are found in one dimension. $^{13}C_{\alpha,\,i}$, $^{13}C_{\alpha,\,i-1}$, $^{13}C_{\beta,\,i}$, and $^{13}C_{\beta,\,i-1}$ are visible in the 3D-spectrum, since the magnetisation is transferred from the amide nitrogen to $^{13}C_{\alpha,\,i}$ and $^{13}C_{\alpha,\,i-1}$ and further to $^{13}C_{\beta,\,i}$ and $^{13}C_{\beta,\,i-1}$, respectively. Thus chemical shifts of the amide proton, the amide nitrogen, the $^{13}C_{\alpha}$, and $^{13}C_{\beta}$ were obtained with HNCA and HNCACB.
Since Nogo-A-Δ20 is a intrinsically disordered segment of the Nogo-A protein, its chemical shift dispersions for ^{1}H, ^{13}C and ^{15}N are rather poor [106]. The small dispersion renders the assignment rather challenging. Therefore, an HNN spectrum was additionally recorded, which connects the N_i to N_{i-1} and N_{i+1} [141]. The informations from the preceding and following chemical shift of an amide nitrogen helped to sequentially assign Nogo-A-Δ20 (figure 5.7).
The amino acid residue assignment was accomplished using the CcpNmr software [144] (figure 5.8).

Using HNCA, HNCACB and HNN, up to 75 % of the C_{α} and C_{β} were assigned (figure 5.9). The assignment was challenging due to many prolines (11 %) in the Nogo-A-Δ20 sequence, which interrupted the sequential assignment. Additionally, the low dispersion in the HNCA and HNCACB spectra and sometimes in the HNN spectrum resulted in a low percentage of assigned C_{α} and C_{β}. The fast degradation of Nogo-A-Δ20 was also a problem due to peaks shifts, which hindered the correlation between different spectra.
To overcome the discontinuity of the protein assignment due to the prolines, it would

be possible to record a HCAN spectrum [145]. The magnetisation is transferred from the H_α to C_α and further to N_i and N_{i-1}. A proline can be connected to its preceding amino acid residue using the HCAN experiment allowing a sequential assignment through prolines.

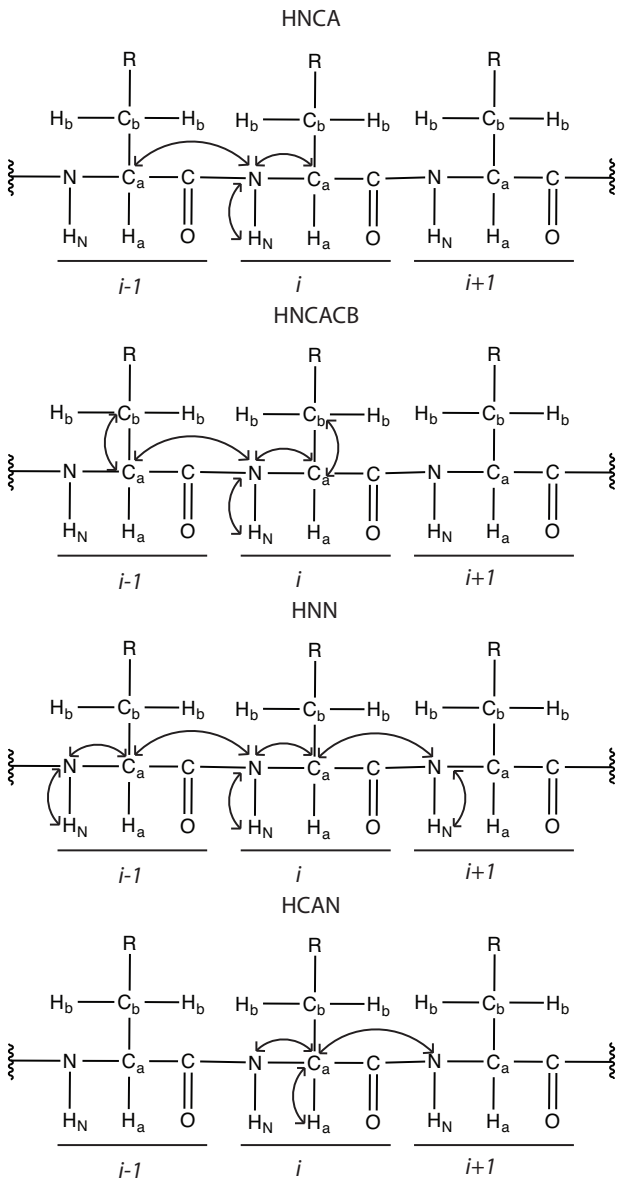

Figure 5.7: Magnetisation transfers for HNCA, HNCACB, HNN, HCAN.

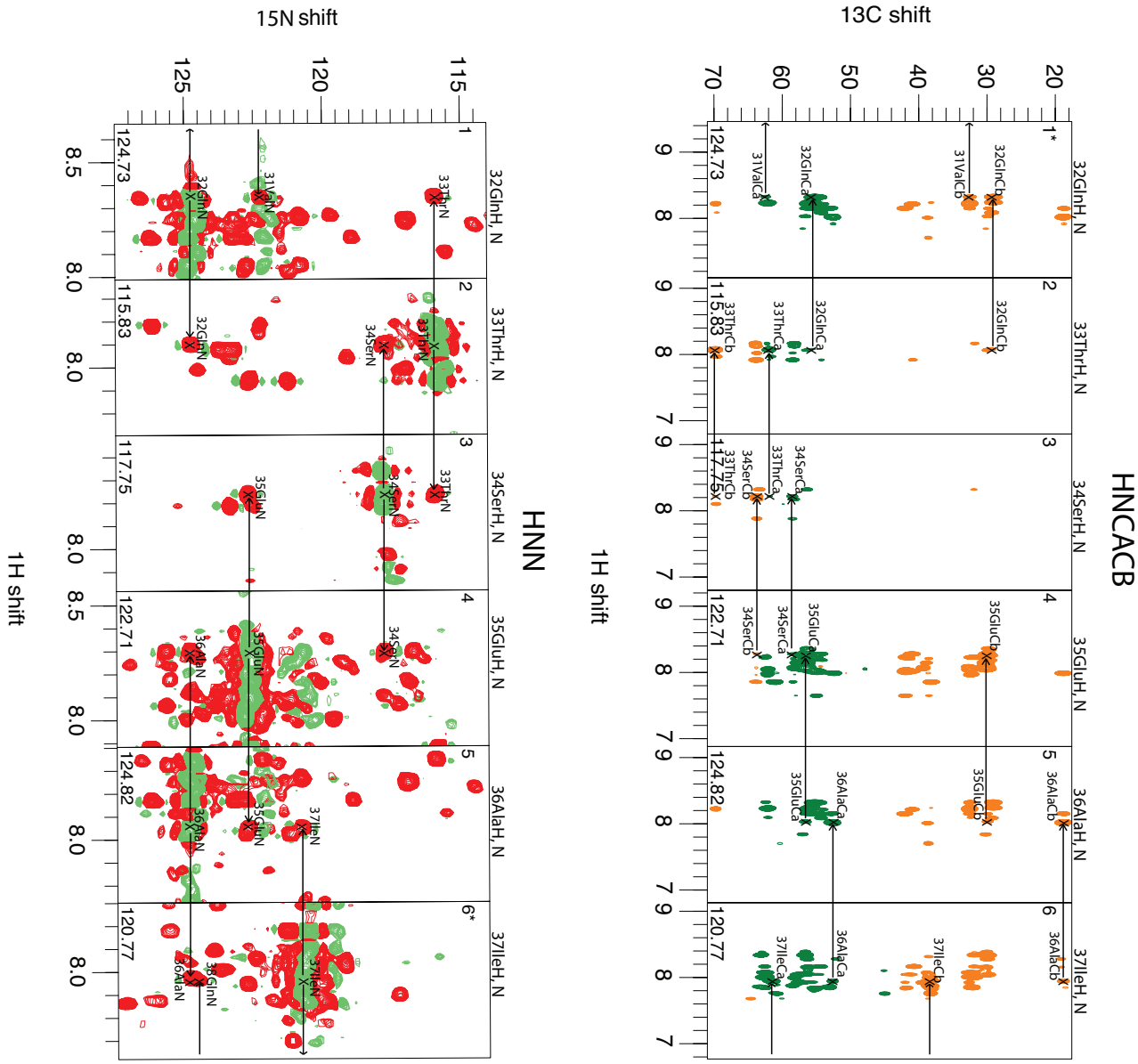

Figure 5.8: Example of a sequential assignment of Nogo-A-Δ20 of the residues 32Gln to 37Gln. Right: strips of the HNCACB spectrum with green and orange contours indicating positive and negative peaks; left: HNN spectrum with red and green contours indicating positive and negative peaks. HNCACB was recorded at the 600 MHz NMR spectrometer and HNN was recorded at the 700 MHz NMR spectrometer at 6 °C at a pH of 7.4.

To obtain information on the secondary structure of Nogo-A-Δ20, secondary chemical shifts $\Delta\delta C_\alpha$ and $\Delta\delta C_\beta$, were calculated by subtracting the random coil values of C_α or C_β for intrinsically disordered proteins [146] from the measured C_α or C_β (figure

5.10). The random coiled values were calculated with an open access software for the pH 7.4 at 6 °C provided by the department of biology, University of Copenhagen. $\Delta\delta C_\alpha$ are positive and $\Delta\delta C_\beta$ negative for a α-helical structure, while $\Delta\delta C_\alpha$ are negative and $\Delta\delta C_\beta$ positive for a β-strands [147]. Nogo-A-Δ20 has few regions with consecutive residues with low δ-values suggesting α-helical structures (Ser34-Ile37, Glu113-Met115, Phe119-Glu201) and a region with β-sheet (Glu187-Ser189) (figure 5.10). Overall, the secondary chemical shifts are randomly distributed with values near random coil indicating no structural conformation for Nogo-A-Δ20 [148].
The combined C_α and C_β secondary chemical shift with values of $\pm$ 2 ppm over several consecutive residues indicate a fully formed secondary structure [149]. If the values are smaller, they indicate a higher fluctuation in the conformation with a transient adoption of a conformation [102, 149]. The combined secondary chemical shifts for Nogo-A-Δ20 indicate a transient conformation with a propensity for α-helical structure (figure 5.11).

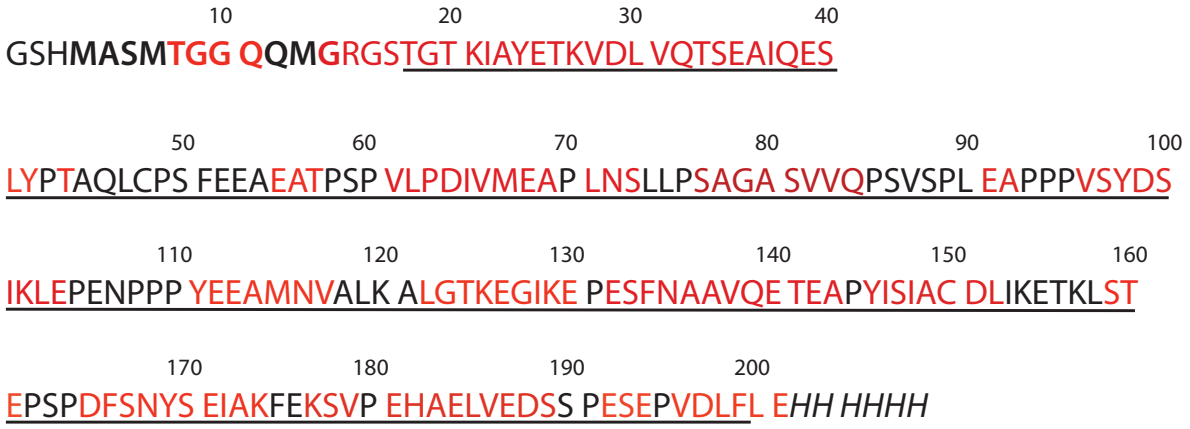

Figure 5.9: Amino acid residues assigned with HNCA, HNCACB, and HNN. Residues in red are assigned, residues in black were not able to be assigned using those three 3D spectra. The underlined residues belong to the Δ20 sequence.

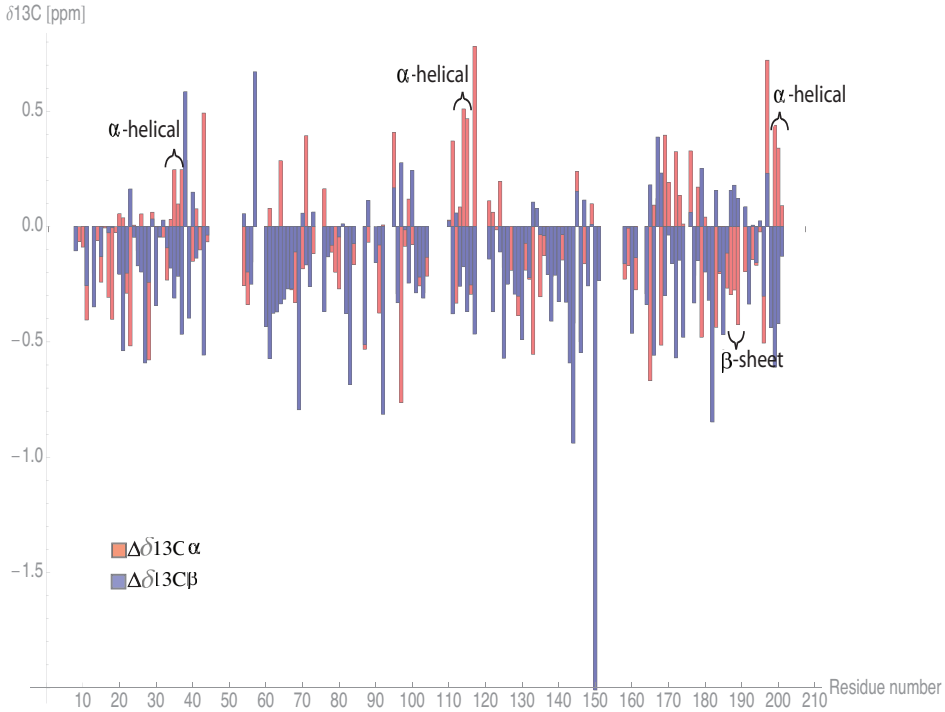

Figure 5.10: $\Delta\delta C_\alpha$ and $\Delta\delta C_\beta$ chemical shifts of Nogo-A-Δ20. δC_α chemical shifts are in red, δC_β are in blue. Propensities for either α-helical structure or β sheet are indicated.

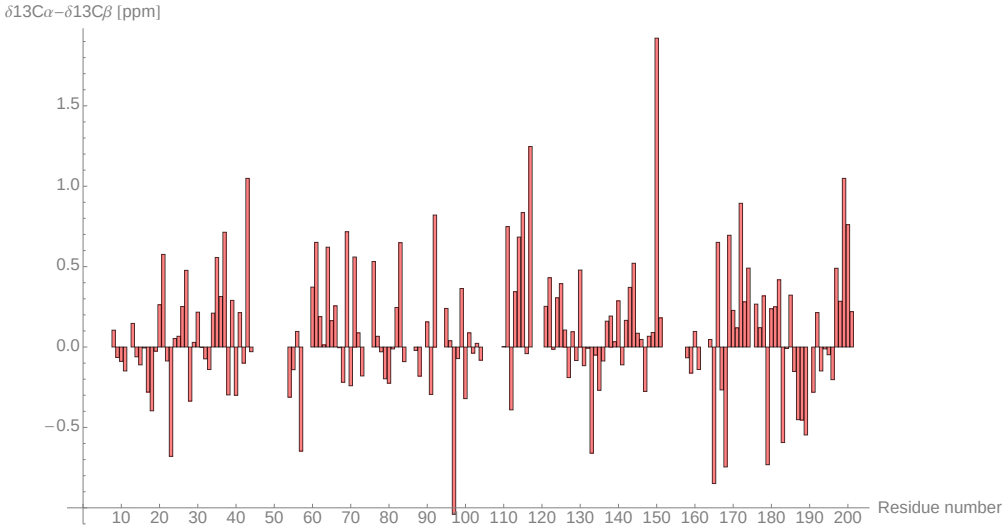

Figure 5.11: Combined $\Delta\delta C_\alpha$ and $\Delta\delta C_\beta$ chemical shifts of Nogo-A-Δ20. Values bigger than $\pm$ 2 ppm over several consecutive residues indicating a fully formed structure [149]. Here, all values are smaller than $\pm$ 2 ppm.

5.3 Titration of the Extracellular Loops of S1PR2 to Nogo-A-△20

It was shown that the sphingosine-1-phosphate receptor 2 (S1PR2) binds to the Nogo-A-△20 segment of the Nogo-A protein [100]. It was hypothesised that the extracellular loops (ECL) of S1PR2 bind to the 181 amino acid residues long Nogo-A-△20 and not its transmembrane domaines, since the size of Nogo-A-△20 might be too big to be diffused into the transmembrane regions.
Published data from Kempf et al. [100] suggest a binding in a few hundred nano molar range for the ECL 2 (280 nM) and ECL 3 (350 nM), while ECL 1 was in the few micro molar range (1.7 µM). Therefore, ECL 2 and 3 were chosen for ligand titration to Nogo-A-△20 using NMR spectroscopy.
For this purpose, 6 L of ^{15}N-labelled Nogo-A-△20 was expressed and purified for the ECL titration, therefore excluding batch to batch variation. The purified Nogo-A-△20 was aliquoted and stored at −80 °C until usage.
ECL 2 was titrated to a 88 µM Nogo-A-△20 solution in different ratio (△20:ECL2, 1:0.1, 1:0.3, 1:0.6, 1:1, 1:2, 1:3). [^{15}N, ^{1}H]-HSQCs were measured for each step at 6 °C and pH 7.4 (figure 5.12). Even with an excess of ECL 2, no peak shifts were detected upon ligand titration (figure 5.13). Upon ligand titration, the peaks of Nogo-A-△20 shift less than 0.01 ppm, indicating no binding of the ECL 2 in the nano molar range. Since pronounced chemical shifts changes were observed for several peaks upon a decrease of pH, a pH change might induce binding. However, an alteration of the pH from 7.4 to 6.4 did not result in any peak shifts, either, upon ligand titration (figure 5.14).
The published results of the ligand binding were performed at higher temperature, therefore it was speculated, whether a temperature increase might induce a binding. However, even an increase of the temperature from 6 °C up to 37 °C did not cause any binding (data not shown).
Additionally, the titration of the ECL 3 to the Nogo-A-△20 segment was examined. However, it was the same case as for the ECL 2, no peak shifts were detected (figure

5.15).

Since no binding could have been confirmed for the ECL 2 and ECL 3, even though they were evaluated to have the highest binding constants of the extracellular loops, the ECL 1 titration was not further investigated.

The reason for not having any chemical shifts for the Nogo-A-Δ20 protein upon ligand titration even though a binding of the ECLs to the protein has been shown, is not clear. The thrombin cleaved Nogo-A-Δ20, which was used for the NMR spectroscopy experiments, has been active. Therefore, it might be rather that the extracellular loops were not structured since the EC-fragments were not in their native environment. However, it is also possible that the ECLs of the S1PR2 are not the native binding partners for the Nogo-A-Δ20 segment.

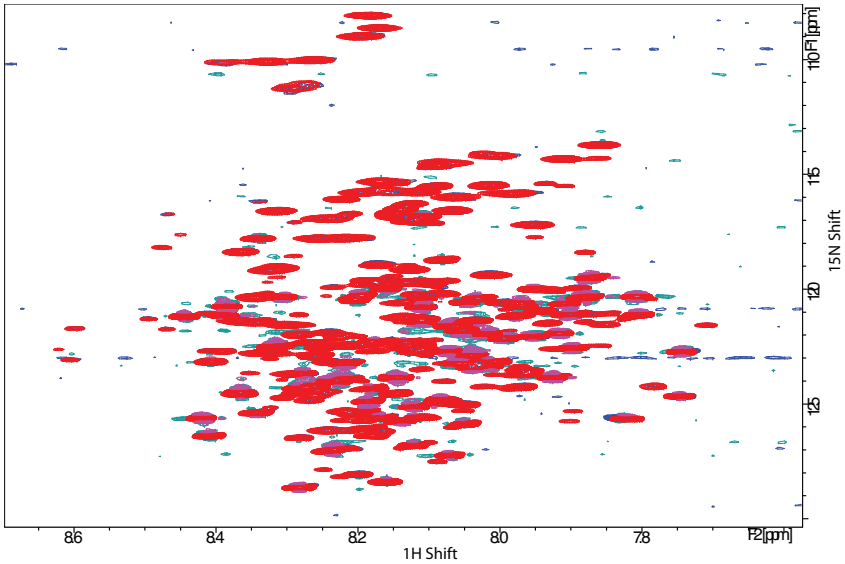

Figure 5.12: [^{15}N, ^{1}H]-HSQC of 88 µM Δ20 alone and in the presence of ECL 2 at pH 7.4. Red spectrum: Δ20 alone; blue spectrum: Nogo-A-Δ20 in the presence of ECL 2, with Nogo-A-Δ20:ECL2=1:3. The spectrum was recorded on a 700 MHz NMR spectrometer at 6 °C. No peak shifts occurred upon ligand titration.

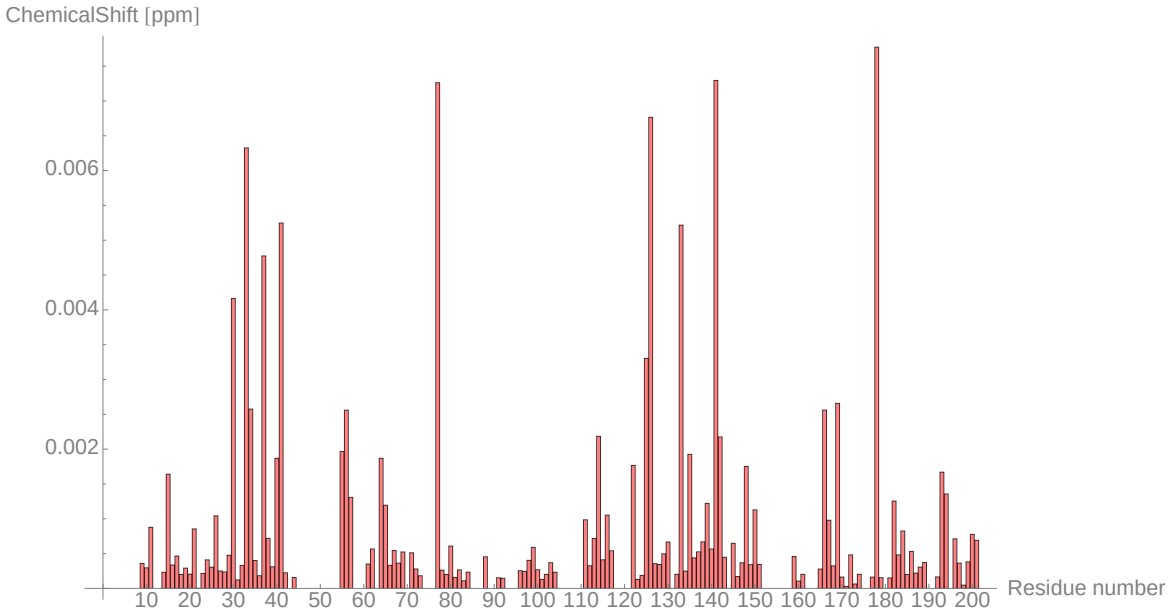

Figure 5.13: Weighted chemical shift differences of ^{1}H and ^{15}N nuclei of Nogo-A-Δ20 alone and upon ligand titration. The formula for the chemical shift perturbation was $\sqrt{0.5 * [\delta_{\mathrm{H}}{}^{2} + (0.14 * \delta_{\mathrm{N}}{}^{2})]}$ [138]. The chemical shifts are smaller than 0.01 ppm upon addition of ECL 2.

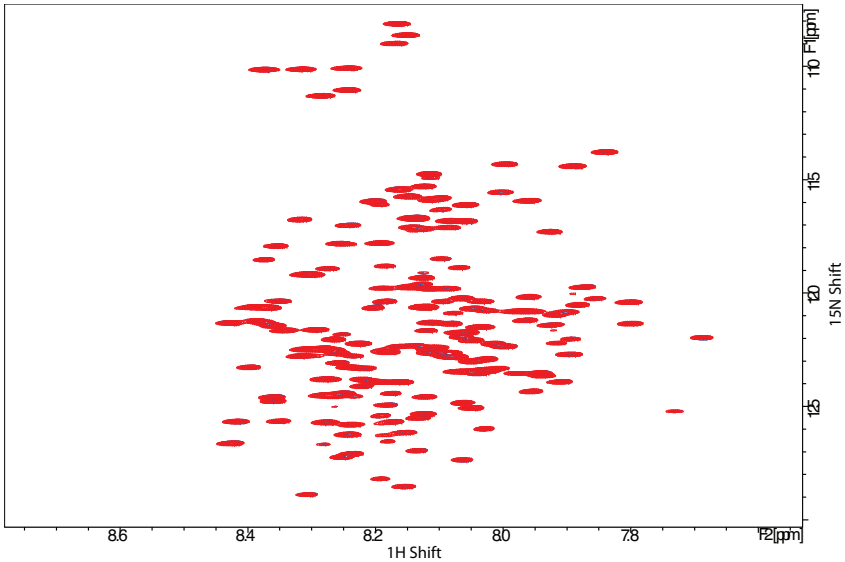

Figure 5.14: [^{15}N, ^{1}H]-HSQC of 88 µM Nogo-A-Δ20 alone and in the presence of ECL 2 at pH 6.40. Red spectrum: Nogo-A-Δ20 alone; blue spectrum: Nogo-A-Δ20 in the presence of ECL 2, with Nogo-A-Δ20:ECL2=1:3. The spectrum was recorded on a 600 MHz NMR spectrometer at 6 °C. No peak shifts occurred upon ligand titration.

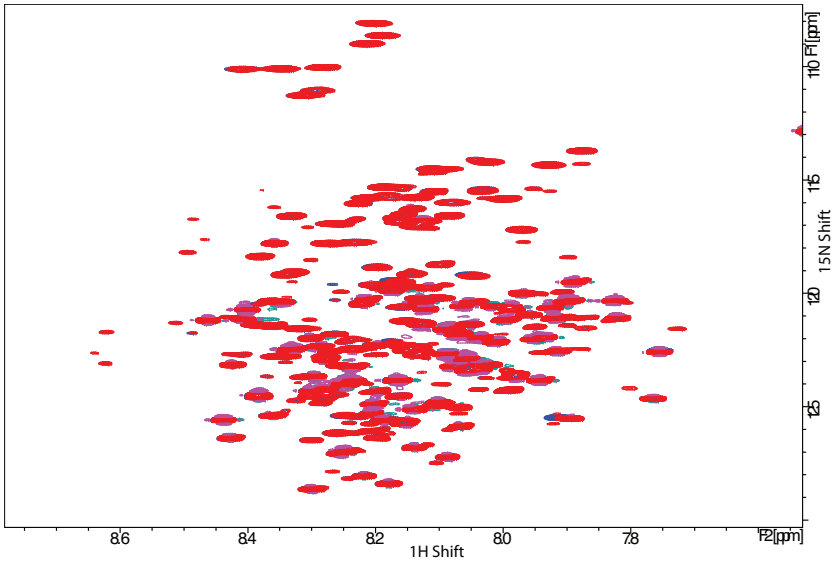

Figure 5.15: [^{15}N, ^{1}H]-HSQC of 88 µM Nogo-A-Δ20 in the presence of ECL 2 and ECL 3 at pH 6.40. Red spectrum: Δ20 with ECL 2; blue spectrum: Nogo-A-Δ20 in the presence of ECL 3, with Nogo-A-Δ20:ECL=1:3. The spectrum was recorded on a 600 MHz NMR spectrometer at 6 °C. No peak shifts occurred upon ligand titration.

Chapter 6

Material and Methods

6.1 Materials

Tris(hydroxymethyl)aminomethan (Tris) for molecular biology was purchased from BiosolveBV (Valkenswaard, Netherlands). Sodium chloride (NaCl), glucose, ammonium chloride (NH_4Cl), ammonium hydroxide (NaOH) were provided by Merck KGaA (Darmstadt, Germany). Lysozyme from chicken egg and calcium chloride ($CaCl_2$) were obtained from Fluka production GmbH (Buchs, Switzerland). Isopropyl β-D-1-thiogalactopyranoside (IPTG), phenylmethanesulfonyl fluoride (PMSF) and ampicilin were provided by AppliChem (Darmstadt, Germany). Hydrochloride acid (HCl), acetic acid, phosphate buffered saline (PBS), sodium phosphate monobase (NaH_2PO_4), glycerol, and guanidinium chloride ($Gu \cdot HCl$) were obtained from Sigma-Aldrich® (Buchs, Switzerland). Complete EDTA-free protease inhibitor (PI) cocktail tablets were purchased from Roch Diagnostics GmbH (Mannheim, Germany). Thrombin from human plasma was obtained either from Sigma-Aldrich® (St. Louis, Missouri, USA) or Calbiochem® (Merck KGaA, Darmstadt, Germany). n-Dodecyl-β-D-maltopyranoside (DDM) Anagrade® (HPLC purity, $99.98\,\%$) was obtained either from Anatrace (Maumee, Ohio, USA) or Avanti® polar lipids, inc (Alabaster, Alabama, USA). Cholesteryl hemisuccinate was provided by Anatrace (Maumee, Ohio, USA). n-Tetradecylphosphocholine

(Fos-choline-14, FC14; HPLC purity, > 99 %) Anagrade®, n-dodecylphosphoscholine (Fos-choline-12, FC12), 1,2-Dimyristoyl-*sn*-glycero-3-phosphocholine (DMPG) were purchased from Affymetrix (Santa Clara, California, USA). 1-Myristoyl-2-hydroxy-*sn*-glycero-3-[phospho-*rac*-(1-glycerol)] sodium salt (LMPG), 1-Myristoyl-2-hydroxy-*sn*-glycero-3-phosphocholin (LMPC), and 1,2-diheptanoyl-*sn*-glycero-3-phosphocholine (DHPC-7) were purchased from Avanti® polar lipids, inc (Alabaster, Alabama, USA). Amicon® Ultra-4 centrifugal filter units, Ultracel® - 10K and Ultracel® - 100k were obtained from Merck Millipore Ltd (Tullagreen, Carrigtwohil, Co. Cork, Irland).

6.2 Strains and Plasmids

The DNA coding sequence for sCRF$_{2\alpha}$R (20-143 amino acid residues) was engineered and cloned into a pET 32a vector (Novagen, Merck KGaA, Darmstadt, Germany) by GeneArt (Burlingame, California, USA). The sCRF$_{2\alpha}$R vector contained a thioredoxin sequence at the N-terminus followed by His$_6$-tag and a thrombin cleavage site. The first extracellular domain (ECD) of CRF$_{2\beta}$R was kindly received from Dr. Marilyn H. Perrin from the Salk institute in San Diego, USA. The ECD construct (38-133 amino acid residues) is similar to the sCRF$_{2\alpha}$R vector, it starts as well with a thioredoxin sequence, followed by a His$_6$-tag and a thrombin cleavage site and ends with the ECD sequence. Mistic-CRF$_{2\beta}$R (27-430 amino acid residues) was engineered by Gateway® destination (Invitrogen) technology including a linker consisting of serines and glutamines between the Mistic- and CRF$_{2\beta}$R-sequence having a His$_8$-tag before and a His$_6$-tag after the Mistic-sequence [127]. pelB-CRF$_{2\beta}$R and CRF$_{2\beta}$R (25-430 amino acid residues) were kindly received from Dr. Roberto Jappelli from the Salk Institute, San Diego, USA [115]. Both constructs have a His$_6$-tag at the C-terminus. The only difference is that the pelB-CRF$_{2\beta}$R construct has an additional pelB leader sequence at the N-terminus.

The plasmid for the rat Nogo-A-Δ20 (544-725 amino acid residues) was cloned in a pET28 vector containing a His$_6$-tag and a T7-tag (kindly shared from Prof Martin E.

Schwab, University of Zurich, Switzerland).
Origami™ B(DE3) (Novagen, Merck KGaA, Darmstadt, Germany), One Shot® BL21 Star™ (DE3) (Invitrogen™ by LifeTechnologies™, LuBioScience GmbH, Lucerne, CH), OverExpress™ C41(DE3) (Lucigen, Middleton, Wisconsin, USA), SHuffle® T7 (New England BioLabs® Inc., Bioconcept, Allschwil, Switzerland) *E. coli* competent cells were used for protein expression. Point mutated proteins were transformed in either ultra competent cells XL 10-Gold from Agilent or DH5alpha. Occasionally, the pET 40b vector from Novagen (Merck KGaA, Darmstadt, Germany) was co-transformed with the $CRF_{2\beta}R$-vector.
The ProtParam tool on the ExPASy server was used for calculating the theoretical molecular weights, the molar extinction coefficients, and the theoretical pI of the fusion proteins [150].

6.3 Point Mutations

Various point mutations were performed on the Mistic-$CRF_{2\beta}R$, pelB-$CRF_{2\beta}R$, and $CRF_{2\beta}R$ expression vectors by PCRs (table 6.1). The PCR reactions were performed with Phusion® High-Fidelity DNA Polymerase kit from Thermo Scientific (Fischer Scientific-Switzerland, Wohlen, Switzerland) according to the manufacturer's instructions together with $0.5\,\mu M$ of each primer (forward and reverse). Oligonucleotides primers were purchased from Microsynth AG (Balgach, Switzerland). In the PCR program, the denaturation of the DNA was performed at $98\,°C$ for $30\,s$, the annealing at $64\,°C$ for $30\,s$, and the extension at $72\,°C$ for $6\,min$. The cycle was repeated 35 times. The template vector was removed by DpnI endonuclease from New England BioLabs® Inc. (Bioconcept, Allschwil, Switzerland). All point mutations were verified by DNA sequencing.

Mutation	Primers
C114S	Fw 5' - TGC GGA GTA TCC GCA GCC TGA GGA ATG TG - 3'
	Rv 5' - CAC ATT CCT CAG GCT GCG GAT ACT CCG CA - 3'
C205A	Fw 5' - ATG TTT GTG GAG GGC GCC TAC CTG CAC ACG GC - 3'
	Rv 5' - GCC GTG TGC AGG TAG GCG CCC TCC ACA AAC AT - 5'
W375Stop	Fw 5' - CGG TGG CAC CGC TAG CAG GAC CAC A - 3'
	Rv 5' - TGT GGT CCT GCT AGC GGT GCC ACC G - 3'
H244Stop	Fw 5' - CAC CAG CGG CAG CGG CTA GCA TCA TCA TCA TCA TAG - 3'
	Rv 5' - CTA TGA TGA TGA TGA TGC TAG CCG CTG CCG CTG GTG - 3'
Y357A	Fw 5' - GTT TCT TTG TGT CCG TTT TCG CCT GCT TCT TCA ATG GAG AGG - 3'
	Rv 5' - CCT CTC CAT TGA AGA AGC AGG CGA AAA CGG ACA CAA AGA AAC - 3'
L368Stop	Fw 5' - GGT GCG CGC GGC CTA GAG AAA GCG GTG G - 3'
	Rv 5' - CCA CCG CTT TCT CTA GGC CGC GCG CAC C - 3'

Table 6.1: Primers used for introducing point mutations into the sequences of mistic-$CRF_{2\beta}R$ and (pelB-)$CRF_{2\beta}R$. Fw - DNA sequence for the forward primer; Rv - DNA sequence for the reverse primer.

6.4 Protein Electrophoresis

To verify the protein purity across protein purifications, denaturing NuPage® 4 % to 12 % Bis-Tris Gel and 12 % Bis-Tris Gel (1 mm X 12 or 15 well) were used from Novex® by Invitrogen™ (LifeTechnologies™, LuBioScience GmbH, Lucerne, Switzerland) with the SeeBlue®Plus2 Pre-Stained Standard from Invitrogen™ or Precision Plus Protein™ Dual colour Standard from Bio-Rad (Hercules, Ca, USA).
For monitoring protein expression and smaller concentrations of protein during protein purifications, Western blot analysis was used with either mouse monoclonal to 6X His tag® from abcam (Cambridge, UK) or rabbit polyclonal CRFHR2 antibody (N-term) from Abgent (San Diego, California, USA) as primary antibodies. A XCell II™ Blot Module from invitrogen was used according to the manufacturer's instructions with a PVDF Transfer Membrane (0.45 µm) from Thermo Scientific (Rockford, Illinois, USA). The protein bands were visualised on Fuji Medical X-ray films from Fujifilm Corporation (Tokyo, Japan).

6.5 Expression and Purification of Recombinant Proteins

6.5.1 soluble $CRF_{2\alpha}$ Receptor

Thioredoxin-$sCRF_{2\alpha}R$ fusion protein plasmid was transformed in the host *E.coli* One Shot® Origami™ B(DE3). Cells were pre-cultured in LB over night at 37 °C, and then transferred to either Terrific Broth (TB) or M9 minimal medium containing 8 gram D-glucose and 1 gram NH_4Cl per litre. Ampicillin (50 mg l^{-1}), kanamycin (15 mg l^{-1}), and tetracycline (12.5 mg l^{-1}) were added as antibiotics. The cells were grown at 37 °C at 100 rpm until the OD_{590} reached 0.7-1.2. The cells were cooled down to either 18° or 20 °C, induced with 0.5 mM IPTG, kept overnight (ca. 15 h) for protein expression, and harvested by centrifugation at 5000 rpm for 15 min at 6 °C (Avanti J-26 XP centrifuge from Beckman Coulter International S.A., Nyon, Switzerland). The wet pellet of 1 L bacteria culture was resuspended in 100 ml lysis buffer (table 6.2). Additionally 0.5 mg ml^{-1} lysozyme per lysis buffer and 2 PI tablets were added. The lysate was stirred at 4 °C for 20 min. The cells were further disrupted by passing twice through a 110S microfluidizer (Microfluidics, Newton, Massachusetts, USA) at 40 PSI. The suspension was centrifuged at 40'000 rpm for 30 min at 4 °C (Optima L-90K Ultracentrifuge, rotor Ti-45, Beckman Coulter International, S.A., Nyon, Switzerland) to pellet cellular debris.
The supernatant of the centrifugation was loaded on 5 ml Ni-NTA Agarose from Qiagen® (Merck KGaA, Darmstadt, Germany) with gravity flow for 2 h. The Ni-NTA was washed with 30 ml wash buffer and eluted with ca. 7 ml elution buffer. The elution buffer was buffer exchanged with a pre-packed and disposable PD-10 desalting column (GE Healthcare Life Sciences, Buckinghamshire, UK) to the cleavage buffer. To the desalted protein, human thrombin was added with the ratio of 2 NIH unit of thrombin to ca. 1 mg of $sCRF_{2\alpha}R$. The cleavage was performed over night at ca. 22 °C.
The cleaved $sCRF_{2\alpha}R$ was further purified either by a second His_6-tag chelating Ni-NTA affinity to bind the His_6-tag followed by RP-HPLC (*vida infra* chapter 'Purification by RP-HPLC') or with the biotinylated-astressin affinity column (*vida infra* chap-

ter 'Ligand-Affinity Chromatography').

Buffer	Composition of Buffer
lysis buffer	50 mM Tris, 300 mM NaCl, 10 mM imidazole, pH 8
wash buffer	50 mM Tris, 300 mM NaCl, 50 mM imidazole, pH 8
elution buffer	50 mM Tris, 300 mM NaCl, 500 mM imidazole, pH 8
cleavage buffer	25 mM Tris, 150 mM NaCl, 10 % glycerol, pH 8

Table 6.2: Buffer used for $sCRF_{2\alpha}R$ and ECD purification.

6.5.2 Extracellular Domain of $CRF_{2\beta}$ Receptor

Thioredoxin-ECD fusion protein plasmid was transformed in the host *E.coli* One Shot® Origami™ B(DE3). Cells were pre-cultured in LB over night at 37 °C and then transferred to either Terrific Broth (TB) or M9 minimal medium containing 8 gram D-glucose and 1 gram NH_4Cl per litre. Ampicillin ($50\,mg\,l^{-1}$), kanamycin ($15\,mg\,l^{-1}$), and tetracycline ($12.5\,mg\,l^{-1}$) were added as antibiotics. The cells were grown at 37 °C at 100 rpm until the OD_{590} reached 1.2, cooled down to 20 °C and induced with 0.5 mM IPTG. They were kept overnight (ca. 15 h) for protein expression and harvested by centrifugation at 5000 rpm for 15 min at 6 °C (Avanti J-26 XP centrifuge from Beckman Coulter International S.A., Nyon, Switzerland). The wet pellet of 1 L bacteria culture was resuspended in 100 ml lysis buffer (table 6.2). Additionally $0.5\,mg\,ml^{-1}$ lysozyme per lysis buffer and 2 PI tablets were added. The lysate was stirred at 4 °C during 20 min. The cells further lysed by passing twice through a 110S microfluidizer (Microfluidics, Newton, Massachusetts, USA) at 40 PSI. The suspension was centrifuged at 40'000 rpm for 30 min at 4 °C (Optima L-90K Ultracentrifuge, rotor Ti-45, Beckman Coulter International, S.A., Nyon, Switzerland) to pellet cellular debris and inclusion bodies.
The supernatant of the centrifugation was loaded on 5 ml Ni-NTA Agarose from Qiagen® (Merck KGaA, Darmstadt, Germany) with gravity flow during 2 h. The Ni-NTA was washed with 30 ml wash buffer and eluted with ca. 7 ml elution buffer. The elution buffer was buffer exchanged with pre-packed and disposable PD-10 desalting column

(GE Healthcare Life Sciences, Buckinghamshire, UK) to the cleavage buffer. Human thrombin was added to the desalted protein, with the ratio of 2 NIH unit of thrombin to ca. 1 mg of ECD. The cleavage was performed over night at ca. 22 °C.
The cleaved ECD was further purified either by a second His_6-tag chelating Ni-NTA affinity column to bind the His_6-tag, while the flow through contained the cleaved ECD followed by RP-HPLC (*vida infra* chapter 'Purification by RP-HPLC') or with the biotinylated-astressin affinity column (*vida infra* chapter 'Ligand-Affinity Chromatography').

6.5.3 Purification by RP-HPLC

Prior RP-HPLC, acetonitrile CHROMASOLV® (gradient grade, for HPLC, $\geq$ 99.9 %), purchased from Sigma-Aldrich (Buchs, Switzerland), was added up to 10 % (initial vol.) to the protein solution. The protein solution was acidified by adding 0.1 % Trifluoroacetic acid (TFA), which was obtained from Fisher Scientific AG (Loughborough, UK). If necessary, conc. HCl was added until a pH of 3 was obtained. The protein solution was centrifuged (eppendorf Centrifuge 5810 R, Faust Laborbedarf AG, Schaffhausen, Switzerland) to pellet protein precipitation due to TFA addition.
The supernatant was loaded on a reverse phase (RP)-column from phenomenex® (Jupiter C4 300A, 25.0 x 10.00 mm, 5 µm Brechenbuehler scientific analytical solutions AG, Zurich, Switzerland). An acetonitrile gradient was used for protein elution (buffer B 10 % to 50 % in 33 min with a flow rate of 2 ml min^{-1}; buffer A - water with 0.1 % TFA; buffer B - acetonitrile with 0.1 % TFA). The 1200 HPLC system (Agilent Technologies (Schweiz) AG, Basel, Switzerland) was equipped with an external manual injector, an automatic fraction collector, and a diode-array detector. The elution was observed by UV absorption at wavelengths 220 nm and 280 nm. For the ECD of $CRF_{2\beta}R$, the largest peak at around 32 % of buffer B was collected and lyophilised. For $sCRF_{2\alpha}R$, the peaks and shoulders were collected separately at around 30 % of buffer B and lyophilised. The lyophilised protein was kept at −20 °C until usage.

6.5.4 $CRF_{2\beta}$ Receptor

Culture Growing

Either Mistic-$CRF_{2\beta}R$ or $CRF_{2\beta}R$ plasmid or its mutated plasmid (table 6.1) was transformed into different One Shot® *E.coli* host cells (BL21 Star™ (DE3), SHuffle® T7, C41(DE3), or BL21 Star™ (DE3) co-transformed with pET40 vector. Cells were precultured in LB over night at 37 °C and then transferred to either Terrific Broth (TB) or M9 minimal medium containing 8 gram D-glucose and 1 gram NH_4Cl per litre. Hutner's trace elements (table 6.3) or unlabelled Celtone® base powered obtained from Cambridge Isotope Laboratories, Inc. (Andover, Massachusetts, USA) were added to the minimal medium as supplement. Alternatively, the unlabelled ready-to-use bioexpress® cell growth media (10X) obtained from Cambridge Isotope Laboratories, Inc. (Andover, Massachusetts, USA) was used. Ampicillin ($50\,mg\,l^{-1}$ for Mistic-$CRF_{2\beta}R$) or kanamycin ($15\,mg\,l^{-1}$ for (pelB-)$CRF_{2\beta}R$) was added as antibiotics. The cells were grown at 37 °C at 110 rpm until the OD_{590} reached 1.0. The cells were transferred to 18 °C and induced with 0.25 mM IPTG (if not specified differently). The cells were kept 20 h at 18° for protein expression and then harvested by centrifugation at 5000 rpm for 15 min at 6 °C (Avanti J-26 XP centrifuge from Beckman Coulter International S.A., Nyon, Switzerland).

Chemical	amount [g]
$ZnSO_4 * 7\,H_2O$	4.4
H_3BO_3	2.2
$MnCl_2 * 4\,H_2O$	1
$CoCl_2 * 6\,H_2O$	0.32
$CuCl_2 * 6\,H_2O$	0.235
$(NH_4)_6Mo_7O_{24} * 4\,H_2O$	0.22

Table 6.3: Hutner's trace metals recipe: First dissolve the listed salts above in 80 ml double-distilled water. Second, dissolve 1 g $FeSO_4$ and 10 g EDTA in 80 ml of double-distilled water. Adjusted pH to 5.5 (a golden yellow solution results). Third, combine both solutions and adjust pH to 6.9 using KOH. Final volume should be 200 ml (solution should become bright green). Store solution at 4 °C. The solution turns purple with time [111].

Preparation of Cells and Extraction

If not stated otherwise, all purification steps were performed at 4 °C.
The wet pellet of 1 L bacteria culture was resuspended in 50 ml lysis buffer (table 6.5). Additionally 0.5 mg ml^{-1} lysozyme per lysis buffer, 0.5 mM PMSF, 1 PI tablet, and DNAse were added. The lysate was stirred at 4 °C for 20 min. The cells were further lysed either by passing twice through a 110S microfluidizer (Microfluidics, Newton, Massachusetts, USA) at 25 PSI or with a dounce homogeniser (Kontes Glass Co., Vineland, New Jersey, USA).
The extraction with different detergents (table 6.4) was either performed on the bacteria lysate (whole cell extraction) or on the membrane protein fraction. The membrane protein fraction was obtained by centrifuging at 10'000 rpm for 30 min at 4 °C (Optima L-90K Ultracentrifuge, rotor Ti-45, Beckman Coulter International, S.A., Nyon, Switzerland) to pellet cellular debris and inclusion bodies and repeated with the supernatant at 40'000 rpm for 90 min at 4 °C (Optima L-90K Ultracentrifuge, rotor Ti-45) to pellet the membrane protein fraction. The membrane fraction was then resuspended in 50 ml lysis buffer.
The extraction was performed with either the resuspended membrane protein fraction or the bacteria lysate using either FC14/CHS (0.5 %/0.06 %) or DDM/CHS (1.0 %/0.12 %) or LMPG (0.5 %) or a mixture of FC14/DDM/CHS (0.25 %/0.25 %/0.06 %) at 4 °C for 3.5 h. Afterwards the suspension was centrifuged at 40'000 rpm for 1 h at 4 °C (Optima L-90K Ultracentrifuge, rotor Ti-45) to pellet the non-extracted debris.

Nickel-Binding

The supernatant was diluted with a dilution buffer so that the total detergent concentration was less then 0.25 %. 3 ml Ni-NTA Agarose from Qiagen® (Merck KGaA, Darmstadt, Germany) was used for His-tag binding to the immobilised metal ion. Gravity flow and batch mode were examined for the best binding conditions like temperatures (22 °C or 4 °C) or binding times (1 h, 2 h, 4 h, over night). The Ni-NTA was washed

Detergent	Detergent concentration [%]
FC14/CHS	0.5/0.06
DDM/CHS	1.0/0.12
DDM/CHS	1.5/0.18
DDM/CHS	2.0/0.24
FC14/DDM/CHS	0.05/0.5/0.06
FC14/DDM/CHS	0.15/0.4/0.06
FC14/DDM/CHS	0.25/0.25/0.06
FC14/DDM/CHS	0.4/0.15/0.06
FC14/DDM/CHS	0.5/0.05/0.06
LMPG	0.5
FC14/LMPG/CHS	0.25/0.25/0.03
FC14/LMPG/CHS	0.1/0.4/0.012
LMPG/ DMPC	0.4/0.1
FC14/LMPG/DMPC/CHS	0.1/0.4/0.1/0.012
LMPG/LMPC	0.1/0.1
DHPC	1.0
FC12	1.0
LDAO	0.5//

Table 6.4: Detergents and its concentrations used in extraction trials.

with 70 mL binding buffer. The protein was eluted with 30 mL elution buffer.
The elution buffer was buffer exchanged with a pre-packed and disposable PD-10 desalting column (GE Healthcare Life Sciences, Buckinghamshire, UK) to the cleavage buffer.

Thrombin Cleavage of Mistic-CRF$_{2\beta}$ Receptor

To cleave the Mistic-tag from MisticCRF$_{2\beta}$R, human thrombin protease was added at different ratios (mg of CRF$_{2\beta}$R:NIH unit of thrombin, 1:7, 1:20, 1:40, 1:60). Additionally, conditions were investigated for different temperatures (ca. 22.5 °C) or 4 °C) and for different time points (2 h, 4 h, 6 h, over night)).
It was investigated if the purity of cleaved Mistic-CRF$_{2\beta}$R increased by loading it on a second Ni-NTA affinity column to bind the His-tagged Mistic, while the flow through

and the wash (using 15 mM Tris, 150 mM NaCl, 50 mM to 100 mM imidazole pH 8, including either FC14/CHS (0.01 %/0.0012 %) or DDM/CHS (0.025 %/0.003 %) or LMPG (0.05 %)) should contain cleaved Mistic-CRF$_{2\beta}$R.

Buffer	Composition of Buffer	Detergent
lysis buffer	50 mM Tris, 500 mM NaCl, 50 mM imidazole, 20 % glycerol, pH 8	-
dilution buffer	50 mM Tris, 500 mM NaCl, 50 mM imidazole, pH 8	-
wash buffer	50 mM Tris, 500 mM NaCl, 50 mM imidazole, 10 % glycerol, pH 8	either 0.01 % FC14/0.0012 % CHS or 0.025 % DDM/ 0.003 % CHS or 0.05 % LMPG
elution buffer	50 mM Tris, 500 mM NaCl, 500 mM imidazole, 10 % glycerol, pH 8	either 0.01 % FC14/0.0012 % CHS or 0.025 % DDM/ 0.003 % CHS or 0.05 % LMPG
cleavage buffer	25 mM Tris, 150 mM NaCl, 10 % glycerol, pH 8	either 0.01 % FC14/0.0012 % CHS or 0.025 % DDM/ 0.003 % CHS or 0.05 % LMPG

Table 6.5: Buffer used for CRF$_{2\beta}$R purification.

6.5.5 Nogo-A-Δ20

The T7-Nogo-A-Δ20 fusion protein plasmid was transformed in the host *E.coli* One Shot® BL21 ™ (DE3) and stored in glycerol stock at −80 °C. Some scraps of the glycerol stock were pre-cultured in LB over night at 37 °C. The next day, the cells were transferred to either Terrific Broth (TB) or M9 minimal medium containing 8 g L^{-1} D-glucose and 1 g L^{-1} NH_4Cl per litre. Kanamycin (15 mg l^{-1}) was added as antibiotics. The cells were grown at 37 °C at 100 rpm until the OD_{590} reached 1.2 and transferred to 30 °C and induced with 1 mM IPTG. They were kept for 8 h for protein expression and harvested by centrifugation at 5000 rpm for 15 min at 6 °C (Avanti J-26 XP centrifuge from Beckman Coulter International S.A., Nyon, Switzerland). The wet pellet was stored at −80 °C.

A frozen pellet of 1 L bacteria culture was thawed on ice and resuspended in 50 ml lysis buffer (20 mM NaH_2PO_4, 500 mM NaCl, 20 mM imidazole, pH 7.4). 0.5 mg ml^{-1} lysozyme, 0.5 mM PMSF, and 1 PI tablets were added. The lysate was stirred at 4 °C for 20 min.

The cells were further disrupted by passing twice through a 110S microfluidizer (Microfluidics, Newton, Massachusetts, USA) at 40 PSI. The suspension was centrifuged at 40'000 rpm for 30 min at 4 °C (Optima L-90K Ultracentrifuge, rotor Ti-45, Beckman Coulter International, S.A., Nyon, Switzerland) to pellet cellular debris.
The supernatant of the centrifugation was bound to 3 ml Ni-NTA Agarose from Qiagen® (Merck KGaA, Darmstadt, Germany) via batch mode during 2 h at 4 °C. The Ni-NTA was washed with 30 ml lysis buffer and eluted with ca. 5 ml elution buffer (20 mM NaH_2PO_4, 500 mM NaCl, 20 mM imidazole, pH 7.4) via gravity flow and collected in 0.5 ml fractions. The fractions were loaded on a denaturing NuPage® 4 % to 12 %. The aliquots with high molecular weight species were pooled and buffer exchanged with pre-packed and disposable PD-10 desalting column (GE Healthcare Life Sciences, Buckinghamshire, UK) to PBS buffer. Bovine thrombin was added with the ratio of 2 NIH unit of thrombin to ca. 1 mg desalted Nogo-A-Δ20. The cleavage was performed for 1 h at 4 °C.
The following day, the cleaved fusion protein was purified on a Highload™ 26/60, Superdex™ 75, (prep grade, GE Healthcare, Uppsala, Sweden).

6.6 Ligand-Affinity Chromatography

The antagonist peptide astressin (biotinylated at the N-terminus, kindly received from Prof Jean E. F. Rivier from the Salk Institute, San Diego, USA) for CRF R was bound to Streptavidin Sepharose™ high performance from GE Healthcare (Uppsala, Sweden) via the byotin-streptavidin non-covalent interaction similar to the already published ligand affinity column by Mesleh et al [151]. Several binding/elution conditions were tested differing in salt compositions and concentrations including different pHs, until the feasible conditions were found (see chapter 'Ligand Affinity Chromatography').

6.6.1 Binding and Elution of ECD of $CRF_{2\beta}$ Receptor and soluble $CRF_{2\alpha}$ Receptor

The biotinylated-astressin affinity column was washed with binding buffer (10 mM Tris, 150 mM NaCl, 5 % glycerol, pH 8) prior usage on a FPLC system (Aekta Purifier from Amersham Pharmacia Biotech Inc, Piscataway, New Jersey, USA) equipped with an automatic fraction collector (Frac-920) and a UV-detector (UV-900). The thrombin cleaved ECD of $CRF_{2\beta}R$ or $sCRF_{2\alpha}R$ was applied on the biotinylated-astressin affinity column using the binding buffer having a flow rate of $1\,\mathrm{ml\,min^{-1}}$. Partially unfolded protein was eluted with the washing buffer (50 mM acetic acid, 50 mM NaCl, pH 3.5) until no more protein was eluted, observed at the wavelength 280 nm. The correctly folded protein was eluted with an elution buffer (10 mM acetic acid, pH 3.5) gradient (50 % to 100 % buffer B in 15 min with a flow rate of $1\,\mathrm{ml\,min^{-1}}$; buffer A - washing buffer, buffer B - elution buffer).

6.6.2 Binding and Elution of $CRF_{2\beta}$ Receptor

The biotinylated-astressin affinity column was washed with binding buffer (10 mM Tris, 500 mM NaCl, 5 % glycerol, pH 8) prior usage on a FPLC system (Aekta Purifier) equipped with an automatic fraction collector (Frac-920) and a UV-detector (UV-900). $CRF_{2\beta}R$ was applied on the biotinylated-astressin affinity column using the binding buffer and a flow rate of $1\,\mathrm{ml\,min^{-1}}$. Impurities were eluted with the washing buffer (10 mM acetic acid, 150 mM NaCl, 5 % glycerol, pH 3.5). The correctly folded protein was eluted with a gradient to the elution buffer (10 mM acetic acid, 5 % glycerol, pH 3.5) (0 % to 100 % buffer B in 20 min with a flow rate of $1\,\mathrm{ml\,min^{-1}}$; buffer A - washing buffer, buffer B - elution buffer).

6.7 NMR Spectroscopy

NMR spectroscopy spectra were measured on either Bruker 700 MHz or 600 MHz spectrometer equipped with cryoprobes. The data were processed with TopSpin 3.1 software (Bruker BioSpin AG, Faellanden, Switzerland). The CCPN software was used for assignment [144].

6.7.1 Protein Labelling

For NMR spectroscopy measurements, the proteins were labelled with different isotopes (^{2}H, ^{15}N, ^{13}C). The protein was expressed in M9 minimal medium with max. $4\,\mathrm{g\,l^{-1}}$ ^{13}C-glucose (^{13}C > 99 %) and $1\,\mathrm{g\,l^{-1}}$ ^{15}N-ammonium chloride ($^{15}NH_4Cl$, ^{15}N > 98 %) and deuterated water (D_2O, D > 99.8 %), which were purchased from Sigma-Aldrich.
Same purification protocols were applied as for unlabelled proteins.

6.7.2 NMR Measurements on soluble $CRF_{2\alpha}$ Receptor or ECD of $CRF_{2\beta}$ Receptor

$sCRF_{2\alpha}R$ and the ECD of $CRF_{2\beta}R$ were buffer exchanged into 12 mM Tris · HCl, 50 mM NaCl, pH 6.1 or 10 mM acetic acid with 50 mM NaCl at pH 6.0. About 5 % deuterated water (D_2O, D > 99.8 %) were added. [^{15}N, ^{1}H]-HSQC were measured at 25 °C with a protein concentration between 100 µM to 300 µM. Eventually, CRF_2R antagonists as astressin or α-helical $CRF_{9\text{-}41}$, originated from solid phase peptide synthesis and received from the Salk Institute, were added.

6.7.3 NMR Measurements on $CRF_{2\beta}$ Receptor

[^{15}N, ^{1}H]-HSQC were recorded for $CRF_{2\beta}R$ on the 700 MHz NMR spectrometer at various temperatures. The buffer for the measurements contained 15 mM Tris · HCl with 50 mM NaCl and 0.01 % FC14, pH 6.85 at the temperatures 22 °C and 37 °C. The concentrations of the $CRF_{2\beta}R$ was ca. 100 µM.

6.7.4 NMR Measurements on Nogo-A-Δ20

[^{15}N, ^{1}H]-HSQC, HNCA, HNCACB and HNN were measured on a 700 MHz NMR spectrometer at 6 °C for the amino acid sequence assignment. The Nogo-A-Δ20 protein had a concentration of 300 µM, which was in a PBS buffer at pH 7.4.
Nogo-A-Δ20 had a concentration of 90 µM for the titrations of the extracellular loops (ECLs) of S1PR2. [^{15}N, ^{1}H]-HSQC were measured on the 600 MHz NMR spectrometer at 6 °C. The ECLs were purchased from JPT Peptide Technologies GmbH (Berlin, Germany) (figure 6.6).

ECL	amino acid sequence
1	LSGHVTLSLTPVQW
2	NCLNQLEACSTVLPLYAKHQVL
3	SILLLDSTCPVRACPVLYK

Table 6.6: Amino acid sequences for the different utilised ECLs of S1PR2.

Conclusion and Outlook

A purification protocol for the corticotropin releasing factor 2β receptor ($CRF_{2\beta}R$) has been established in this thesis. A functionally active receptor was purified using ligand-affinity chromatography, which is a crucial step in the purification. For this, an antagonist of the CFR receptors, astressin, is used as the ligand and bound to a resin via a biotin-streptavidin interaction. The functionality of the ligand-affinity chromatography has been validated using the first extracellular domain (ECD) of the $CRF_{2\beta}R$. Additionally, a new expression protocol has been established for $CRF_{2\beta}R$ in an alternative medium, which is capable of isotopically labelling the receptor.
It has been shown in this thesis that the purified $CRF_{2\beta}R$ is able to bind its antagonist astressin with high affinity to its N-terminal domain using radioactive-ligand binding assays. However, it is still not clear, if the transmembrane region of the $CRF_{2\beta}R$ is correctly structured. A nucleotide-exchange assay could confirm this by an interaction of a G protein to the purified receptor [78, 152, 153]. A non-hydrolysable GTP analogue, GTPγS, is used in the nucleotide-exchange assay, which is exchanged for a GDP if the G protein binds to the receptor. Unbound GTPγS can be readily washed away by filtration [154]. Depending on the labelling of the GTPγS, the quantity of the bound GTPγS can be measured either with fluorescence [155] or radioactivity [156]. This assay would be suitable to assess if the $CRF_{2\beta}R$ is able to transfer signals upon ligand binding and thus, if the transmembrane region of $CRF_{2\beta}R$ is correctly structured. Due to the tendency of GPCRs to aggregate even in the presence of detergents [71], a possibility to stabilise $CRF_{2\beta}R$ further would be to insert the receptors into nan-

odiscs. Nanodiscs are synthetic model membrane systems [75]. They consists of two membrane scaffolds proteins (MSP) wrapped around a certain number of lipids [157]. Rhodopsin was one of the first GPCR transferred into nanodiscs [79] showing a higher stability in nanodiscs than in common detergents such as DM [158]. Therefore, it would be highly desirable to test this approach with $CRF_{2\beta}R$ as well to ensure higher stability in solution and thereby allowing more profound investigations using liquid state NMR spectroscopy studies. Our preliminary results suggest that it is still challenging to estimate the correct MSP to lipid to GPCR ratio to reconstitute the membrane protein-nanodiscs complex. Additionally, the separation of nanodiscs with and without receptors can be laborious.

Additional constraints of GPCRs is the spectral crowding, when measuring NMR spectroscopy spectra. This can be disadvantageous for interpreting a 420 amino acid residues long receptor. This might be overcome by selective labelling, where only a small number of amino acid residues are labelled and thus are NMR detectable [159–161]. Fewer peaks are observed in the NMR spectra rendering the spectra more comprehensible. If each of the peaks can be assigned to, for example with mutagenesis, further NMR studies can be performed. This has been accomplished, for example, for the β2-adrenergic receptor, where different kinds of ligands were added and its peak shifts were interpreted [73]. A similar study could be realised for the $CRF_{2\beta}R$ using a homology model for the $CRF_{2\beta}R$, since the crystal structure for the transmembrane region of the CRF_1 receptor is known.

The slower tumbling time of larger particles is a disadvantage for liquid state NMR as they cause broadening of the line widths. Therefore solid state NMR spectroscopy could be recorded on a solid sample using the magic angle spinning (MAS). MAS can average the anisotropic interactions resulting in sharper line widths [162]. Due to this, most of the NMR spectroscopy studies on GPCRs were performed with solid state NMR, such as the first NMR derived structure of the chemokine receptor CXCR1 [85], and functional studies on the rhodopsin receptor [94]. Thus, ligand-receptor interactions, dynamic pictures of the $CRF_{2\beta}R$ structures or intermediates of an activated

receptor could be deduced from NMR spectroscopy.
Another approach would be to label the ligands instead of the receptors. The binding of a ligand to a CRF receptor is assumed to be in two steps, first the C-terminus of the ligand binds to the extracellular domain (ECD), which then moves the N-terminus of the ligand to the transmembrane region of the receptor resulting in the activation of the receptor. The exact amino acid residues of the antagonist astressin or the agonist α-helical CRF involved in the interactions with the ECD of the CRF receptors have been extensively studied [27, 39]. Using instead of the ECD the full length receptor, the amino acid residues of the ligand involved in the transmembrane binding could be now investigated. Since the C-terminus of the ca. 44 amino acid residue long ligands have to be amidated for high affinity binding, this might not be so trivial.
Besides NMR measurements, other biochemical methods could also be used to investigate different structural aspects of the $CRF_{2\beta}R$, such as mass spectroscopy (MS), where intact membrane proteins complexes were studied using gas-phase activation [163]. Dimerisation occurs often in GPCRs, some being induced by ligand binding [164, 165] and some were dissociated upon ligand binding [166]. Since dimerisation upon ligand binding were found for the CRF binding protein [167], but non for the CRF_1 receptor [168], the influence of the ligand on the $CRF_{2\beta}R$ might be investigated with native MS. A single band was found at the molecular weight of a monomer before and high molecular weigh species were found after the ligand-affinity chromatography on a denaturing NuPAGE® Bis-Tris gel. If the high molecular weight species were induced by pH, higher concentrations of receptor or indeed due to its ligand, could be investigated with native MS. Furthermore, using limited proteolysis, a possible binding site and affinity for cholesterol in $CRF_{2\beta}R$ could be probed.

A purification protocol has also been established for a soluble isoform of the $CRF_{2\alpha}$ receptor ($sCRF_{2\alpha}R$). Interestingly, when eluted from the astressin-affinity column, a mixture of folded and unfolded protein was present.
It is suspected that the unfolded $sCRF_{2\alpha}R$ binds unspecifically to the resin instead to

the folded $sCRF_{2\alpha}R$ or to astressin. Thus, instead of using a pH gradient for the elution, a competitive ligand could be added to the elution buffer of the astressin-affinity chromatography to dissociate the astressin-$sCRF_{2\alpha}R$ complex. However, it is also possible to use a reverse phase HPLC after the astressin-affinity chromatography to separate folded from unfolded soluble receptor. The structure of the $sCRF_{2\alpha}R$ would be interesting to compare to the structures of the ECD of the $CRF_{2\beta}R$ and of the CRF_1R, since $sCRF_{2\alpha}R$ exhibits a unique hydrophilic C-terminus compared to the other ECDs.

Another part of the thesis is about the intrinsically disordered segment Nogo-A-Δ20 of Nogo-A, which has been expressed with isotopes suitable for NMR spectroscopy measurements. Nogo-A-Δ20 has been purified and several 3D NMR spectra have been recorded for a sequential amino acid residue assignment. Up to 75 % of the residues were accomplished to assign. Further, a potential interaction between Nogo-A-Δ20 and the extracellular loops (ECL) of its natural binding partner, the sphingosine-1-phosphate receptor 2 (S1PR2), have been investigated. Neither of the ECLs showed a binding to Nogo-A-Δ20 upon titration and investigation with NMR spectroscopy.
A second biochemical method could be used to reevaluate, whether the ECLs bind to the Nogo-A-Δ20 segment. There is a possibility that the binding was not able to be detected by NMR spectroscopy measurements. Isothermal titration calorimetry (ITC) is a widely used technique to measure affinities of ligand binding by measuring the energy release or absorption upon ligand binding. Binding affinities up to a μmolar range can be investigated using ITC. Thus it could be examined if our observation of lack of peak shifts were due to a weak binding or no binding at all.
There is also the possibility that the used ECLs are unstructured due to their segmentations and the solid phase synthesise is the reason that no binding is observed. Therefore binding studies including the full S1PR2 receptor should be favoured.
Additionally, the percentage of assigned amino acid residues could be increased by additionally measuring *e.g.* a HCAN spectrum, where the preceding amino acid residue of a proline could be determined and thus the discontinuity of the sequential assign-

ment could be overcome due to proline residues.

Summarised, the established purification protocol for CRF receptor isomers together with the ligand affinity chromatography allows new investigations on the purified receptors. Especially the functional active $CRF_{2\beta}R$, defined by its capability to bind its ligand, has a great potential for many investigations with numerous techniques and subsequent experiments, which might provide new insights into the structure and function of $CRF_{2\beta}R$.
For the Nogo-A-Δ20 segment, it has to be first investigated, which fragments of the S1PR2 bind to Nogo-A-Δ20 prior any further experiments.

List of Tables

List of Figures

Appendix A

Chemical Shifts of Nogo-A-△20

		H	N	HA	CA	CB
5	Ala	-	-	-	52.82	-
6	Ser	8.06	114.49	-	58.38	-
7	Met	-	-	-	55.61	-
8	Thr	-	-	-	61.98	-
8	Thr	7.96	114.17	-	-	-
9	Gly	8.26	111.20	3.72	45.40	-
10	Gly	8.13	108.54	-	45.23	-
11	Gln	8.13	119.66	-	55.71	29.07
13	Met	-	-	-	55.50	32.32
14	Gly	8.30	110.09	-	45.32	-
15	Arg	8.10	120.52	-	56.19	30.40
16	Gly	8.35	110.10	-	45.25	-
17	Ser	8.13	115.64	-	58.23	63.69
18	Thr	8.11	115.23	4.12	62.01	69.66
19	Gly	8.22	110.98	3.74	45.23	-
20	Thr	7.87	114.37	-	62.02	69.73
21	Lys	8.21	124.49	-	56.31	32.61
22	Ile	8.00	123.35	-	60.94	38.34
23	Ala	8.13	128.52	4.02	52.02	19.15
24	Tyr	7.93	120.16	4.11	57.84	38.73
25	Glu	8.15	122.51	4.03	56.28	30.21
26	Thr	8.03	116.84	4.03	61.99	69.67
27	Lys	8.24	124.94	3.95	56.10	32.64
28	Val	8.03	122.05	-	62.10	32.62
29	Asp	8.22	124.38	4.30	54.23	40.94
30	Leu	8.02	122.97	4.21	54.92	41.86
31	Val	7.99	122.21	3.76	62.48	32.58
32	Gln	8.33	124.75	4.14	55.62	29.18
33	Thr	8.08	115.86	4.03	61.80	69.82
34	Ser	8.23	117.76	4.16	58.59	63.71
35	Glu	8.28	122.70	3.96	56.73	29.93

36	Ala	8.04	124.84	-	52.61	18.81
37	Ile	7.95	120.82	-	61.43	38.25
38	Gln	8.24	124.71	-	56.11	29.63
39	Glu	8.24	122.47	3.92	56.78	29.91
40	Ser	8.08	116.33	4.17	58.44	63.58
41	Leu	7.92	123.65	3.99	55.26	42.10
42	Tyr	7.83	120.23	4.25	55.62	37.92
43	Pro	-	-	-	63.26	31.83
44	Thr	8.09	114.89	4.01	61.95	69.80
45	Ala	8.15	126.50	-	52.51	18.97
54	Ala	-	-	-	52.44	19.08
55	Glu	8.16	120.37	3.92	56.24	30.06
56	Ala	8.16	125.70	4.05	52.29	19.02
57	Thr	8.11	117.18	4.27	59.76	69.68
58	Pro	-	139.44	4.16	61.23	31.97
59	Ser	8.35	118.45	4.43	56.53	62.99
60	Pro	-	137.95	4.16	62.95	31.82
61	Val	8.09	121.64	4.00	62.24	32.24
62	Leu	8.28	128.85	-	52.67	41.32
63	Pro	-	-	-	62.66	31.85
64	Asp	8.17	120.61	-	54.41	40.82
65	Ile	7.90	121.38	-	60.95	38.33
66	Val	8.13	126.14	-	62.35	32.25
67	Met	8.32	125.63	-	55.06	32.47
68	Glu	8.23	123.03	-	56.07	30.23
69	Ala	8.22	127.05	-	50.47	17.75
70	Pro	-	-	-	62.79	32.05
71	Leu	8.23	122.60	-	55.74	41.88
72	Asn	8.28	119.15	-	53.13	38.43
73	Ser	8.03	116.04	-	58.49	63.65
76	Pro	-	-	-	63.20	31.80
77	Ser	8.17	115.91	-	58.22	63.74
78	Ala	8.22	126.17	-	52.76	18.94
79	Gly	8.14	108.07	3.66	45.03	-
80	Ala	7.91	123.48	4.06	52.35	19.12
81	Ser	8.13	115.40	4.19	58.21	63.76
82	Val	7.97	122.29	3.85	62.21	32.40
83	Val	8.10	125.48	3.78	62.17	32.29
84	Gln	8.40	126.58	4.32	53.27	28.42
85	Pro	-	136.92	4.17	62.82	31.96
86	Ser	8.29	116.70	4.17	58.22	63.82
87	Val	8.04	121.86	3.82	61.98	32.46
88	Ser	8.31	121.62	-	56.23	63.22
90	Leu	-	-	-	-	42.14
91	Glu	8.02	121.67	4.28	55.89	30.24
92	Ala	8.11	126.89	4.29	50.25	17.86
93	Pro	-	136.81	-	-	-
95	Pro	-	136.22	4.16	63.29	32.25
96	Val	8.02	120.61	4.12	62.33	32.52

97	Ser	8.10	119.27	4.17	57.42	63.97
98	Tyr	8.21	123.22	-	57.95	38.42
99	Asp	8.05	121.28	-	54.34	40.91
100	Ser	7.93	115.85	-	58.46	63.74
101	Ile	7.87	122.65	-	61.17	38.20
102	Lys	8.16	126.26	-	55.91	32.58
103	Leu	8.16	124.93	-	54.77	42.13
104	Glu	8.19	123.32	-	54.23	29.36
110	Pro	-	-	-	63.14	32.24
111	Tyr	8.00	120.78	-	58.20	38.39
112	Glu	7.95	123.51	-	56.09	30.42
113	Glu	8.06	122.74	-	56.83	29.92
114	Ala	8.15	124.81	-	53.14	18.77
115	Met	8.05	118.82	-	55.92	32.32
116	Asn	8.17	119.78	-	52.85	38.40
117	Val	7.86	120.52	-	63.44	32.29
118	Ala	8.00	125.95	3.98	52.99	18.57
119	Leu	7.85	120.51	4.28	55.57	41.87
120	Lys	7.89	121.63	-	56.53	32.45
121	Ala	7.92	124.27	4.00	52.53	18.74
122	Leu	7.93	121.15	-	55.52	41.97
123	Gly	8.14	108.92	-	45.31	-
124	Thr	7.81	113.76	-	61.93	69.84
125	Lys	8.25	123.71	-	56.30	32.54
126	Glu	8.24	122.01	-	56.69	29.96
127	Gly	8.22	110.03	-	45.11	-
128	Ile	7.77	120.35	-	60.92	38.30
129	Lys	8.25	126.63	-	55.78	32.71
130	Glu	8.33	124.57	-	54.44	29.12
131	Pro	-	-	-	63.05	31.88
132	Glu	8.40	121.25	-	56.66	29.94
133	Ser	8.11	116.59	-	57.98	63.82
134	Phe	8.08	122.39	-	57.90	39.41
135	Asn	8.09	121.22	-	52.73	38.70
136	Ala	8.02	125.00	-	52.63	18.94
137	Ala	8.00	122.88	-	52.48	18.81
138	Val	7.85	119.74	-	62.26	32.51
139	Gln	8.25	124.49	-	55.64	29.15
140	Glu	8.37	123.24	-	56.65	29.90
141	Thr	8.07	115.73	-	61.95	69.82
142	Glu	8.25	123.77	-	56.24	30.22
143	Ala	8.22	127.19	-	50.43	17.74
144	Pro	-	-	-	62.67	31.24
145	Tyr	8.05	120.86	-	57.87	38.64
146	Ile	7.70	125.15	-	60.31	38.40
147	Ser	8.06	120.32	-	58.07	63.70
148	Ile	7.98	123.25	-	60.91	38.48
149	Ala	8.17	128.16	-	52.67	18.94
150	Cys	8.15	118.95	-	58.61	27.89

151	Asp	8.20	122.82	-	54.36	40.66
158	Leu	-	-	-	54.97	42.15
159	Ser	8.21	116.95	3.99	58.23	63.66
160	Thr	7.98	115.54	4.08	61.49	69.56
161	Glu	8.10	124.55	4.31	54.26	29.38
162	Pro	-	137.21	4.14	62.55	31.93
163	Ser	8.33	117.89	4.44	56.38	63.32
164	Pro	-	137.94	4.07	63.20	31.78
165	Asp	8.06	119.75	4.24	53.86	40.85
166	Phe	8.01	121.52	4.17	57.98	38.88
167	Ser	8.06	117.09	4.03	58.79	63.86
168	Asn	8.04	120.17	4.41	53.18	38.44
169	Tyr	7.88	120.91	4.22	58.56	38.25
170	Ser	7.89	117.25	4.04	58.49	63.74
171	Glu	8.06	122.58	-	56.67	29.88
172	Ile	7.78	121.36	-	61.48	38.12
173	Ala	8.04	127.39	-	52.69	18.74
174	Lys	7.86	120.05	-	56.43	32.59
175	Phe	7.93	120.83	-	57.73	39.35
176	Glu	8.07	122.84	-	56.63	30.16
177	Lys	8.09	122.58	-	56.19	32.75
178	Ser	8.18	117.84	-	58.25	63.69
179	Val	8.04	123.39	4.15	59.74	32.39
180	Pro	-	139.43	4.09	63.05	31.89
181	Glu	8.35	121.16	3.86	56.60	29.99
182	His	8.11	119.62	4.35	55.71	30.09
183	Ala	8.10	125.65	4.00	52.30	19.22
184	Glu	8.28	120.42	3.93	56.32	29.90
185	Leu	8.13	123.92	4.30	54.78	41.87
186	Val	8.05	122.89	3.82	62.14	32.48
187	Glu	8.39	125.75	4.00	56.31	30.23
188	Asp	8.29	122.51	4.34	54.21	40.98
189	Ser	8.11	116.72	4.20	58.01	63.82
190	Ser	8.28	119.36	4.47	56.56	63.10
191	Pro	-	137.96	4.16	63.13	31.88
192	Glu	8.34	120.72	3.98	56.62	29.92
193	Ser	8.07	116.89	4.16	58.14	63.93
194	Glu	8.20	123.92	4.30	54.32	29.37
195	Pro	-	137.67	4.16	62.96	32.19
196	Val	8.08	120.56	3.77	62.10	32.61
197	Asp	8.19	124.07	4.30	54.82	41.01
198	Leu	8.01	123.51	-	55.35	41.71
199	Phe	8.11	119.83	4.20	57.98	38.45
200	Leu	7.66	122.51	-	55.32	41.97
201	Glu	8.05	120.71	-	56.79	29.87

Appendix B

Chemical Shifts of the ECD of $CRF_{2\beta}R$

		H	N	NE	HA	HB	HG	HD	HE	C
16	His	-	-	-	-	3.44,2.79	-	-	-	-
17	Met	7.14	107.98	-	-	-	-	-	-	4.37
21	Asp	-	-	-	4.07	-	-	-	-	-
22	Leu	8.20	125.08	-	3.95	1.42	-	-	-	-
23	Gly	7.96	121.59	-	4.07	-	-	-	-	1.18
24	Thr	8.02	121.42	-	4.09	-	-	-	-	1.21
25	Thr	7.92	118.50	-	4.05	1.83	-	-	-	-
26	Leu	8.02	120.56	-	4.08	-	-	-	-	-
27	Leu	-	-	-	4.28	1.85	-	-	-	-
28	Glu	8.27	119.75	-	4.11	1.55	1.37	-	-	-
29	Gln	7.81	119.46	109.89	3.98	1.82,1.72	2.29	-	6.45,6.55	-
30	Tyr	8.36	120.98	-	4.15	-	-	-	-	-
31	Cys	8.03	114.96	-	4.11	1.86,1.75	-	-	-	-
32	His	8.24	119.93	-	4.45	2.53,2.43	-	-	-	-
33	Arg	7.98	115.07	-	4.57	3.69	-	-	-	-
34	Thr	3.62	-	-	4.26	2.08	-	-	-	1.74
35	Thr	8.17	118.36	-	4.44	2.58	-	-	-	-
36	Ile	8.06	121.91	-	4.14	-	1.05	-	-	1.48
37	Gly	8.29	107.26	-	3.82	-	-	-	-	-
38	Asn	7.88	112.56	-	4.15	4.09	-	-	-	1.04
39	Phe	8.01	114.95	-	4.13	4.10	-	-	-	1.06
40	Ser	8.07	122.22	-	4.11	1.49,1.39	1.45	-	-	0.70
41	Gly	1.41	120.02	-	4.02	-	-	-	-	1.51
42	Pro	-	118.55	-	3.86	8.06	2.08	-	-	-
43	Tyr	6.63	117.72	-	4.13	1.83	-	-	-	2.11
47	Asn	1.86	111.73	-	3.68	2.05	-	-	-	2.57
48	Thr	8.01	117.00	-	4.09	4.36	1.05	-	-	-
49	Thr	-	-	-	4.26	-	-	-	-	-
50	Leu	8.02	122.08	-	4.05	1.69	1.48	0.73	-	1.04
51	Asp	8.20	111.05	-	-	-	-	-	-	3.71

52	Gln	7.33	117.21	-	4.12	2.14,1.80	-	-	-	-	
54	Gly	-	-	-	4.37	-	-	-	-	3.67	
55	Thr	7.80	109.38	-	-	-	-	-	-	3.86	
56	Cys	3.33	-	-	4.27	1.84,1.59	-	-	-	1.35	
57	Trp	7.77	118.32	-	4.48	2.87,2.61	-	-	-	6.92	
58	Pro	-	113.46	-	4.02	3.88	-	-	-	0.90	
59	Gln	7.39	118.38	-	4.33	2.70,2.54	-	-	-	6.62	
60	Ser	8.36	115.87	-	3.95	1.25,1.07	-	-	-	-	
61	Ala	6.89	120.01	-	4.58	2.68,2.78	-	-	-	-	
62	Pro	-	118.08	-	4.83	3.87	-	-	-	1.04	
63	Gly	3.84	120.91	-	4.52	-	-	-	-	0.64	
64	Ala	1.46	126.88	-	5.06	1.26,1.47	-	-	-	0.58	
65	Leu	8.40	122.96	-	4.73	3.36,2.42	-	-	-	-	
66	Val	8.42	113.86	-	3.98	2.02	-	-	-	2.34	
67	Glu	7.80	115.69	-	4.14	2.01	1.10	-	-	0.34	
68	Arg	7.78	107.47	-	4.17	-	-	-	-	-	
69	Pro	-	121.24	-	3.71	3.90	8.39	-	-	-0.18	
70	Cys	8.30	124.62	-	4.54	2.62	-	-	-	-	
71	Pro	-	167.80	-	4.30	2.06	10.45	6.39	-	-	
72	Glu	-	-	-	4.37	-	-	-	-	-	
73	Tyr	6.63	119.41	-	4.09	1.82,1.71	-	-	-	2.04	
74	Phe	5.41	119.99	-	4.84	3.47,3.16	-	-	-	-	
75	Asn	8.33	124.63	-	3.69	1.00	-	-	-	-	
76	Gly	2.08	-	-	-	-	-	-	-	-	
77	Ile	7.78	112.66	-	4.00	-	-	-	-	-	
78	Lys	7.60	122.14	-	4.11	1.21	-	-	-	-	
79	Tyr	8.22	122.09	-	4.52	1.72,1.32	-	-	-	0.69	
80	Asn	8.80	129.49	-	4.15	2.60	-	-	-	1.26	
81	Thr	8.37	124.61	-	5.16	1.77	-	-	-	1.84	
82	Thr	8.36	121.80	-	4.42	-	-	-	-	1.08	
83	Arg	-	-	-	4.48	2.33	-	-	-	-	
84	Asn	8.41	119.93	-	3.94	2.70	-	-	-	-	
85	Ala	-	-	-	4.34	1.81	-	-	-	-	
86	Tyr	8.41	119.81	-	4.08	1.58	-	-	-	2.04	
87	Arg	7.92	117.53	-	4.28	2.81,2.91	-	6.94	-	-	
89	Cys	6.46	110.42	-	-	2.71	-	-	-	7.04	
90	Leu	7.96	101.32	-	3.94	-	-	-	-	-	
91	Glu	7.51	121.39	-	4.05	1.82	1.30	-	-	0.44	
92	Asn	8.06	125.03	-	4.51	1.64,1.44	-	-	-	1.14	
93	Gly	2.56	123.83	-	4.34	-	-	-	-	6.70	
94	Thr	8.55	120.03	-	5.20	-	-	-	-	7.47	
95	Trp	8.18	114.50	-	4.05	-	-	-	-	1.06	
96	Ala	7.98	110.23	-	4.20	-	-	-	-	1.10	
97	Ser	7.05	119.48	-	4.33	1.87,1.73	-	-	-	3.09	
98	Arg	8.22	116.61	-	5.05	2.06,1.83	-	-	-	6.87	
99	Val	8.99	120.21	-	4.33	-	-	-	-	0.91	
100	Asn	7.55	112.57	-	5.82	2.76,2.53	-	-	-	-	6.75:956
101	Tyr	1.26	122.33	-	4.25	0.39,-0.30	-	0.99	-	6.46	
102	Ser	8.60	126.52	-	4.73	1.70,1.84	1.93	-	-	-	

103	His	8.85	124.14	-	4.34	2.55,1.70	-	-	-	-
104	Cys	1.54	127.24	-	4.32	2.09,1.31	-	-	-	0.66
105	Glu	8.36	116.05	-	3.60	1.83,1.57	2.08	-	-	-
106	Pro	-	112.55	-	4.38	7.32,7.32	-	6.98	-	-
107	Ile	8.17	105.96	-	3.55	-	-	-	-	-
108	Leu	6.62	108.34	-	4.29	3.87	-	-	-	0.90
109	Asp	7.12	121.92	-	4.51	2.70,2.85	-	-	-	-
110	Asp	8.85	123.12	-	4.18	1.54	-	-	-	-
111	Lys	-	-	-	-	3.80	-	-	-	-
112	Gln	7.40	118.42	-	4.33	1.56	1.31	-	-	3.01
113	Arg	8.09	123.73	-	3.60	1.48	-	-	-	0.42
114	Lys	8.62	121.45	-	4.71	3.01,2.58	-	7.40	-	-
115	Tyr	8.98	126.90	-	4.72	2.41	-	6.80	-	-
116	Asp	8.52	116.48	-	4.00	3.78	-	-	-	-
117	Leu	9.53	119.13	-	4.54	3.25	-	6.99	-	-
118	His	7.79	116.00	-	4.51	2.72,2.63	-	-	-	-
119	Tyr	8.11	122.24	-	-	1.83	-	-	-	-

Acknowledgment

A lot of support was received from many different people, intentionally and unintentionally.
First, I would like to thank Prof. Roland Riek for giving me the opportunity to do my PhD in his group.
As well, I would like to thank Prof. Gebhard Schertler for his time and accepting this manuscript for corrections and his group, with which I had many fruitful discussions.
I would like to acknowledge Dr. Marilyn Perrin for measuring my protein samples, sometimes even on short notice and for her great work on the activity assays.
Additionally, I would like to thank Prof. Jean Rivier for the biotinylated Astressin.
I would like to thank Dr. Christos Tzitzilonis for his teachings about protein purification and his introduction to membrane proteins. Unforgettable will be his great sense of humour and his not-so-children-approved vocabulary during daily routines, which made the quotidian so much more fun.
I would like to thank Dr. Stefan Bibow for his great help regarding NMR spectroscopy measurements and teaching me with patience the secrets about NMR.
I would like to thank Michael Arzt from the Prof. Martin Schwab group for participating in a collaboration and entrusting me with parts of his projects such as the assignment of $\Delta 20$.
I am very grateful for Kristina, she is a solid rock in our turbulent and sometimes chaotic world.
I would like to acknowledge Marielle and Marianne. She was a great help, when moral

support was needed, and was the sacrificial person to read through the first draft of my thesis. The rescue of the fishes will stay forever in my memories, also the unfortunately not growing cherry tree.
I express also my gratitude to Michael, for reading through parts of my thesis, his help on mathematica and his fast participation in celebrating or mourning, when needed.
A big thanks goes to Silvia, also for reading large parts of my thesis. I hope Tommaso learned some new techniques as well during the corrections.
I would like to thank Franziska, Reto and Dominik for keeping me active and getting me through bad days without mercy.
I would like to thank as well T, M, and S for showing me the sweet life of breaks and for all the enjoyable and sometimes squabbling game nights that kept my mind off my minor problems.
I am blessed to have such a great family, who supported me and kept me motivated. Dominik for giving me an asylum, when my world consisted of nothing but my bed and my office and Benjamin for the music he shared with me that kept me motivated during non-motivating days; Veronika and René for showing me the world of the grown up PhDs. Unforgettable will be the Tuesday evenings, where drawbacks were sarcastically dissected, those evenings kept me cheerful and pragmatic. A big thank you goes to my parents, who always believed in me; the cakes kept me going through Mondays.
Notamment, Bas. Je pourrais dire tant de choses, mais je ferais court: Merci de m'avoir gardée optimiste.

Curriculum vitae

Viviane Dominika Zelenay

Date of Birth: 16.06.1987
Nationality: Swiss
Marital Status: Single

Education and Academic Degrees

05.2011– Present	PhD at the Swiss Federal Institute of Technology Zurich (ETH Zurich), Switzerland and the Salk Institute, San Diego, USA.
09.2009 – 01.2011	Studies in Chemistry at the ETH Zurich, Switzerland and the National University of Singapore (NUS), Singapore. Degree: Master of Science (MSc) ETH in Chemistry.
09.2006 – 09.2009	Studies in Chemistry at the ETH Zurich, Switzerland. Degree: Bachelor of Science (BSc) ETH in Chemistry.
09.2006	Federal Maturity Diploma at Kantonsschule Oerlikon (High School), Switzerland.

Thesis

05.2011 – Present	PhD thesis Supervised by Prof. Roland Riek at the ETH Zurich, Switzerland — *Development of Purification Protocols for CRF Receptor Isomers and Structural Investigations of Potential Interactions Between Nogo-A-Δ20 and S1PR2-Fragments*.
08.2010 – 12.2010	Master thesis Supervised by Prof. Roland Sigel at the University of Zurich, Switzerland and Prof. Roland Riek at the ETH, Switzerland — btuB *Riboswitch and its Structural Changes Upon Binding to Coenzyme* B_{12}.

Projects & Practical Trainings

01.2014	Practical training in Computer-Assisted Drug Design supervised by Prof. Gisbert Schneider at the ETH Zurich, Switzerland (2 weeks).
06.2011 – 10.2011	Research studies supervised by Prof. Senyon Choe and Prof. Wylie Vale at the Salk Institute, San Diego, USA, as Part of PhD.
02.2010 – 08.2010	Research project in the analytical chemistry group of Prof. Lee Hian Kee at NUS, Singapur — *Micro-Extraction of Organic Compounds Analysed by Gas Chromatography.*
02.2009 – 06.2009	Research project in the bioinorganic chemistry group of Prof. Willhelm H. Koppenol at ETH Zurich, Switzerland — *Kinetics of Ascorbate Depletion by Amino Acids Radicals.*
02.2009 – 05.2009	Scientific and Technical English (B2) at the ETH Zurich, Switzerland.

Bibliography

[1] Robert Fredriksson, Malin C Lagerstrom, Lars-Gustav Lundin, and Helgi B Schioth. The g-protein-coupled receptors in the human genome form five main families. phylogenetic analysis, paralogon groups, and fingerprints. *Mol Pharmacol*, 63(6):1256–1272, Jun 2003. ISSN 0026-895X (Print); 0026-895X (Linking).

[2] Jung-Soon Mo, Hyun Woo Park, and Kun-Liang Guan. The hippo signaling pathway in stem cell biology and cancer. *EMBO Rep*, 15(6):642–656, Jun 2014. ISSN 1469-3178 (Electronic); 1469-221X (Linking).

[3] Jose L Moreno, Terrell Holloway, and Javier Gonzalez-Maeso. G protein-coupled receptor heterocomplexes in neuropsychiatric disorders. *Prog Mol Biol Transl Sci*, 117:187–205, 2013. ISSN 1878-0814 (Electronic); 1877-1173 (Linking).

[4] Kinga Szafran, Agata Faron-Gorecka, Magdalena Kolasa, Maciej Kusmider, Joanna Solich, Dariusz Zurawek, and Marta Dziedzicka-Wasylewska. Potential role of g protein-coupled receptor (gpcr) heterodimerization in neuropsychiatric disorders: a focus on depression. *Pharmacol Rep*, 65(6):1498–1505, 2013. ISSN 1734-1140 (Print); 1734-1140 (Linking).

[5] Richard L Hauger, Victoria Risbrough, Robert H Oakley, J Alberto Olivares-Reyes, and Frank M Dautzenberg. Role of crf receptor signaling in stress vulnerability, anxiety, and depression. *Ann N Y Acad Sci*, 1179:120–143, Oct 2009. ISSN 1749-6632 (Electronic); 0077-8923 (Linking).

[6] Alan Wise, Katy Gearing, and Stephen Rees. Target validation of g-protein coupled receptors. *Drug Discov Today*, 7(4):235–246, Feb 2002. ISSN 1359-6446 (Print); 1359-6446 (Linking).

[7] John P Overington, Bissan Al-Lazikani, and Andrew L Hopkins. How many drug targets are there? *Nat Rev Drug Discov*, 5(12):993–996, Dec 2006. ISSN 1474-1776 (Print); 1474-1776 (Linking).

[8] Malin C. Lagerstrom and Helgi B. Schioth. Structural diversity of g protein-coupled receptors and significance for drug discovery. *Nat Rev Drug Discov*, 7 (4):339–357, 04 2008. ISBN 1474-1776. URL `http://dx.doi.org/10.1038/nrd2518`.

[9] K Palczewski, T Kumasaka, T Hori, C A Behnke, H Motoshima, B A Fox, I Le Trong, D C Teller, T Okada, R E Stenkamp, M Yamamoto, and M Miyano. Crystal structure of rhodopsin: A g protein-coupled receptor. *Science*, 289 (5480):739–745, Aug 2000. ISSN 0036-8075 (Print); 0036-8075 (Linking).

[10] A J Venkatakrishnan, Xavier Deupi, Guillaume Lebon, Christopher G Tate, Gebhard F Schertler, and M Madan Babu. Molecular signatures of g-protein-coupled receptors. *Nature*, 494(7436):185–194, Feb 2013. ISSN 1476-4687 (Electronic); 0028-0836 (Linking).

[11] Theresa M Cabrera-Vera, Jurgen Vanhauwe, Tarita O Thomas, Martina Medkova, Anita Preininger, Maria R Mazzoni, and Heidi E Hamm. Insights into g protein structure, function, and regulation. *Endocr Rev*, 24(6):765–781, Dec 2003. ISSN 0163-769X (Print); 0163-769X (Linking).

[12] Kurt Kristiansen. Molecular mechanisms of ligand binding, signaling, and regulation within the superfamily of g-protein-coupled receptors: molecular modeling and mutagenesis approaches to receptor structure and function. *Pharmacol Ther*, 103(1):21–80, Jul 2004. ISSN 0163-7258 (Print); 0163-7258 (Linking).

[13] Dong Soo Kang, Xufan Tian, and Jeffrey L Benovic. Role of beta-arrestins and arrestin domain-containing proteins in g protein-coupled receptor trafficking. *Curr Opin Cell Biol*, 27:63–71, Apr 2014. ISSN 1879-0410 (Electronic); 0955-0674 (Linking).

[14] Robert P Millar and Claire L Newton. The year in g protein-coupled receptor research. *Mol Endocrinol*, 24(1):261–274, Jan 2010. ISSN 1944-9917 (Electronic); 0888-8809 (Linking).

[15] L F Jr Kolakowski. Gcrdb: a g-protein-coupled receptor database. *Receptors Channels*, 2(1):1–7, 1994. ISSN 1060-6823 (Print); 1060-6823 (Linking).

[16] Juan A. Ballesteros and Harel Weinstein. Integrated methods for the construction of three-dimensional models and computational probing of structure-function relations in g protein-coupled receptors. In Stuart C. Sealfon, editor, *Receptor Molecular Biology*, volume 25, pages 366 – 428. Academic Press, 1995. ISSN 1043-9471. URL `http://www.sciencedirect.com/science/article/pii/S1043947105800497`.

[17] Denise Wootten, John Simms, Laurence J. Miller, Arthur Christopoulos, and Patrick M. Sexton. Polar transmembrane interactions drive formation of ligand-specific and signal pathway-biased family b g protein-coupled receptor conformations. *Proceedings of the National Academy of Sciences*, 110(13): 5211–5216, 2013. URL `http://www.pnas.org/content/110/13/5211.abstract`.

[18] Jean-Michel Neumann, Alain Couvineau, Samuel Murail, Jean-Jacques Lacapere, Nadege Jamin, and Marc Laburthe. Class-b gpcr activation: is ligand helix-capping the key? *Trends Biochem Sci*, 33(7):314–319, Jul 2008. ISSN 0968-0004 (Print); 0968-0004 (Linking).

[19] M Arai, I Q Assil, and A B Abou-Samra. Characterization of three corticotropin-releasing factor receptors in catfish: a novel third receptor is predominantly expressed in pituitary and urophysis. *Endocrinology*, 142(1):446–454, Jan 2001. ISSN 0013-7227 (Print); 0013-7227 (Linking).

[20] Edward W Hillhouse and Dimitris K Grammatopoulos. The molecular mechanisms underlying the regulation of the biological activity of corticotropin-releasing hormone receptors: implications for physiology and pathophysiology. *Endocr Rev*, 27(3):260–286, May 2006. ISSN 0163-769X (Print); 0163-769X (Linking).

[21] E Nishimura, N Billestrup, M Perrin, and W Vale. Identification and characterization of a pituitary corticotropin-releasing factor binding protein by chemical cross-linking. *J Biol Chem*, 262(27):12893–12896, Sep 1987. ISSN 0021-9258 (Print); 0021-9258 (Linking).

[22] Alon M Chen, Marilyn H Perrin, Michael R Digruccio, Joan M Vaughan, Bhawanjit K Brar, Carlos M Arias, Kathy A Lewis, Jean E Rivier, Paul E Sawchenko, and Wylie W Vale. A soluble mouse brain splice variant of type 2alpha corticotropin-releasing factor (crf) receptor binds ligands and modulates their activity. *Proc Natl Acad Sci U S A*, 102(7):2620–2625, Feb 2005. ISSN 0027-8424 (Print); 0027-8424 (Linking).

[23] Christopher G Tate and Gebhard F X Schertler. Engineering g protein-coupled receptors to facilitate their structure determination. *Curr Opin Struct Biol*, 19 (4):386–395, Aug 2009. ISSN 1879-033X (Electronic); 0959-440X (Linking).

[24] Christoph Parthier, Steffen Reedtz-Runge, Rainer Rudolph, and Milton T Stubbs. Passing the baton in class b gpcrs: peptide hormone activation via helix induction? *Trends Biochem Sci*, 34(6):303–310, Jun 2009. ISSN 0968-0004 (Print); 0968-0004 (Linking).

[25] S M Nielsen, L Z Nielsen, S A Hjorth, M H Perrin, and W W Vale. Constitutive activation of tethered-peptide/corticotropin-releasing factor receptor chimeras. *Proc Natl Acad Sci U S A*, 97(18):10277–10281, Aug 2000. ISSN 0027-8424 (Print); 0027-8424 (Linking).

[26] Christy Rani R Grace, Laura Cervini, Jozsef Gulyas, Jean Rivier, and Roland Riek. Astressin-amide and astressin-acid are structurally different in dimethylsulfoxide. *Biopolymers*, 87(2-3):196–205, Oct 2007. ISSN 0006-3525 (Print); 0006-3525 (Linking).

[27] Christy Rani R Grace, Marilyn H Perrin, Jozsef Gulyas, Michael R Digruccio, Jeffrey P Cantle, Jean E Rivier, Wylie W Vale, and Roland Riek. Structure of the n-terminal domain of a type b1 g protein-coupled receptor in complex with a peptide ligand. *Proc Natl Acad Sci U S A*, 104(12):4858–4863, Mar 2007. ISSN 0027-8424 (Print); 0027-8424 (Linking).

[28] Augen A Pioszak, Naomi R Parker, Kelly Suino-Powell, and H Eric Xu. Molecular recognition of corticotropin-releasing factor by its g-protein-coupled receptor crfr1. *J Biol Chem*, 283(47):32900–32912, Nov 2008. ISSN 0021-9258 (Print); 0021-9258 (Linking).

[29] Christy Rani R Grace, Marilyn H Perrin, Jeffrey P Cantle, Wylie W Vale, Jean E Rivier, and Roland Riek. Common and divergent structural features of a se-

ries of corticotropin releasing factor-related peptides. *J Am Chem Soc*, 129(51): 16102–16114, Dec 2007. ISSN 1520-5126 (Electronic); 0002-7863 (Linking).

[30] J W Tams, S M Knudsen, and J Fahrenkrug. Proposed arrangement of the seven transmembrane helices in the secretin receptor family. *Receptors Channels*, 5 (2):79–90, 1998. ISSN 1060-6823 (Print); 1060-6823 (Linking).

[31] Sam R J Hoare, Sue K Sullivan, David A Schwarz, Nicholas Ling, Wylie W Vale, Paul D Crowe, and Dimitri E Grigoriadis. Ligand affinity for amino-terminal and juxtamembrane domains of the corticotropin releasing factor type i receptor: regulation by g-protein and nonpeptide antagonists. *Biochemistry*, 43(13): 3996–4011, Apr 2004. ISSN 0006-2960 (Print); 0006-2960 (Linking).

[32] M H Perrin, S Sutton, D L Bain, W T Berggren, and W W Vale. The first extracellular domain of corticotropin releasing factor-r1 contains major binding determinants for urocortin and astressin. *Endocrinology*, 139(2):566–570, Feb 1998. ISSN 0013-7227 (Print); 0013-7227 (Linking).

[33] S Wille, S Sydow, M R Palchaudhuri, J Spiess, and F M Dautzenberg. Identification of amino acids in the n-terminal domain of corticotropin-releasing factor receptor 1 that are important determinants of high-affinity ligand binding. *J Neurochem*, 72(1):388–395, Jan 1999. ISSN 0022-3042 (Print); 0022-3042 (Linking).

[34] Shiva Kumar, Augen Pioszak, Chenghai Zhang, Kunchithapadam Swaminathan, and H Eric Xu. Crystal structure of the pac1r extracellular domain unifies a consensus fold for hormone recognition by class b g-protein coupled receptors. *PLoS One*, 6(5):e19682, 2011. ISSN 1932-6203 (Electronic); 1932-6203 (Linking).

[35] Christoph Parthier, Martin Kleinschmidt, Piotr Neumann, Rainer Rudolph, Susanne Manhart, Dagmar Schlenzig, Jorg Fanghanel, Jens-Ulrich Rahfeld, Hans-Ulrich Demuth, and Milton T Stubbs. Crystal structure of the incretin-bound extracellular domain of a g protein-coupled receptor. *Proc Natl Acad Sci U S A*, 104(35):13942–13947, Aug 2007. ISSN 0027-8424 (Print); 0027-8424 (Linking).

[36] Steffen Runge, Henning Thogersen, Kjeld Madsen, Jesper Lau, and Rainer Rudolph. Crystal structure of the ligand-bound glucagon-like peptide-1 receptor extracellular domain. *J Biol Chem*, 283(17):11340–11347, Apr 2008. ISSN 0021-9258 (Print); 0021-9258 (Linking).

[37] Augen A Pioszak and H Eric Xu. Molecular recognition of parathyroid hormone by its g protein-coupled receptor. *Proc Natl Acad Sci U S A*, 105(13):5034–5039, Apr 2008. ISSN 1091-6490 (Electronic); 0027-8424 (Linking).

[38] Christy R R Grace, Marilyn H Perrin, Michael R DiGruccio, Charleen L Miller, Jean E Rivier, Wylie W Vale, and Roland Riek. Nmr structure and peptide hormone binding site of the first extracellular domain of a type b1 g protein-coupled receptor. *Proc Natl Acad Sci U S A*, 101(35):12836–12841, Aug 2004. ISSN 0027-8424 (Print); 0027-8424 (Linking).

[39] Christy Rani R Grace, Marilyn H Perrin, Jozsef Gulyas, Jean E Rivier, Wylie W Vale, and Roland Riek. Nmr structure of the first extracellular domain of corticotropin-releasing factor receptor 1 (ecd1-crf-r1) complexed with a high affinity agonist. *J Biol Chem*, 285(49):38580–38589, Dec 2010. ISSN 1083-351X (Electronic); 0021-9258 (Linking).

[40] Chaohong Sun, Danying Song, Rachel A Davis-Taber, Leo W Barrett, Victoria E Scott, Paul L Richardson, Ana Pereda-Lopez, Marie E Uchic, Larry R Solomon, Marc R Lake, Karl A Walter, Philip J Hajduk, and Edward T Olejniczak. Solution structure and mutational analysis of pituitary adenylate cyclase-activating polypeptide binding to the extracellular domain of pac1-rs. *Proc Natl Acad Sci U S A*, 104(19):7875–7880, May 2007. ISSN 0027-8424 (Print); 0027-8424 (Linking).

[41] Marilyn H Perrin, Christy R R Grace, Michael R Digruccio, Wolfgang H Fischer, Samir K Maji, Jeffrey P Cantle, Sean Smith, Gerard Manning, Wylie W Vale, and Roland Riek. Distinct structural and functional roles of conserved residues in the first extracellular domain of receptors for corticotropin-releasing factor and related g-protein-coupled receptors. *J Biol Chem*, 282(52):37529–37536, Dec 2007. ISSN 0021-9258 (Print); 0021-9258 (Linking).

[42] Kaspar Hollenstein, Chris de Graaf, Andrea Bortolato, Ming-Wei Wang, Fiona H. Marshall, and Raymond C. Stevens. Insights into the structure of class b {GPCRs}. *Trends in Pharmacological Sciences*, 35(1):12 – 22, 2014. ISSN 0165-6147. URL `http://www.sciencedirect.com/science/article/pii/S0165614713002095`.

[43] Kaspar Hollenstein, James Kean, Andrea Bortolato, Robert K Y Cheng, Andrew S Dore, Ali Jazayeri, Robert M Cooke, Malcolm Weir, and Fiona H Marshall. Struc-

ture of class b gpcr corticotropin-releasing factor receptor 1. *Nature*, 499(7459): 438–443, Jul 2013. ISSN 1476-4687 (Electronic); 0028-0836 (Linking).

[44] Maria J Serrano-Vega, Francesca Magnani, Yoko Shibata, and Christopher G Tate. Conformational thermostabilization of the beta1-adrenergic receptor in a detergent-resistant form. *Proc Natl Acad Sci U S A*, 105(3):877–882, Jan 2008. ISSN 1091-6490 (Electronic); 0027-8424 (Linking).

[45] S A Hjorth, C Orskov, and T W Schwartz. Constitutive activity of glucagon receptor mutants. *Mol Endocrinol*, 12(1):78–86, Jan 1998. ISSN 0888-8809 (Print); 0888-8809 (Linking).

[46] R S Heller, T J Kieffer, and J F Habener. Point mutations in the first and third intracellular loops of the glucagon-like peptide-1 receptor alter intracellular signaling. *Biochem Biophys Res Commun*, 223(3):624–632, Jun 1996. ISSN 0006-291X (Print); 0006-291X (Linking).

[47] E Schipani, K Kruse, and H Juppner. A constitutively active mutant pth-pthrp receptor in jansen-type metaphyseal chondrodysplasia. *Science*, 268(5207):98–100, Apr 1995. ISSN 0036-8075 (Print); 0036-8075 (Linking).

[48] Sam R J Hoare, Brock T Brown, Mark A Santos, Siobhan Malany, Stephen F Betz, and Dimitri E Grigoriadis. Single amino acid residue determinants of non-peptide antagonist binding to the corticotropin-releasing factor1 (crf1) receptor. *Biochem Pharmacol*, 72(2):244–255, Jul 2006. ISSN 0006-2952 (Print); 0006-2952 (Linking).

[49] Fai Yiu Siu, Min He, Chris de Graaf, Gye Won Han, Dehua Yang, Zhiyun Zhang, Caihong Zhou, Qingping Xu, Daniel Wacker, Jeremiah S. Joseph, Wei Liu, Jesper Lau, Vadim Cherezov, Vsevolod Katritch, Ming-Wei Wang, and Raymond C. Stevens. Structure of the human glucagon class b g-protein-coupled receptor. *Nature*, advance online publication:, 07 17, 2013. ISBN 1476-4687. URL `http://dx.doi.org/10.1038/nature12393`.

[50] Vsevolod Katritch, Vadim Cherezov, and Raymond C Stevens. Diversity and modularity of g protein-coupled receptor structures. *Trends Pharmacol Sci*, 33 (1):17–27, Jan 2012. ISSN 1873-3735 (Electronic); 0165-6147 (Linking).

[51] Ryan T Evans and Audrey F Seasholtz. Soluble corticotropin-releasing hormone receptor 2alpha splice variant is efficiently translated but not trafficked for secretion. *Endocrinology*, 150(9):4191–4202, Sep 2009. ISSN 1945-7170 (Electronic); 0013-7227 (Linking).

[52] Eric Kubat, Shilpi Mahajan, Min Liao, Larry Ackerman, Peter T Ohara, Eileen F Grady, and Aditi Bhargava. Corticotropin-releasing factor receptor 2 mediates sex-specific cellular stress responses. *Mol Med*, 19:212–222, 2013. ISSN 1528-3658 (Electronic); 1076-1551 (Linking).

[53] Caroline M Hostetler and Andrey E Ryabinin. The crf system and social behavior: a review. *Front Neurosci*, 7:92, 2013. ISSN 1662-4548 (Print); 1662-453X (Linking).

[54] Debra A Bangasser. Sex differences in stress-related receptors: "micro" differences with "macro" implications for mood and anxiety disorders. *Biol Sex Differ*, 4(1):2, 2013. ISSN 2042-6410 (Electronic); 2042-6410 (Linking).

[55] Kendall M Carlin, Wylie W Vale, and Tracy L Bale. Vital functions of corticotropin-releasing factor (crf) pathways in maintenance and regulation of energy homeostasis. *Proc Natl Acad Sci U S A*, 103(9):3462–3467, Feb 2006. ISSN 0027-8424 (Print); 0027-8424 (Linking).

[56] Jill M Weathington and Bradley M Cooke. Corticotropin-releasing factor receptor binding in the amygdala changes across puberty in a sex-specific manner. *Endocrinology*, 153(12):5701–5705, Dec 2012. ISSN 1945-7170 (Electronic); 0013-7227 (Linking).

[57] E Dermitzaki, C Tsatsanis, V Minas, E Chatzaki, I Charalampopoulos, M Venihaki, A Androulidaki, M Lambropoulou, J Spiess, E Michalodimitrakis, A Gravanis, and A N Margioris. Corticotropin-releasing factor (crf) and the urocortins differentially regulate catecholamine secretion in human and rat adrenals, in a crf receptor type-specific manner. *Endocrinology*, 148(4):1524–1538, Apr 2007. ISSN 0013-7227 (Print); 0013-7227 (Linking).

[58] Efi Kokkotou, Daniel Torres, Alan C Moss, Michael O'Brien, Dimitri E Grigoriadis, Katia Karalis, and Charalabos Pothoulakis. Corticotropin-releasing

hormone receptor 2-deficient mice have reduced intestinal inflammatory responses. *J Immunol*, 177(5):3355–3361, Sep 2006. ISSN 0022-1767 (Print); 0022-1767 (Linking).

[59] Yael Kuperman, Orna Issler, Joan Vaughan, Louise Bilezikjian, Wylie Vale, and Alon Chen. Expression and regulation of corticotropin-releasing factor receptor type 2beta in developing and mature mouse skeletal muscle. *Mol Endocrinol*, 25(1):157–169, Jan 2011. ISSN 1944-9917 (Electronic); 0888-8809 (Linking).

[60] Yehezkel Sztainberg, Yael Kuperman, Orna Issler, Shosh Gil, Joan Vaughan, Jean Rivier, Wylie Vale, and Alon Chen. A novel corticotropin-releasing factor receptor splice variant exhibits dominant negative activity: a putative link to stress-induced heart disease. *FASEB J*, 23(7):2186–2196, Jul 2009. ISSN 1530-6860 (Electronic); 0892-6638 (Linking).

[61] Tracy L Bale, Frank J Giordano, Reed P Hickey, Yan Huang, Anjali K Nath, Kirk L Peterson, Wylie W Vale, and Kuo-Fen Lee. Corticotropin-releasing factor receptor 2 is a tonic suppressor of vascularization. *Proc Natl Acad Sci U S A*, 99(11): 7734–7739, May 2002. ISSN 0027-8424 (Print); 0027-8424 (Linking).

[62] E M Fekete, Y Zhao, A Szucs, V Sabino, P Cottone, J Rivier, W W Vale, G F Koob, and E P Zorrilla. Systemic urocortin 2, but not urocortin 1 or stressin 1-a, suppresses feeding via crf2 receptors without malaise and stress. *Br J Pharmacol*, 164(8):1959–1975, Dec 2011. ISSN 1476-5381 (Electronic); 0007-1188 (Linking).

[63] Sebastian Pollandt, Jie Liu, Luis Orozco-Cabal, Dimitri E Grigoriadis, Wylie W Vale, Joel P Gallagher, and Patricia Shinnick-Gallagher. Cocaine withdrawal enhances long-term potentiation induced by corticotropin-releasing factor at central amygdala glutamatergic synapses via crf, nmda receptors and pka. *Eur J Neurosci*, 24(6):1733–1743, Sep 2006. ISSN 0953-816X (Print); 0953-816X (Linking).

[64] Bin Wang, Zhi-Bing You, Kenner C Rice, and Roy A Wise. Stress-induced relapse to cocaine seeking: roles for the crf(2) receptor and crf-binding protein in the ventral tegmental area of the rat. *Psychopharmacology (Berl)*, 193(2):283–294, Aug 2007. ISSN 0033-3158 (Print); 0033-3158 (Linking).

[65] Yuan He, Kan Wang, and Nieng Yan. The recombinant expression systems for structure determination of eukaryotic membrane proteins. *Protein Cell*, 5(9): 658–672, Sep 2014. ISSN 1674-8018 (Electronic); 1674-800X (Linking).

[66] Jean-Louis Baneres, Jean-Luc Popot, and Bernard Mouillac. New advances in production and functional folding of g-protein-coupled receptors. *Trends Biotechnol*, 29(7):314–322, Jul 2011. ISSN 1879-3096 (Electronic); 0167-7799 (Linking).

[67] Reinhard Grisshammer. Purification of recombinant g-protein-coupled receptors. *Methods Enzymol*, 463:631–645, 2009. ISSN 1557-7988 (Electronic); 0076-6879 (Linking).

[68] Edward C Hulme and Mike A Trevethick. Ligand binding assays at equilibrium: validation and interpretation. *Br J Pharmacol*, 161(6):1219–1237, Nov 2010. ISSN 1476-5381 (Electronic); 0007-1188 (Linking).

[69] V Sarramegn, I Muller, A Milon, and F Talmont. Recombinant g protein-coupled receptors from expression to renaturation: a challenge towards structure. *Cell Mol Life Sci*, 63(10):1149–1164, May 2006. ISSN 1420-682X (Print); 1420-682X (Linking).

[70] Annela M Seddon, Paul Curnow, and Paula J Booth. Membrane proteins, lipids and detergents: not just a soap opera. *Biochim Biophys Acta*, 1666(1-2):105–117, Nov 2004. ISSN 0006-3002 (Print); 0006-3002 (Linking).

[71] Christopher G Tate. Practical considerations of membrane protein instability during purification and crystallisation. *Methods Mol Biol*, 601:187–203, 2010. ISSN 1940-6029 (Electronic); 1064-3745 (Linking).

[72] Eugene Serebryany, Gefei Alex Zhu, and Elsa C Y Yan. Artificial membrane-like environments for in vitro studies of purified g-protein coupled receptors. *Biochim Biophys Acta*, 1818(2):225–233, Feb 2012. ISSN 0006-3002 (Print); 0006-3002 (Linking).

[73] Yutaka Kofuku, Takumi Ueda, Junya Okude, Yutaro Shiraishi, Keita Kondo, Takuya Mizumura, Shiho Suzuki, and Ichio Shimada. Functional dynamics of deuterated beta2 -adrenergic receptor in lipid bilayers revealed by nmr spectroscopy. *Angew Chem Int Ed Engl*, 53(49):13376–13379, Dec 2014. ISSN 1521-3773 (Electronic); 1433-7851 (Linking).

[74] Stefan Bibow, Marta G Carneiro, T Michael Sabo, Claudia Schwiegk, Stefan Becker, Roland Riek, and Donghan Lee. Measuring membrane protein bond orientations in nanodiscs via residual dipolar couplings. *Protein Sci*, 23(7):851–856, Jul 2014. ISSN 1469-896X (Electronic); 0961-8368 (Linking).

[75] Natanya R Civjan, Timothy H Bayburt, Mary A Schuler, and Stephen G Sligar. Direct solubilization of heterologously expressed membrane proteins by incorporation into nanoscale lipid bilayers. *Biotechniques*, 35(3):556–560, Sep 2003. ISSN 0736-6205 (Print); 0736-6205 (Linking).

[76] T K Ritchie, Y V Grinkova, T H Bayburt, I G Denisov, J K Zolnerciks, W M Atkins, and S G Sligar. Chapter 11 - reconstitution of membrane proteins in phospholipid bilayer nanodiscs. *Methods Enzymol*, 464:211–231, 2009. ISSN 1557-7988 (Electronic); 0076-6879 (Linking).

[77] Andrew J Leitz, Timothy H Bayburt, Alexander N Barnakov, Barry A Springer, and Stephen G Sligar. Functional reconstitution of beta2-adrenergic receptors utilizing self-assembling nanodisc technology. *Biotechniques*, 40(5):601–602, May 2006. ISSN 0736-6205 (Print); 0736-6205 (Linking).

[78] Nivedita Mitra, Yuting Liu, Jian Liu, Eugene Serebryany, Victoria Mooney, Brian T DeVree, Roger K Sunahara, and Elsa C Y Yan. Calcium-dependent ligand binding and g-protein signaling of family b gpcr parathyroid hormone 1 receptor purified in nanodiscs. *ACS Chem Biol*, 8(3):617–625, Mar 2013. ISSN 1554-8937 (Electronic); 1554-8929 (Linking).

[79] Timothy H Bayburt, Andrew J Leitz, Guifu Xie, Daniel D Oprian, and Stephen G Sligar. Transducin activation by nanoscale lipid bilayers containing one and two rhodopsins. *J Biol Chem*, 282(20):14875–14881, May 2007. ISSN 0021-9258 (Print); 0021-9258 (Linking).

[80] Satita Tapaneeyakorn, Alan D Goddard, Joanne Oates, Christine L Willis, and Anthony Watts. Solution- and solid-state nmr studies of gpcrs and their ligands. *Biochim Biophys Acta*, 1808(6):1462–1475, Jun 2011. ISSN 0006-3002 (Print); 0006-3002 (Linking).

[81] Maciej Wiktor, Sebastien Morin, Hans-Jurgen Sass, Fabian Kebbel, and Stephan Grzesiek. Biophysical and structural investigation of bacterially expressed and

engineered ccr5, a g protein-coupled receptor. *J Biomol NMR*, 55(1):79–95, Jan 2013. ISSN 1573-5001 (Electronic); 0925-2738 (Linking).

[82] Antoine Gautier, John P Kirkpatrick, and Daniel Nietlispach. Solution-state nmr spectroscopy of a seven-helix transmembrane protein receptor: backbone assignment, secondary structure, and dynamics. *Angew Chem Int Ed Engl*, 47(38): 7297–7300, 2008. ISSN 1521-3773 (Electronic); 1433-7851 (Linking).

[83] K Pervushin, R Riek, G Wider, and K Wuthrich. Attenuated t2 relaxation by mutual cancellation of dipole-dipole coupling and chemical shift anisotropy indicates an avenue to nmr structures of very large biological macromolecules in solution. *Proc Natl Acad Sci U S A*, 94(23):12366–12371, Nov 1997. ISSN 0027-8424 (Print); 0027-8424 (Linking).

[84] Charles R Sanders and Frank Sonnichsen. Solution nmr of membrane proteins: practice and challenges. *Magn Reson Chem*, 44 Spec No:S24–40, Jul 2006. ISSN 0749-1581 (Print); 0749-1581 (Linking).

[85] Sang Ho Park, Bibhuti B Das, Fabio Casagrande, Ye Tian, Henry J Nothnagel, Mignon Chu, Hans Kiefer, Klaus Maier, Anna A De Angelis, Francesca M Marassi, and Stanley J Opella. Structure of the chemokine receptor cxcr1 in phospholipid bilayers. *Nature*, 491(7426):779–783, Nov 2012. ISSN 1476-4687 (Electronic); 0028-0836 (Linking).

[86] Rie Nygaard, Yaozhong Zou, Ron O Dror, Thomas J Mildorf, Daniel H Arlow, Aashish Manglik, Albert C Pan, Corey W Liu, Juan Jose Fung, Michael P Bokoch, Foon Sun Thian, Tong Sun Kobilka, David E Shaw, Luciano Mueller, R Scott Prosser, and Brian K Kobilka. The dynamic process of beta(2)-adrenergic receptor activation. *Cell*, 152(3):532–542, Jan 2013. ISSN 1097-4172 (Electronic); 0092-8674 (Linking).

[87] Antoine Gautier, Helen R Mott, Mark J Bostock, John P Kirkpatrick, and Daniel Nietlispach. Structure determination of the seven-helix transmembrane receptor sensory rhodopsin ii by solution nmr spectroscopy. *Nat Struct Mol Biol*, 17 (6):768–774, Jun 2010. ISSN 1545-9985 (Electronic); 1545-9985 (Linking).

[88] Johann P Klare, Igor Chizhov, and Martin Engelhard. Microbial rhodopsins: scaffolds for ion pumps, channels, and sensors. *Results Probl Cell Differ*, 45: 73–122, 2008. ISSN 0080-1844 (Print); 0080-1844 (Linking).

[89] Tomohiro Kimura, Krishna Vukoti, Diane L Lynch, Dow P Hurst, Alan Grossfield, Michael C Pitman, Patricia H Reggio, Alexei A Yeliseev, and Klaus Gawrisch. Global fold of human cannabinoid type 2 receptor probed by solid-state 13c-, 15n-mas nmr and molecular dynamics simulations. *Proteins*, 82(3): 452–465, Mar 2014. ISSN 1097-0134 (Electronic); 0887-3585 (Linking).

[90] M Katragadda, M W Maciejewski, and P L Yeagle. Structural studies of the putative helix 8 in the human beta(2) adrenergic receptor: an nmr study. *Biochim Biophys Acta*, 1663(1-2):74–81, May 2004. ISSN 0006-3002 (Print); 0006-3002 (Linking).

[91] Elvis K Tiburu, Sergiy Tyukhtenko, Han Zhou, David R Janero, Jochem Struppe, and Alexandros Makriyannis. Human cannabinoid 1 gpcr c-terminal domain interacts with bilayer phospholipids to modulate the structure of its membrane environment. *AAPS J*, 13(1):92–98, Mar 2011. ISSN 1550-7416 (Electronic); 1550-7416 (Linking).

[92] Angela Shuyi Chen, Young Mee Kim, Shovanlal Gayen, Qiwei Huang, Manfred Raida, and Congbao Kang. Nmr structural study of the intracellular loop 3 of the serotonin 5-ht(1a) receptor and its interaction with calmodulin. *Biochim Biophys Acta*, 1808(9):2224–2232, Sep 2011. ISSN 0006-3002 (Print); 0006-3002 (Linking).

[93] Gaetan Bellot, Robert Pascal, Christiane Mendre, Serge Urbach, Bernard Mouillac, and Helene Demene. Expression, purification and nmr characterization of the cyclic recombinant form of the third intracellular loop of the vasopressin type 2 receptor. *Protein Expr Purif*, 78(2):131–138, Aug 2011. ISSN 1096-0279 (Electronic); 1046-5928 (Linking).

[94] Andreyah Pope, Markus Eilers, Philip J Reeves, and Steven O Smith. Amino acid conservation and interactions in rhodopsin: probing receptor activation by nmr spectroscopy. *Biochim Biophys Acta*, 1837(5):683–693, May 2014. ISSN 0006-3002 (Print); 0006-3002 (Linking).

[95] Tao Wang, Jian-Qiong Xiong, Xiao-Bao Ren, and Wei Sun. The role of nogo-a in neuroregeneration: a review. *Brain Res Bull*, 87(6):499–503, Apr 2012. ISSN 1873-2747 (Electronic); 0361-9230 (Linking).

[96] Andrea B Huber, Oliver Weinmann, Christian Brosamle, Thomas Oertle, and Martin E Schwab. Patterns of nogo mrna and protein expression in the developing and adult rat and after cns lesions. *J Neurosci*, 22(9):3553–3567, May 2002. ISSN 1529-2401 (Electronic); 0270-6474 (Linking).

[97] M S Chen, A B Huber, M E van der Haar, M Frank, L Schnell, A A Spillmann, F Christ, and M E Schwab. Nogo-a is a myelin-associated neurite outgrowth inhibitor and an antigen for monoclonal antibody in-1. *Nature*, 403(6768):434–439, Jan 2000. ISSN 0028-0836 (Print); 0028-0836 (Linking).

[98] Vincent Pernet and Martin E Schwab. The role of nogo-a in axonal plasticity, regrowth and repair. *Cell Tissue Res*, 349(1):97–104, Jul 2012. ISSN 1432-0878 (Electronic); 0302-766X (Linking).

[99] Martin E Schwab. Functions of nogo proteins and their receptors in the nervous system. *Nat Rev Neurosci*, 11(12):799–811, Dec 2010. ISSN 1471-0048 (Electronic); 1471-003X (Linking).

[100] Anissa Kempf, Bjoern Tews, Michael E Arzt, Oliver Weinmann, Franz J Obermair, Vincent Pernet, Marta Zagrebelsky, Andrea Delekate, Cristina Iobbi, Ajmal Zemmar, Zorica Ristic, Miriam Gullo, Peter Spies, Dana Dodd, Daniel Gygax, Martin Korte, and Martin E Schwab. The sphingolipid receptor s1pr2 is a receptor for nogo-a repressing synaptic plasticity. *PLoS Biol*, 12(1):e1001763, Jan 2014. ISSN 1545-7885 (Electronic); 1544-9173 (Linking).

[101] Onanong Chivatakarn, Shinjiro Kaneko, Zhigang He, Marc Tessier-Lavigne, and Roman J Giger. The nogo-66 receptor ngr1 is required only for the acute growth cone-collapsing but not the chronic growth-inhibitory actions of myelin inhibitors. *J Neurosci*, 27(27):7117–7124, Jul 2007. ISSN 1529-2401 (Electronic); 0270-6474 (Linking).

[102] Nasrollah Rezaei-Ghaleh, Martin Blackledge, and Markus Zweckstetter. Intrinsically disordered proteins: from sequence and conformational properties toward drug discovery. *Chembiochem*, 13(7):930–950, May 2012. ISSN 1439-7633 (Electronic); 1439-4227 (Linking).

[103] M Madan Babu, Robin van der Lee, Natalia Sanchez de Groot, and Jorg Gsponer. Intrinsically disordered proteins: regulation and disease. *Curr Opin Struct Biol*, 21(3):432–440, Jun 2011. ISSN 1879-033X (Electronic); 0959-440X (Linking).

[104] A J Venkatakrishnan, Tilman Flock, Daniel Estevez Prado, Matt E Oates, Julian Gough, and M Madan Babu. Structured and disordered facets of the gpcr fold. *Curr Opin Struct Biol*, 27:129–137, Aug 2014. ISSN 1879-033X (Electronic); 0959-440X (Linking).

[105] Nathalie Sibille and Pau Bernado. Structural characterization of intrinsically disordered proteins by the combined use of nmr and saxs. *Biochem Soc Trans*, 40(5):955–962, Oct 2012. ISSN 1470-8752 (Electronic); 0300-5127 (Linking).

[106] Robert Konrat. Nmr contributions to structural dynamics studies of intrinsically disordered proteins. *J Magn Reson*, 241:74–85, Apr 2014. ISSN 1096-0856 (Electronic); 1090-7807 (Linking).

[107] Claudia Rutz, Armin Renner, Martina Alken, Katharina Schulz, Michael Beyermann, Burkhard Wiesner, Walter Rosenthal, and Ralf Schulein. The corticotropin-releasing factor receptor type 2a contains an n-terminal pseudo signal peptide. *J Biol Chem*, 281(34):24910–24921, Aug 2006. ISSN 0021-9258 (Print); 0021-9258 (Linking).

[108] L Debarbieux and J Beckwith. On the functional interchangeability, oxidant versus reductant, of members of the thioredoxin superfamily. *J Bacteriol*, 182 (3):723–727, Feb 2000. ISSN 0021-9193 (Print); 0021-9193 (Linking).

[109] J L Martin. Thioredoxin–a fold for all reasons. *Structure*, 3(3):245–250, Mar 1995. ISSN 0969-2126 (Print); 0969-2126 (Linking).

[110] Christopher Horst Lillig, Carsten Berndt, and Arne Holmgren. Glutaredoxin systems. *Biochim Biophys Acta*, 1780(11):1304–1317, Nov 2008. ISSN 0006-3002 (Print); 0006-3002 (Linking).

[111] SH Hutner, L Provasoli, A Schatz, and CP Haskins. Some approaches to the study of the role of metals in the metabolism of microorganisms. *Proc. Am. Philos. Soc.*, 94:152–170, 1950.

[112] Marilyn H Perrin, Michael R DiGruccio, Steven C Koerber, Jean E Rivier, Koichi S Kunitake, Deborah L Bain, Wolfgang H Fischer, and Wylie W Vale. A soluble form of the first extracellular domain of mouse type 2beta corticotropin-releasing factor receptor reveals differential ligand specificity. *J Biol Chem*, 278 (18):15595–15600, May 2003. ISSN 0021-9258 (Print); 0021-9258 (Linking).

[113] P Jeffrey Conn, Arthur Christopoulos, and Craig W Lindsley. Allosteric modulators of gpcrs: a novel approach for the treatment of cns disorders. *Nat Rev Drug Discov*, 8(1):41–54, Jan 2009. ISSN 1474-1784 (Electronic); 1474-1776 (Linking).

[114] Tony Warne, Jill Chirnside, and Gebhard F X Schertler. Expression and purification of truncated, non-glycosylated turkey beta-adrenergic receptors for crystallization. *Biochim Biophys Acta*, 1610(1):133–140, Feb 2003. ISSN 0006-3002 (Print); 0006-3002 (Linking).

[115] Roberto Jappelli, Marilyn H Perrin, Kathy A Lewis, Joan M Vaughan, Christos Tzitzilonis, Jean E Rivier, Wylie W Vale, and Roland Riek. Expression and functional characterization of membrane-integrated mammalian corticotropin releasing factor receptors 1 and 2 in escherichia coli. *PLoS One*, 9(1):e84013, 2014. ISSN 1932-6203 (Electronic); 1932-6203 (Linking).

[116] Bice Chini and Marco Parenti. G-protein-coupled receptors, cholesterol and palmitoylation: facts about fats. *J Mol Endocrinol*, 42(5):371–379, May 2009. ISSN 1479-6813 (Electronic); 0952-5041 (Linking).

[117] Md. Jafurulla, Shrish Tiwari, and Amitabha Chattopadhyay. Identification of cholesterol recognition amino acid consensus (crac) motif in g-protein coupled receptors. *Biochemical and Biophysical Research Communications*, 404(1): 569 – 573, 2011. ISSN 0006-291X. URL `http://www.sciencedirect.com/science/article/pii/S0006291X10022564`.

[118] G Gimpl, K Burger, and F Fahrenholz. Cholesterol as modulator of receptor function. *Biochemistry*, 36(36):10959–10974, Sep 1997. ISSN 0006-2960 (Print); 0006-2960 (Linking).

[119] Joanne Oates and Anthony Watts. Uncovering the intimate relationship between lipids, cholesterol and gpcr activation. *Curr Opin Struct Biol*, 21(6):802–807, Dec 2011. ISSN 1879-033X (Electronic); 0959-440X (Linking).

[120] Rob Phillips, Tristan Ursell, Paul Wiggins, and Pierre Sens. Emerging roles for lipids in shaping membrane-protein function. *Nature*, 459(7245):379–385, May 2009. ISSN 1476-4687 (Electronic); 0028-0836 (Linking).

[121] Yoko Shibata, Jim F White, Maria J Serrano-Vega, Francesca Magnani, Amanda L Aloia, Reinhard Grisshammer, and Christopher G Tate. Thermostabilization of

the neurotensin receptor nts1. *J Mol Biol*, 390(2):262–277, Jul 2009. ISSN 1089-8638 (Electronic); 0022-2836 (Linking).

[122] Guillaume Lebon, Kirstie Bennett, Ali Jazayeri, and Christopher G Tate. Thermostabilisation of an agonist-bound conformation of the human adenosine a(2a) receptor. *J Mol Biol*, 409(3):298–310, Jun 2011. ISSN 1089-8638 (Electronic); 0022-2836 (Linking).

[123] Casim A Sarkar, Igor Dodevski, Manca Kenig, Stefan Dudli, Anja Mohr, Emmanuel Hermans, and Andreas Pluckthun. Directed evolution of a g protein-coupled receptor for expression, stability, and binding selectivity. *Proc Natl Acad Sci U S A*, 105(39):14808–14813, Sep 2008. ISSN 1091-6490 (Electronic); 0027-8424 (Linking).

[124] Christopher G Tate. A crystal clear solution for determining g-protein-coupled receptor structures. *Trends Biochem Sci*, 37(9):343–352, Sep 2012. ISSN 0968-0004 (Print); 0968-0004 (Linking).

[125] S P Lei, H C Lin, S S Wang, J Callaway, and G Wilcox. Characterization of the erwinia carotovora pelb gene and its product pectate lyase. *J Bacteriol*, 169(9): 4379–4383, Sep 1987. ISSN 0021-9193 (Print); 0021-9193 (Linking).

[126] B C Berks, F Sargent, and T Palmer. The tat protein export pathway. *Mol Microbiol*, 35(2):260–274, Jan 2000. ISSN 0950-382X (Print); 0950-382X (Linking).

[127] Tarmo P Roosild, Jason Greenwald, Mark Vega, Samantha Castronovo, Roland Riek, and Senyon Choe. Nmr structure of mistic, a membrane-integrating protein for membrane protein expression. *Science*, 307(5713):1317–1321, Feb 2005. ISSN 1095-9203 (Electronic); 0036-8075 (Linking).

[128] F William Studier. Protein production by auto-induction in high density shaking cultures. *Protein Expr Purif*, 41(1):207–234, May 2005. ISSN 1046-5928 (Print); 1046-5928 (Linking).

[129] L E Petrovskaya, A A Shulga, O V Bocharova, Ya S Ermolyuk, E A Kryukova, V V Chupin, M J J Blommers, A S Arseniev, and M P Kirpichnikov. Expression of g-protein coupled receptors in escherichia coli for structural studies. *Biochemistry (Mosc)*, 75(7):881–891, Jul 2010. ISSN 1608-3040 (Electronic); 0006-2979 (Linking).

[130] Alexander I Alexandrov, Mauro Mileni, Ellen Y T Chien, Michael A Hanson, and Raymond C Stevens. Microscale fluorescent thermal stability assay for membrane proteins. *Structure*, 16(3):351–359, Mar 2008. ISSN 0969-2126 (Print); 0969-2126 (Linking).

[131] Ana Sofia Pina, Christopher R Lowe, and Ana Cecilia A Roque. Challenges and opportunities in the purification of recombinant tagged proteins. *Biotechnol Adv*, 32(2):366–381, Mar-Apr 2014. ISSN 1873-1899 (Electronic); 0734-9750 (Linking).

[132] D S Hage. Affinity chromatography: a review of clinical applications. *Clin Chem*, 45(5):593–615, May 1999. ISSN 0009-9147 (Print); 0009-9147 (Linking).

[133] T Ohtaki, Y Masuda, Y Ishibashi, C Kitada, A Arimura, and M Fujino. Purification and characterization of the receptor for pituitary adenylate cyclase-activating polypeptide. *J Biol Chem*, 268(35):26650–26657, Dec 1993. ISSN 0021-9258 (Print); 0021-9258 (Linking).

[134] E Hazum, I Schvartz, Y Waksman, and D Keinan. Solubilization and purification of rat pituitary gonadotropin-releasing hormone receptor. *J Biol Chem*, 261(28): 13043–13048, Oct 1986. ISSN 0021-9258 (Print); 0021-9258 (Linking).

[135] Ann T Du, Done Onan, Diem T Dinh, Michael J Lew, James Ziogas, Marie-Isabel Aguilar, Leonard K Pattenden, and Walter G Thomas. Ligand-supported purification of the urotensin-ii receptor. *Mol Pharmacol*, 78(4):639–647, Oct 2010. ISSN 1521-0111 (Electronic); 0026-895X (Linking).

[136] J M Gibbins, R J Woods, and P J Lowry. Affinity purification of 61- and 65-kda rat brain corticotropin-releasing factor receptors and receptor-associated g proteins. *Int J Biochem Cell Biol*, 28(9):1017–1029, Sep 1996. ISSN 1357-2725 (Print); 1357-2725 (Linking).

[137] Hugo O Villar, Jiangli Yan, and Mark R Hansen. Using nmr for ligand discovery and optimization. *Curr Opin Chem Biol*, 8(4):387–391, Aug 2004. ISSN 1367-5931 (Print); 1367-5931 (Linking).

[138] Mike P Williamson. Using chemical shift perturbation to characterise ligand binding. *Prog Nucl Magn Reson Spectrosc*, 73:1–16, Aug 2013. ISSN 1873-3301 (Electronic); 0079-6565 (Linking).

[139] Thomas Oertle, Marjan E van der Haar, Christine E Bandtlow, Anna Robeva, Patricia Burfeind, Armin Buss, Andrea B Huber, Marjo Simonen, Lisa Schnell, Christian Brosamle, Klemens Kaupmann, Rudiger Vallon, and Martin E Schwab. Nogo-a inhibits neurite outgrowth and cell spreading with three discrete regions. *J Neurosci*, 23(13):5393–5406, Jul 2003. ISSN 1529-2401 (Electronic); 0270-6474 (Linking).

[140] Maike Gallwitz, Mattias Enoksson, Michael Thorpe, and Lars Hellman. The extended cleavage specificity of human thrombin. *PLoS One*, 7(2):e31756, 2012. ISSN 1932-6203 (Electronic); 1932-6203 (Linking).

[141] S C Panchal, N S Bhavesh, and R V Hosur. Improved 3d triple resonance experiments, hnn and hn(c)n, for hn and 15n sequential correlations in (13c, 15n) labeled proteins: application to unfolded proteins. *J Biomol NMR*, 20(2):135–147, Jun 2001. ISSN 0925-2738 (Print); 0925-2738 (Linking).

[142] Lewis E Kay, Mitsuhiko Ikura, Rolf Tschudin, and Ad Bax. Three-dimensional triple-resonance {NMR} spectroscopy of isotopically enriched proteins. *Journal of Magnetic Resonance (1969)*, 89(3):496 – 514, 1990. ISSN 0022-2364. URL `http://www.sciencedirect.com/science/article/pii/0022236490903335`.

[143] Stephan Grzesiek and Ad Bax. An efficient experiment for sequential backbone assignment of medium-sized isotopically enriched proteins. *Journal of Magnetic Resonance (1969)*, 99(1):201 – 207, 1992. ISSN 0022-2364. URL `http://www.sciencedirect.com/science/article/pii/0022236492901698`.

[144] Wim F Vranken, Wayne Boucher, Tim J Stevens, Rasmus H Fogh, Anne Pajon, Miguel Llinas, Eldon L Ulrich, John L Markley, John Ionides, and Ernest D Laue. The ccpn data model for nmr spectroscopy: development of a software pipeline. *Proteins*, 59(4):687–696, Jun 2005. ISSN 1097-0134 (Electronic); 0887-3585 (Linking).

[145] Maayan Gal, Katherine A Edmonds, Alexander G Milbradt, Koh Takeuchi, and Gerhard Wagner. Speeding up direct (15)n detection: hcan 2d nmr experiment. *J Biomol NMR*, 51(4):497–504, Dec 2011. ISSN 1573-5001 (Electronic); 0925-2738 (Linking).

[146] Magnus Kjaergaard and Flemming M Poulsen. Sequence correction of random coil chemical shifts: correlation between neighbor correction factors and changes in the ramachandran distribution. *J Biomol NMR*, 50(2):157–165, Jun 2011. ISSN 1573-5001 (Electronic); 0925-2738 (Linking).

[147] D S Wishart and B D Sykes. The 13c chemical-shift index: a simple method for the identification of protein secondary structure using 13c chemical-shift data. *J Biomol NMR*, 4(2):171–180, Mar 1994. ISSN 0925-2738 (Print); 0925-2738 (Linking).

[148] Jiri Novacek, Lukas Zidek, and Vladimir Sklenar. Toward optimal-resolution nmr of intrinsically disordered proteins. *J Magn Reson*, 241:41–52, Apr 2014. ISSN 1096-0856 (Electronic); 1090-7807 (Linking).

[149] Tanja Mittag and Julie D Forman-Kay. Atomic-level characterization of disordered protein ensembles. *Curr Opin Struct Biol*, 17(1):3–14, Feb 2007. ISSN 0959-440X (Print); 0959-440X (Linking).

[150] M R Wilkins, E Gasteiger, A Bairoch, J C Sanchez, K L Williams, R D Appel, and D F Hochstrasser. Protein identification and analysis tools in the expasy server. *Methods Mol Biol*, 112:531–552, 1999. ISSN 1064-3745 (Print); 1064-3745 (Linking).

[151] Michael F Mesleh, William A Shirley, Christopher E Heise, Nicholas Ling, Richard A Maki, and Richard P Laura. Nmr structural characterization of a minimal peptide antagonist bound to the extracellular domain of the corticotropin-releasing factor1 receptor. *J Biol Chem*, 282(9):6338–6346, Mar 2007. ISSN 0021-9258 (Print); 0021-9258 (Linking).

[152] William M Oldham, Ned Van Eps, Anita M Preininger, Wayne L Hubbell, and Heidi E Hamm. Mechanism of the receptor-catalyzed activation of heterotrimeric g proteins. *Nat Struct Mol Biol*, 13(9):772–777, Sep 2006. ISSN 1545-9993 (Print); 1545-9985 (Linking).

[153] Dar'ya S Redka, Takefumi Morizumi, Gwendolynne Elmslie, Pranavan Paranthaman, Rabindra V Shivnaraine, John Ellis, Oliver P Ernst, and James W Wells. Coupling of g proteins to reconstituted monomers and tetramers of the m2 muscarinic receptor. *J Biol Chem*, 289(35):24347–24365, Aug 2014. ISSN 1083-351X (Electronic); 0021-9258 (Linking).

[154] Ru Zhang and Xin Xie. Tools for gpcr drug discovery. *Acta Pharmacol Sin*, 33(3): 372–384, Mar 2012. ISSN 1745-7254 (Electronic); 1671-4083 (Linking).

[155] Heini Frang, Veli-Matti Mukkala, Rita Syysto, Pia Ollikka, Pertti Hurskainen, Mika Scheinin, and Ilkka Hemmila. Nonradioactive gtp binding assay to monitor activation of g protein-coupled receptors. *Assay Drug Dev Technol*, 1(2): 275–280, Apr 2003. ISSN 1540-658X (Print); 1540-658X (Linking).

[156] J K Northup, M D Smigel, and A G Gilman. The guanine nucleotide activating site of the regulatory component of adenylate cyclase. identification by ligand binding. *J Biol Chem*, 257(19):11416–11423, Oct 1982. ISSN 0021-9258 (Print); 0021-9258 (Linking).

[157] Mary A Schuler, Ilia G Denisov, and Stephen G Sligar. Nanodiscs as a new tool to examine lipid-protein interactions. *Methods Mol Biol*, 974:415–433, 2013. ISSN 1940-6029 (Electronic); 1064-3745 (Linking).

[158] Sourabh Banerjee, Thomas Huber, and Thomas P Sakmar. Rapid incorporation of functional rhodopsin into nanoscale apolipoprotein bound bilayer (nabb) particles. *J Mol Biol*, 377(4):1067–1081, Apr 2008. ISSN 1089-8638 (Electronic); 0022-2836 (Linking).

[159] P Brodin, T Drakenberg, E Thulin, S Forsen, and T Grundstrom. Selective proton labelling of amino acids in deuterated bovine calbindin d9k. a way to simplify 1h-nmr spectra. *Protein Eng*, 2(5):353–357, Jan 1989. ISSN 0269-2139 (Print); 0269-2139 (Linking).

[160] V Ramesh, R O Frederick, S E Syed, C F Gibson, J C Yang, and G C Roberts. The interactions of escherichia coli trp repressor with tryptophan and with an operator oligonucleotide. nmr studies using selectively 15n-labelled protein. *Eur J Biochem*, 225(2):601–608, Oct 1994. ISSN 0014-2956 (Print); 0014-2956 (Linking).

[161] Peter S C Wu, Kiyoshi Ozawa, Slobodan Jergic, Xun-Cheng Su, Nicholas E Dixon, and Gottfried Otting. Amino-acid type identification in 15n-hsqc spectra by combinatorial selective 15n-labelling. *J Biomol NMR*, 34(1):13–21, Jan 2006. ISSN 0925-2738 (Print); 0925-2738 (Linking).

[162] E. R. ANDREW, A. BRADBURY, and R. G. EADES. Nuclear magnetic resonance spectra from a crystal rotated at high speed. *Nature*, 182(4650):1659, 12 13, 1958. URL `http://dx.doi.org/10.1038/1821659a0`.

[163] Nelson P Barrera, Natalie Di Bartolo, Paula J Booth, and Carol V Robinson. Micelles protect membrane complexes from solution to vacuum. *Science*, 321 (5886):243–246, Jul 2008. ISSN 1095-9203 (Electronic); 0036-8075 (Linking).

[164] Chang-Cheng Zhu, Laurie B Cook, and Patricia M Hinkle. Dimerization and phosphorylation of thyrotropin-releasing hormone receptors are modulated by agonist stimulation. *J Biol Chem*, 277(31):28228–28237, Aug 2002. ISSN 0021-9258 (Print); 0021-9258 (Linking).

[165] Ramesh C Patel, Ujendra Kumar, Don C Lamb, John S Eid, Magalie Rocheville, Michael Grant, Aruna Rani, Theodore Hazlett, Shutish C Patel, Enrico Gratton, and Yogesh C Patel. Ligand binding to somatostatin receptors induces receptor-specific oligomer formation in live cells. *Proc Natl Acad Sci U S A*, 99 (5):3294–3299, Mar 2002. ISSN 0027-8424 (Print); 0027-8424 (Linking).

[166] Z J Cheng and L J Miller. Agonist-dependent dissociation of oligomeric complexes of g protein-coupled cholecystokinin receptors demonstrated in living cells using bioluminescence resonance energy transfer. *J Biol Chem*, 276(51): 48040–48047, Dec 2001. ISSN 0021-9258 (Print); 0021-9258 (Linking).

[167] R J Woods, K M Kennedy, J M Gibbins, D Behan, W Vale, and P J Lowry. Corticotropin-releasing factor binding protein dimerizes after association with ligand. *Endocrinology*, 135(2):768–773, Aug 1994. ISSN 0013-7227 (Print); 0013-7227 (Linking).

[168] Oliver Kraetke, Burkhard Wiesner, Jenny Eichhorst, Jens Furkert, Michael Bienert, and Michael Beyermann. Dimerization of corticotropin-releasing factor receptor type 1 is not coupled to ligand binding. *J Recept Signal Transduct Res*, 25(4-6):251–276, 2005. ISSN 1079-9893 (Print); 1079-9893 (Linking).